

# Thermal Conductivity and Theory of Inelastic Scattering of Phonons by Collective Fluctuations

Léo Mangeolle,<sup>1</sup> Leon Balents,<sup>2,3</sup> and Lucile Savary<sup>1,2</sup>

<sup>1</sup>*Université de Lyon, École Normale Supérieure de Lyon, Université Claude Bernard Lyon I, CNRS, Laboratoire de physique, 46, allée d'Italie, 69007 Lyon*

<sup>2</sup>*Kavli Institute for Theoretical Physics, University of California, Santa Barbara, CA 93106-4030*

<sup>3</sup>*Canadian Institute for Advanced Research, Toronto, Ontario, Canada*

(Dated: October 28, 2022)

We study the intrinsic scattering of phonons by a general quantum degree of freedom, i.e. a fluctuating “field”  $Q$ , which may have completely general correlations, restricted only by unitarity and translational invariance. From the induced scattering rates, generalizing the model studied in a companion paper, Ref. [1], we obtain the consequences on the thermal conductivity tensor of the phonons. We confirm that, even within our generalized model, the off-diagonal scattering rates involve a minimum of three- to four-point correlation functions of the  $Q$  fields, and discuss the “semiclassical” vs “quantum” nature of all contributions. We obtain general and explicit forms for these correlations which isolate the contributions to the Hall conductivity, and provide a general discussion of the implications of symmetry and equilibrium; this elaborates on, and extends, the results of Ref. [1]. We also extend the discussion and evaluation of these two- (diagonal scattering) and four-point correlation functions, and hence the thermal transport, for the illustrative example of an ordered two dimensional antiferromagnet, where the  $Q$  field is a composite of magnon operators arising from spin-lattice coupling, and confirm numerically that the results, while satisfying all the necessary symmetry restrictions, lead to non-vanishing scattering and Hall effects. In particular, we investigate, both analytically and numerically, the dependence of such intrinsic scattering on a crucial parameter – the magnon to phonon velocity ratio  $v$ . We in particular confirm that within some range of  $v$  of order 1 the skew-scattering mechanism leads to comparable thermal Hall conductivity for thermal currents within and normal to the plane of the antiferromagnetism, and discover that the temperature scaling of the longitudinal conductivity displays a threshold effect and a non-universal, *continuous* variation of the scaling exponent with  $v$ .

## CONTENTS

		A. Summary of results and method	29
		B. About (anti-)detailed balance	29
I. Introduction	2	C. Relation to other work	30
		D. General observations	30
II. Setup	3	E. Future directions	30
A. Derivation	3		
B. Discussion	4	Acknowledgments	31
III. Formal expressions for the thermal conductivity	4	References	31
A. Formal expressions	4		
B. Model	5	A. Strain tensor	32
C. Scattering rates	5	B. General hydrodynamics of phonons	34
D. The collision integral as correlation functions	7		
IV. Relations and symmetries	9	C. From interaction terms to the collision integral	35
A. Time-reversal symmetry: reversal of the momenta	9	1. General method and definitions	35
B. Point-group symmetries	10	2. Computation at first Born order	35
		3. Energy shift of the phonons	37
V. Application to an ordered magnet	11	4. Computation at second Born order	37
A. Magnon dynamics	11	5. Computation at third Born’s order	40
B. Formal couplings	13	D. Generalizations	40
C. Phenomenological coupling Hamiltonian	15	1. Generalized model and higher perturbative orders	40
D. Solutions of the delta functions	17	2. Special properties of first Born’s order	41
E. Scaling and orders of magnitude	19	E. Application—further technical details	43
F. Numerical results	23	1. Solving the delta functions	43
G. Discussion of the results in absolute scales	29	2. Choice of polarization vectors	43
VI. Conclusions	29		

3. Numerical implementation	45
4. Details of the derivation of the general forms of the scaling relations	45
F. Application—further physical details	46
1. Microscopic derivation of the coupling constants	46
2. Contributions to intervalley couplings	47
3. Derivation of the gaps from a sigma model	47
G. Application—Supplementary figures	49

## I. INTRODUCTION

Two-point correlation functions are ubiquitous in the study of condensed matter systems. They are often the building blocks of response functions in scattering and other experiments and appear in Feynman diagrams, as well as Monte Carlo simulations. They are the central elements of linear response theory, as is evident from Kubo’s formula [2, 3]. They are often independent of the arbitrary phase choice of the wave function.

Higher-order correlation functions have witnessed renewed interest recently. They arise theoretically in the measurement of chaos. A particular type of four-point correlation function, the “out-of-time-ordered” correlator, has been shown to be related to the Lyapunov exponent, which measures the rate at which the result of a measurement diverges after a weak initial perturbation [4]. Multi-point correlations also naturally describe non-linear response, e.g. in non-linear optics such as second harmonic generation, and in “multi-dimensional spectroscopy” [5]. They may also arise in scattering measurements at resonance, such as RIXS [6, 7]. From a statistical point of view, higher order correlation functions measure the non-Gaussianity of the distribution of an observable. The more strongly correlated a state is, i.e. the more it deviates from a free-particle description, the more significant the non-Gaussianity. Hence multi-point functions are essential harbingers of strong correlations.

In a companion paper [1], we present the study of the thermal conductivity due to phonons *linearly* coupled to another degree of freedom, for example an electronic or a magnetic one. We summarize the results of that paper in this paragraph. First, it is demonstrated that this coupling induces two types of scattering of phonons: those which are symmetric in the sense of respecting detailed balance, and those which are antisymmetric and obey an “anti-detailed balance” relation. Only the latter “skew scattering” events contribute to a thermal Hall effect of phonons, as proven by formulating and solving the associated Boltzmann transport equations. Finally, the results are applied to an example calculation of the diagonal and Hall components of the thermal conductivity for the case of a two-dimensional antiferromagnet.

The purpose of the present paper is to extend the problem of Ref. [1] to the most general case, and to give full

detail of the corresponding scattering contributions and their derivation. We allow the phonons to be both linearly and quadratically coupled to the fluctuating degree of freedom, i.e. with an interaction Hamiltonian density (c.f. Eq. (16))

$$H' = \sum_{\mathbf{n}\mathbf{k}} \sum_{q=\pm} a_{\mathbf{n}\mathbf{k}}^q Q_{\mathbf{n}\mathbf{k}}^q + \frac{1}{\sqrt{N_{\text{uc}}}} \sum_{\mathbf{n}\mathbf{k} \neq \mathbf{n}'\mathbf{k}'} \sum_{q,q'=\pm} a_{\mathbf{n}\mathbf{k}}^q a_{\mathbf{n}'\mathbf{k}'}^{q'} Q_{\mathbf{n}\mathbf{k}\mathbf{n}'\mathbf{k}'}^{qq'}, \quad (1)$$

where  $a_{\mathbf{n}\mathbf{k}}^- \equiv a_{\mathbf{n}\mathbf{k}}$ ,  $a_{\mathbf{n}\mathbf{k}}^+ \equiv a_{\mathbf{n}\mathbf{k}}^\dagger$  are the phonon annihilation and creation operators for the  $n^{\text{th}}$  phonon mode with momentum  $\mathbf{k}$ , and  $Q_{\mathbf{n}\mathbf{k}}^q$ ,  $Q_{\mathbf{n}\mathbf{k}\mathbf{n}'\mathbf{k}'}^{qq'}$  are the collective fluctuating “fields” coupled to the phonons (we discuss even more general forms in the Appendices). The quantity  $N_{\text{uc}}$  is the number of unit cells in the sample. We provide a full discussion of all the different scattering contributions generated by these terms (up to quartic order in the phonon coupling, see Sec. III D), and give a full exposition of the expressions of the corresponding rates in terms of correlation functions. We also give a thorough discussion of the consequences of symmetries and detailed-balance relations on the Hall conductivity, and show in particular that the conclusion that two-point correlations functions do not contribute to a Hall effect, arrived at in Ref. [1] for the linear coupling model, continues to hold in full generality.

Up to fourth order in  $\lambda$ , where  $\lambda$  captures the size of the coupling between one phonon and one  $Q$  operator, and terms involving  $p$  phonon operators are assumed to be of order  $\lambda^p$ , the longitudinal scattering rate is

$$D_{\mathbf{n}\mathbf{k}} = D_{\mathbf{n}\mathbf{k}}^{(1)} + D_{\mathbf{n}\mathbf{k}}^{(2)} + \check{D}_{\mathbf{n}\mathbf{k}} \quad (2)$$

where  $D^{(1)}$  and  $D^{(2)}$  are obtained in our perturbative expansion at orders  $\lambda^2$  and  $\lambda^4$ , respectively, and  $\check{D}_{\mathbf{n}\mathbf{k}}$  encompasses contributions due to other scattering processes as well as higher-order terms of the expansion.

The skew scattering rate can be similarly expanded in terms at different orders in  $\lambda$ . At fourth order, we find the full set of scattering rates generalizing the results of Ref. [1] to include the two-phonon couplings and quantum interference terms:

$$\begin{aligned} \mathfrak{W}_{\mathbf{n}\mathbf{k}\mathbf{n}'\mathbf{k}'}^{\ominus,[1,1];[1,1],qq'} &\sim \langle [Q_{\mathbf{n}\mathbf{k}}^{-q}, Q_{\mathbf{n}'\mathbf{k}'}^{-q'}] \{ Q_{\mathbf{n}'\mathbf{k}'}^{q'}, Q_{\mathbf{n}\mathbf{k}}^q \} \rangle, \\ \mathfrak{W}_{\mathbf{n}\mathbf{k}\mathbf{n}'\mathbf{k}'}^{\oplus,[1,1];[1,1],qq'} &\sim \langle \{ Q_{\mathbf{n}\mathbf{k}}^{-q}, Q_{\mathbf{n}'\mathbf{k}'}^{-q'} \} \{ Q_{\mathbf{n}'\mathbf{k}'}^{q'}, Q_{\mathbf{n}\mathbf{k}}^q \} \rangle \\ &\quad - \langle [Q_{\mathbf{n}\mathbf{k}}^{-q}, Q_{\mathbf{n}'\mathbf{k}'}^{-q'}] [Q_{\mathbf{n}'\mathbf{k}'}^{q'}, Q_{\mathbf{n}\mathbf{k}}^q] \rangle, \\ \mathfrak{W}_{\mathbf{n}\mathbf{k}\mathbf{n}'\mathbf{k}'}^{\oplus,[2];[2],qq'} &\sim \langle Q_{\mathbf{n}\mathbf{k}\mathbf{n}'\mathbf{k}'}^{-q-q'} Q_{\mathbf{n}\mathbf{k}\mathbf{n}'\mathbf{k}'}^{q+q'} \rangle, \\ \mathfrak{W}_{\mathbf{n}\mathbf{k}\mathbf{n}'\mathbf{k}'}^{\oplus,[1,1];[2],qq'} &\sim \langle Q_{\mathbf{n}\mathbf{k}\mathbf{n}'\mathbf{k}'}^{-q,-q'} [Q_{\mathbf{n}'\mathbf{k}'}^{q'}, Q_{\mathbf{n}\mathbf{k}}^q] \rangle, \\ \mathfrak{W}_{\mathbf{n}\mathbf{k}\mathbf{n}'\mathbf{k}'}^{\ominus,[1,1];[2],qq'} &\sim \langle Q_{\mathbf{n}\mathbf{k}\mathbf{n}'\mathbf{k}'}^{-q,-q'} \{ Q_{\mathbf{n}'\mathbf{k}'}^{q'}, Q_{\mathbf{n}\mathbf{k}}^q \} \rangle, \\ \mathfrak{W}_{\mathbf{n}\mathbf{k}\mathbf{n}'\mathbf{k}'}^{\ominus,[2,1];[1],qq'} &\sim \langle Q_{\mathbf{n}\mathbf{k}}^{-q} \{ Q_{\mathbf{n}'\mathbf{k}'}^{-q'}, Q_{\mathbf{n}\mathbf{k}\mathbf{n}'\mathbf{k}'}^{qq'} \} \rangle, \\ \mathfrak{W}_{\mathbf{n}\mathbf{k}\mathbf{n}'\mathbf{k}'}^{\ominus,[1,1,1];[1],qq'} &\sim \langle Q_{\mathbf{n}\mathbf{k}}^{-q} \left( Q_{\mathbf{n}'\mathbf{k}'}^{-q'}, Q_{\mathbf{n}\mathbf{k}}^q, Q_{\mathbf{n}'\mathbf{k}'}^{q'} \right) \rangle. \quad (3) \end{aligned}$$

The full scattering rate is the total of all the contributions, summed over  $\sigma = \pm 1 = \oplus, \ominus$ ,  $q, q' = \pm 1$ , and the  $[\cdot], [\cdot]'$  indices which denote the “internal” states of the scattering process and will be explained in Sec. III C 1. The  $(\cdot, \cdot', \cdot'')$  notation in the last term is explained in

Appendix C 5. The first term,  $\mathfrak{W}_{n\mathbf{k}n'\mathbf{k}'}^{\ominus, [1,1]; [1,1], qq'}$  is that discussed in Ref. [1].

Most importantly, we have separated the processes into those which satisfy detailed ( $\sigma = 1$ ) and “anti-detailed” ( $\sigma = -1$ ) balance relations,

$$\mathfrak{W}_{n\mathbf{k}n'\mathbf{k}'}^{\sigma, qq'} = \sigma e^{-\beta(q\omega_{n\mathbf{k}} + q'\omega_{n'\mathbf{k}'})} \mathfrak{W}_{n\mathbf{k}n'\mathbf{k}'}^{\sigma, -q - q'}, \quad \sigma = \pm \text{ or } \oplus, \ominus. \quad (4)$$

When these rates are used as input to the Boltzmann equation, we observe that *only the anti-detailed balance terms can generate a thermal Hall effect*. A discussion of these (anti-)detailed balance relations can be found in Secs. III C 2, IV A 2.

After the derivation of these relations and their relation to the thermal conductivity tensor, and a discussion of the consequences of symmetry for the latter, we turn to the specific problem of the antiferromagnet introduced in Ref. [1]. Notably, we significantly extend the treatment there to unveil the dependence of the thermal conductivity upon the ratio  $v = v_m/v_{\text{ph}}$  of the magnon and phonon velocities, which is striking and non-trivial. In particular  $\kappa_L$  has the scaling behavior

$$\kappa_L \sim \begin{cases} T^{-1} & \text{for } v < 3 \\ T^{3-8/(v-1)} & \text{for } v > 3 \end{cases}, \quad (5)$$

exhibiting a threshold effect and a non-universal, *continuous* variation of the scaling exponent with  $v$ , as shown in Fig. 1. Furthermore, we find that the Hall resistivity dramatically decreases as  $v$  increases, due to the reduction of the allowed phase space for scattering.

The remainder of the paper is organized as follows. We first (Secs. II, III) provide an expanded derivation of the skew and longitudinal scattering rates, including those terms which result from “higher-order”  $Q$ -phonon interactions and are not present in Ref. [1]. We then (Sec. IV) provide a detailed discussion of the consequences of symmetries and “detailed balance”-like relations on the Hall conductivity. The final section (Sec. V) is an application of the results to an ordered antiferromagnet, as in Ref. [1], which we expand on in considerably more detail, both regarding the longitudinal and skew scattering rates. We obtain analytical results for the longitudinal conductivity  $\kappa_L$  and Hall resistivity  $\rho_H$  in terms of multidimensional integrals, whose scaling we analyze and verify through numerical evaluation. Seven appendices provide all details and further generalizations not given in the main text.

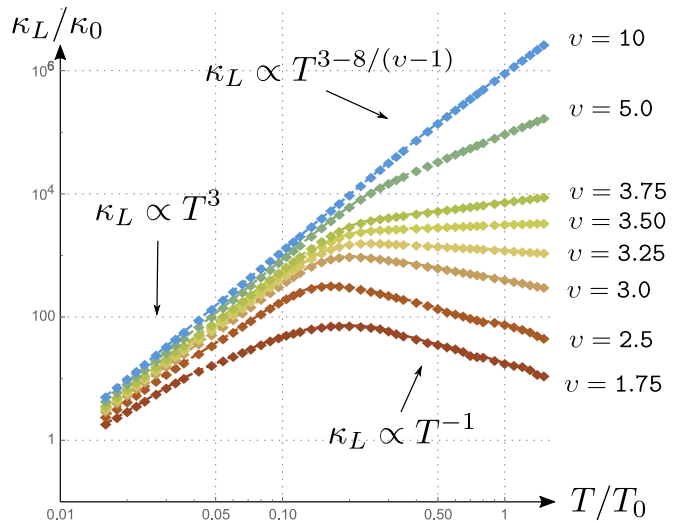


FIG. 1: Dependence upon  $v = v_m/v_{\text{ph}}$  of the longitudinal conductivity as a function of temperature, in log-log scale, for  $\bar{D}_{n\mathbf{k}} = \gamma_{\text{ext}} = 10^{-6}(v_{\text{ph}}/a)$ . We highlight the change of scaling behaviors for  $T > T_\lambda^*$  (defined in Eq. (100)) at  $v_m/v_{\text{ph}} = 3$ , above which the temperature scaling exponent of  $\kappa_L$  is a continuous function of  $v_m/v_{\text{ph}}$ , see Eq. (5) or Eq. (117).

## II. SETUP

### A. Derivation

The quasiparticle nature of phonons justifies treating their dynamics within the Boltzmann equation,

$$\partial_t \bar{N}_{n\mathbf{k}} + \mathbf{v}_{n\mathbf{k}} \cdot \nabla_{\mathbf{r}} \bar{N}_{n\mathbf{k}} = \mathcal{C}_{n\mathbf{k}}[\{\bar{N}_{n'\mathbf{k}'}\}], \quad (6)$$

where  $N_{n\mathbf{k}}(i_p) = \langle i_p | a_{n\mathbf{k}}^\dagger a_{n\mathbf{k}} | i_p \rangle$  is the number of  $(n, \mathbf{k})$  phonons ( $\mathbf{k}$  is the phonon momentum and  $n$  an extra phonon label, containing the band index and polarization) in the  $|i_p\rangle$  state,  $\bar{N}_{n\mathbf{k}} = \sum_{i_p} N_{n\mathbf{k}}(i_p) p_{i_p}$  is the average population, and  $\mathbf{v}_{n\mathbf{k}} = \nabla_{\mathbf{k}} \omega_{n\mathbf{k}}$ , with  $\omega_{n\mathbf{k}}$  the dispersion of phonons, is the group velocity of phonons.  $\mathcal{C}$  is the “collision integral,” which captures in particular the scattering of phonons with other degrees of freedom ( $Q$  fields whose coupling to the phonons is given by  $H'$  in Eq. (1)). In turn, using Born’s approximation, we have the following perturbative expansion of the scattering matrix:

$$T_{\mathbf{i} \rightarrow \mathbf{f}} = T_{\mathbf{f}\mathbf{i}} = \langle \mathbf{f} | H' | \mathbf{i} \rangle + \sum_{\mathbf{n}} \frac{\langle \mathbf{f} | H' | \mathbf{n} \rangle \langle \mathbf{n} | H' | \mathbf{i} \rangle}{E_{\mathbf{i}} - E_{\mathbf{n}} + i\eta} + \dots, \quad (7)$$

where the  $|\mathbf{i}, \mathbf{f}, \mathbf{n}\rangle$  states are product states in the  $Q$  (index  $s$ ) and phonon (index  $p$ ) Hilbert space,  $|\mathbf{g}\rangle = |g_s\rangle |g_p\rangle$  for  $g = i, f, n$ , and  $E_{\mathbf{g}}$  is the energy of the unperturbed Hamiltonians of the  $Q$  and phonons in state  $\mathbf{g}$ .  $\eta \rightarrow 0^+$  is a small regularization parameter. The expression Eq. (7) can be derived from time-dependent perturbation (scattering) theory, in which  $\eta$  captures causality and the regularizability of  $1/(E_{\mathbf{i}} - E_{\mathbf{n}})$  in the case of a continuous

energy spectrum, appropriate for scattering (unbounded) states which we are interested in [8].

The rate of transitions from state  $\mathbf{i}$  to state  $\mathbf{f}$  is obtained using Fermi's golden rule,

$$\Gamma_{\mathbf{i} \rightarrow \mathbf{f}} = \frac{2\pi}{\hbar} |T_{\mathbf{i} \rightarrow \mathbf{f}}|^2 \delta(E_{\mathbf{i}} - E_{\mathbf{f}}). \quad (8)$$

Note that  $\Gamma_{\mathbf{i} \rightarrow \mathbf{f}}$  is a transition rate in the full combined phonon- $Q$  system. This in turn determines the collision integral through the master equation

$$\mathcal{C}_{n\mathbf{k}} = \sum_{i_p, f_p} \tilde{\Gamma}_{i_p \rightarrow f_p} (N_{n\mathbf{k}}(f_p) - N_{n\mathbf{k}}(i_p)) p_{i_p}, \quad (9)$$

where  $p_{i_p} = \sum_{i_s} p_i$ , where  $p_i = \frac{1}{Z} e^{-\beta E_i}$  is the probability to find the system in state  $\mathbf{i}$ , and  $Z$  is the partition function of the two subsystems. Here

$$\tilde{\Gamma}_{i_p \rightarrow f_p} = \sum_{i_s, f_s} \Gamma_{\mathbf{i} \rightarrow \mathbf{f}} p_{i_s} \quad (10)$$

is the transition rate between just phonon states, with  $p_{i_s} = \frac{1}{Z_s} e^{-\beta E_{i_s}}$ .

## B. Discussion

The above approach is ‘‘semiclassical’’ in two respects. First, it ultimately treats phonons as quasiparticles within a Boltzmann equation. This is justified whenever the scattering rate is small compared to the energy of the particles. Second, we use the Fermi's golden rule relation, Eq. (8), to determine the scattering rates. This approximation leads to slight differences from an exact calculation of the quantum rates, but preserves all symmetries and physical processes, and we expect it to capture all the key features of a fully quantum approach. We proceed with the T-matrix approach here which has the advantage of (relative) physical transparency, as every effect can be directly identified with a scattering process.

One can understand the need for effects beyond the first Born approximation entirely through the symmetries of the T-matrix. Specifically, since the time reversal (TR) operator is anti-unitary, and requires complex conjugation, one can see from Eq. (7) that under time reversal,  $\text{TR} : T \mapsto T^\dagger$  ( $\eta \rightarrow -\eta$  under complex conjugation). Since TR invariance is sufficient to enforce a vanishing Hall effect, the hermiticity of  $T$  is enough to guarantee a vanishing Hall effect. From Eq. (7),  $T$  is indeed always hermitian within the first Born approximation, because  $H'$  itself must be hermitian.

Finally, we note that we are focusing on collisional effects, i.e. on *real* transitions induced by interactions,

rather than Berry phase contributions, which arise from entirely virtual transitions and manifest as modifications to the semiclassical equations of motion for phonons, e.g. an anomalous velocity. Formally, real transitions are captured within the collision integral on the right hand side of the Boltzmann equation [9], while Berry phase contributions enter the left hand side and in the definition of the currents. For phonons, our focus on collisions is justified by strong phase space constraints on the Berry curvature effects which are typical to acoustic bosonic modes. Specifically, as shown in Ref. [10], the Berry phase contributions are described by an emergent vector potential which at small momenta must by symmetry be at least second order in gradients, making it a formally ‘‘irrelevant’’ perturbation to the phonon Lagrangian, and strongly suppressing its effects at low temperature [11].

## III. FORMAL EXPRESSIONS FOR THE THERMAL CONDUCTIVITY

### A. Formal expressions

To solve Eq. (6), we expand  $\bar{N}_{n\mathbf{k}} = N_{n\mathbf{k}}^{\text{eq}} + \delta\bar{N}_{n\mathbf{k}}$  around the equilibrium distribution  $N_{n\mathbf{k}}^{\text{eq}}$ , which solves Boltzmann's equation at  $\nabla T = \mathbf{0}$ , keep terms up to linear order in  $\delta\bar{N}_{n\mathbf{k}}$  in the collision integral and for convenience separate the diagonal  $D_{n\mathbf{k}}$  and off-diagonal  $M_{n\mathbf{k}, n'\mathbf{k}'}$  parts, i.e. we write the collision integral

$$\mathcal{C}_{n\mathbf{k}} = \sum_{n'\mathbf{k}'} (-\delta_{nn'} \delta_{\mathbf{k}\mathbf{k}'} D_{n\mathbf{k}} + M_{n\mathbf{k}, n'\mathbf{k}'} \delta\bar{N}_{n'\mathbf{k}'} + O(\delta\bar{N}^2)), \quad (11)$$

where by definition  $M_{n\mathbf{k}, n\mathbf{k}} = 0$ . The equation  $\mathcal{C}_{n\mathbf{k}}[\{N_{n'\mathbf{k}'}^{\text{eq}}\}] = 0$  —i.e. the collision integral is zero in equilibrium—should be considered the *definition* of the equilibrium densities  $\{N_{n'\mathbf{k}'}^{\text{eq}}\}$  of the interacting phonons (see Appendix C 3).

Using Fourier's law,

$$\mathbf{j} = -\boldsymbol{\kappa} \cdot \nabla T = V^{-1} \sum_{n\mathbf{k}} \bar{N}_{n\mathbf{k}} \mathbf{v}_{n\mathbf{k}} \omega_{n\mathbf{k}}, \quad (12)$$

and formally inverting the collision integral leads to the following expressions for the longitudinal  $\kappa_L^{\mu\mu}$ , and Hall (antisymmetric)  $\kappa_H^{\mu\nu} = (\kappa^{\mu\nu} - \kappa^{\nu\mu})/2$  conductivities (along the  $\mu$  direction and in the  $\mu\nu$  plane, respectively):

$$\kappa_{L/H}^{\mu\nu} = \frac{\hbar^2}{k_B T^2} \frac{1}{V} \sum_{n\mathbf{k} n'\mathbf{k}'} J_{n\mathbf{k}}^\mu K_{n\mathbf{k} n'\mathbf{k}'}^{L/H} J_{n'\mathbf{k}'}^\nu, \quad (13)$$

where  $\nu = \mu$  for  $\kappa_L$ . Assuming  $\sum_{n'\mathbf{k}'} M_{n\mathbf{k} n'\mathbf{k}'} \ll D_{n\mathbf{k}}$ , one can effectively invert the collision integral to obtain the kernels



$$K_{n\mathbf{k}n'\mathbf{k}'}^L = \frac{e^{\beta\hbar\omega_{n\mathbf{k}}}}{D_{n\mathbf{k}}} \delta_{nn'} \delta_{\mathbf{k},\mathbf{k}'} + \frac{e^{\beta\hbar(\omega_{n\mathbf{k}}+\omega_{n'\mathbf{k}'})/2}}{2D_{n\mathbf{k}}D_{n'\mathbf{k}'}} \left( \frac{\sinh(\beta\hbar\omega_{n\mathbf{k}}/2)}{\sinh(\beta\hbar\omega_{n'\mathbf{k}'}/2)} M_{n\mathbf{k},n'\mathbf{k}'} + (n\mathbf{k} \leftrightarrow n'\mathbf{k}') \right), \quad (14)$$

$$K_{n\mathbf{k}n'\mathbf{k}'}^H = \frac{e^{\beta\hbar(\omega_{n\mathbf{k}}+\omega_{n'\mathbf{k}'})/2}}{2D_{n\mathbf{k}}D_{n'\mathbf{k}'}} \left( \frac{\sinh(\beta\hbar\omega_{n\mathbf{k}}/2)}{\sinh(\beta\hbar\omega_{n'\mathbf{k}'}/2)} M_{n\mathbf{k},n'\mathbf{k}'} - (n\mathbf{k} \leftrightarrow n'\mathbf{k}') \right). \quad (15)$$

Here we identified the equilibrium phonon current  $J_{n\mathbf{k}}^\mu = N_{n\mathbf{k}}^{\text{eq}} \omega_{n\mathbf{k}} v_{n\mathbf{k}}^\mu$ , and made the ‘‘standard’’ approximation  $\nabla_{\mathbf{r}} \bar{N}_{n\mathbf{k}} \approx \nabla_{\mathbf{r}} N_{n\mathbf{k}}^{\text{eq}}$ , and looked for a stationary solution ( $\partial_t \bar{N} = 0$ ) to Boltzmann’s equation. While the sign of  $\kappa_H$  depends on the details of the system (see later), the second law of thermodynamics imposes  $\kappa_L > 0$ . Considering Eq. (14), we therefore expect  $D_{n\mathbf{k}} > 0$ .

Clearly, only contributions to  $K_{n\mathbf{k},n'\mathbf{k}'}^{L/H}$  which are symmetric (resp. antisymmetric) in exchanging  $(n\mathbf{k} \leftrightarrow n'\mathbf{k}')$  contribute to  $\kappa_L$  (resp.  $\kappa_H$ ). The special case of the term diagonal in  $n\mathbf{k}, n'\mathbf{k}'$ , being symmetric, does not contribute to the Hall conductivity. Below we will isolate the correlation functions of the  $Q$  operators which give anti-symmetric (in  $n\mathbf{k} \leftrightarrow n'\mathbf{k}'$ ) contributions to  $\frac{\sinh(\beta\hbar\omega_{n\mathbf{k}}/2)}{\sinh(\beta\hbar\omega_{n'\mathbf{k}'}/2)} M_{n\mathbf{k},n'\mathbf{k}'}$ , and hence contribute to  $\kappa_H$ . These correspond to scattering processes which violate detailed balance.

## B. Model

To describe the interaction between the phonons and another degree of freedom, we introduce general coupling terms between phonon annihilation (creation) operators  $a_{n\mathbf{k}}^{(\dagger)}$  and general, for now unspecified, fields  $Q_{\{n_j, \mathbf{k}_j\}}^{\{q_j\}}$  which are operators acting in their own Hilbert space. In what follows we only consider the first two terms of the expansion with respect to phonon operators (see also Eq. (1)), i.e. we write the interaction hamiltonian as  $H' = H'_{[1]} + H'_{[2]}$ , where

$$H'_{[1]} = \sum_{n\mathbf{k}} \sum_{q=\pm} a_{n\mathbf{k}}^q Q_{n\mathbf{k}}^q, \quad (16)$$

$$H'_{[2]} = \frac{1}{\sqrt{N_{\text{uc}}}} \sum_{n\mathbf{k} \neq n'\mathbf{k}'} \sum_{q, q'=\pm} a_{n\mathbf{k}}^q a_{n'\mathbf{k}'}^{q'} Q_{n\mathbf{k}n'\mathbf{k}'}^{qq'},$$

$$T_{i \rightarrow f}^{[1]} = \sum_{n\mathbf{k}q} \sqrt{N_{n\mathbf{k}}^i + \frac{1+q}{2}} \langle f_s | Q_{n\mathbf{k}}^q | i_s \rangle \mathbb{I}(i_p \xrightarrow{q \cdot n\mathbf{k}} f_p), \quad (18)$$

$$T_{i \rightarrow f}^{[2]} = \frac{1}{\sqrt{N_{\text{uc}}}} \sum_{n\mathbf{k}q, n'\mathbf{k}'q'} \sqrt{N_{n\mathbf{k}}^i + \frac{1+q}{2}} \sqrt{N_{n'\mathbf{k}'}^i + \frac{1+q'}{2}} \langle f_s | Q_{n\mathbf{k}n'\mathbf{k}'}^{qq'} | i_s \rangle \mathbb{I}(i_p \xrightarrow{q \cdot n\mathbf{k}} f_p), \quad (19)$$

$$T_{i \rightarrow f}^{[1,1]} = \sum_{n\mathbf{k}q, n'\mathbf{k}'q'} \sqrt{N_{n\mathbf{k}}^i + \frac{1+q}{2}} \sqrt{N_{n'\mathbf{k}'}^f + \frac{1-q'}{2}} \sum_{m_s} \frac{\langle f_s | Q_{n'\mathbf{k}'}^{q'} | m_s \rangle \langle m_s | Q_{n\mathbf{k}}^q | i_s \rangle}{E_{i_s} - E_{m_s} - q\omega_{n\mathbf{k}} + i\eta} \mathbb{I}(i_p \xrightarrow{q \cdot n\mathbf{k}} f_p), \quad (20)$$

and  $T_{i \rightarrow f}^{[1,2]}$  and  $T_{i \rightarrow f}^{[1,1,1]}$  are given in Appendices C4

and in the following, we consider Eq. (16) as a perturbative expansion with respect to a small parameter  $\lambda$ , such that formally  $Q_{n\mathbf{k}} \sim \lambda$ ,  $Q_{n\mathbf{k}n'\mathbf{k}'}^{qq'} \sim \lambda^2$ , etc. Note we consider generalizations of this model in Appendix D.

In the above expression we used  $a_{n\mathbf{k}}^+ \equiv a_{n\mathbf{k}}^\dagger$  and  $a_{n\mathbf{k}}^- \equiv a_{n\mathbf{k}}$ . The hermiticity of  $H'$  imposes  $Q_{\{n_i, \mathbf{k}_i\}}^+ \equiv Q_{\{n_i, \mathbf{k}_i\}}^\dagger$  and  $Q_{\{n_i, \mathbf{k}_i\}}^- \equiv Q_{\{n_i, \mathbf{k}_i\}}$ , and for many-phonon terms, we have  $Q_{\{n_j, \mathbf{k}_j\}}^{-q_1, \dots, -q_M} = (Q_{\{n_j, \mathbf{k}_j\}}^{q_1 \dots q_M})^\dagger$ . The single-phonon interaction terms, which may physically be seen as single-phonon scattering off the  $Q$  degrees of freedom, corresponds in particular to a coupling of the  $Q$  operators to the strain tensor  $\mathcal{E}^{\alpha\beta}(\mathbf{r})$ ,

$$\mathcal{E}^{\alpha\beta}(\mathbf{r}) = \frac{i\hbar^{1/2}}{\sqrt{N_{\text{uc}}}} \sum_{\mathbf{k}n} e^{i\mathbf{k} \cdot \mathbf{r}} \frac{(k^\alpha \varepsilon_{\mathbf{k}n}^\beta + k^\beta \varepsilon_{\mathbf{k}n}^\alpha)}{\sqrt{2M_{\text{uc}}\omega_{\mathbf{k}n}}} (a_{\mathbf{k}n} + a_{-\mathbf{k}n}^\dagger), \quad (17)$$

where  $M_{\text{uc}}$  is the unit cell mass and  $\varepsilon_{n\mathbf{k}}$  is the polarization vector of the  $|n\mathbf{k}\rangle$  phonon. The two-phonon terms capture quadratic coupling of the lattice displacements to the electrons/spins, as is often considered for example in treatments of Raman scattering [12, 13]. A priori, the quadratic terms are much smaller than the linear ones, but the former may be important if they give rise to distinct effects or contribute at a lower order in perturbation theory than the linear ones.

## C. Scattering rates

### 1. T-matrix elements

The transition matrix elements are  $T_{\mathbf{f}\mathbf{i}} = \sum_l T_{\mathbf{f}\mathbf{i}}^{[l_1, \dots]}$  (the  $l_i$  represent which  $H_{[l_i]}$  appear successively in  $T$ , so that the number of  $l_i$  appearing in  $T_{\mathbf{f}\mathbf{i}}^{[l_1, \dots]}$  is the order of the Born approximation used for that term), where

(Eq. (C50)) and C5 (Eq. (C54)), respectively. Here,

$\mathbb{I}(i_p \xrightarrow{q \cdot n\mathbf{k}} f_p)$  (resp.  $\mathbb{I}(i_p \xrightarrow{q \cdot n\mathbf{k}}_{q' \cdot n'\mathbf{k}'} f_p)$ ) is a large product of delta functions which enforce  $N_{n''\mathbf{k}''}^f = N_{n''\mathbf{k}''}^i \forall n''\mathbf{k}'' \neq n\mathbf{k}$  (resp.  $\forall n''\mathbf{k}'' \neq (n\mathbf{k}, n'\mathbf{k}')$ ), and  $N_{n\mathbf{k}}^f = N_{n\mathbf{k}}^i + q$  (resp.  $N_{n\mathbf{k}}^f = N_{n\mathbf{k}}^i + q, N_{n'\mathbf{k}'}^f = N_{n'\mathbf{k}'}^i + q'$ ). Note that the cases where  $n\mathbf{k} = n'\mathbf{k}'$  require a formal correction. However, at any given order in the  $\lambda$  expansion, such terms are smaller than all others by a factor  $1/N_{\text{uc}}$ , where  $N_{\text{uc}}$  is the number of unit cells, and therefore vanish in the thermodynamic limit. In what follows we thus use  $\sum_{n\mathbf{k}, n'\mathbf{k}'}$  and  $\sum_{n\mathbf{k} \neq n'\mathbf{k}'}$  exchangeably, unless we specify otherwise.

The scattering rate as given by Eq. (8), involves the squares of the elements of the total transition matrix (see Appendices C 4, C 5 for computational details). Its full expression to perturbative order  $\lambda^4$  is

$$\Gamma_{i \rightarrow f} = \Gamma_{i \rightarrow f}^{\text{sc}} + \Gamma_{i \rightarrow f}^{\text{Q1}} + \Gamma_{i \rightarrow f}^{\text{Q2}}, \quad (21)$$

where

$$\begin{aligned} & \left[ \Gamma_{i \rightarrow f}^{\text{sc}} ; \Gamma_{i \rightarrow f}^{\text{Q2}} ; \Gamma_{i \rightarrow f}^{\text{Q1}} \right] = \frac{2\pi}{\hbar} \delta(E_i - E_f) \\ & \times \begin{bmatrix} |T_{i \rightarrow f}^{[1]}|^2 + |T_{i \rightarrow f}^{[1,1]}|^2 + |T_{i \rightarrow f}^{[2]}|^2 & ; \\ 2\Re \left\{ (T_{i \rightarrow f}^{[1,1]})^* T_{i \rightarrow f}^{[2]} \right\} & ; \\ 2\Re \left\{ (T_{i \rightarrow f}^{[1,2]})^* T_{i \rightarrow f}^{[1]} + (T_{i \rightarrow f}^{[1,1,1]})^* T_{i \rightarrow f}^{[1]} \right\} \end{bmatrix}. \quad (22) \end{aligned}$$

This decomposition into three terms is discussed in Sec. III D 3.

## 2. Collision matrix elements

Following Eq. (9), the scattering rates  $\Gamma_{i \rightarrow f}$  give access to the collision integral, i.e. to  $M_{n\mathbf{k}, n'\mathbf{k}'}$  and  $D_{n\mathbf{k}}$ . We decompose the latter as  $D_{n\mathbf{k}} = D_{n\mathbf{k}}^{(1)} + D_{n\mathbf{k}}^{(2)} + \check{D}_{n\mathbf{k}}$ , where  $D^{(1)}$  and  $D^{(2)}$  are obtained in our perturbative expansion at orders  $\lambda^2$  and  $\lambda^4$ , respectively, and  $\check{D}_{n\mathbf{k}}$  encompasses contributions due to other scattering processes as well as higher-order terms of the expansion. In the following, we also use the “[ $l_i$ ]; [ $l'_j$ ]” superscripts to denote a term obtained from the product of  $T_{i \rightarrow f}^{[l_i]}$  and  $T_{i \rightarrow f}^{[l'_j]}$  within  $|T_{i \rightarrow f}|^2$ . For instance, at order  $\lambda^2$ , we have

$$D_{n\mathbf{k}}^{(1)} = D_{n\mathbf{k}}^{[1];[1]}. \quad (23)$$

Details of the derivation are given in Sec. III D 1 and Appendix C 2. At order  $\lambda^4$ , the diagonal and off-diagonal

contributions to the collision integral take the forms

$$D_{n\mathbf{k}}^{(2)} = -\frac{1}{N_{\text{uc}}} \sum_{n'\mathbf{k}'} \sum_{qq'} q \left( N_{n'\mathbf{k}'}^{\text{eq}} + \frac{q'+1}{2} \right) \left[ \mathfrak{W}_{n\mathbf{k}n'\mathbf{k}'}^{qq'} \right], \quad (24)$$

and

$$M_{n\mathbf{k}n'\mathbf{k}'} = \frac{1}{N_{\text{uc}}} \sum_{q, q' = \pm} q \left( N_{n\mathbf{k}}^{\text{eq}} + \frac{q+1}{2} \right) \left[ \mathfrak{W}_{n\mathbf{k}n'\mathbf{k}'}^{qq'} \right], \quad (25)$$

respectively, where  $\mathfrak{W}_{n\mathbf{k}, n'\mathbf{k}'}^{qq'}$  is an off-diagonal scattering rate which involves two different phonon states  $|n\mathbf{k}\rangle$  and  $|n'\mathbf{k}'\rangle$ . More precisely,  $\mathfrak{W}^{+,+}$  (resp.  $\mathfrak{W}^{-,-}$ ) corresponds to scattering processes where two phonons are emitted (resp. absorbed), and  $\mathfrak{W}^{+,-}, \mathfrak{W}^{-,+}$  to processes where one phonon is emitted and one is absorbed.  $D_{n\mathbf{k}}$  is the diagonal scattering rate, i.e. it is associated with variations in  $\delta \bar{N}_{n\mathbf{k}}$  only.

We will now decompose the  $\mathfrak{W}_{n\mathbf{k}, n'\mathbf{k}'}^{qq'}$  scattering rates into

$$\mathfrak{W}_{n\mathbf{k}, n'\mathbf{k}'}^{qq'} = \mathfrak{W}_{n\mathbf{k}n'\mathbf{k}'}^{\oplus, qq'} + \mathfrak{W}_{n\mathbf{k}n'\mathbf{k}'}^{\ominus, qq'}, \quad (26)$$

where  $\mathfrak{W}_{n\mathbf{k}, n'\mathbf{k}'}^{\oplus/\ominus, qq'}$  satisfy detailed ( $\sigma = 1$ ) or “anti-detailed” ( $\sigma = -1$ ) balance equations

$$\mathfrak{W}_{n\mathbf{k}n'\mathbf{k}'}^{\sigma, qq'} = \sigma e^{-\beta(q\omega_{n\mathbf{k}} + q'\omega_{n'\mathbf{k}'})} \mathfrak{W}_{n\mathbf{k}n'\mathbf{k}'}^{\sigma, -q-q'}, \quad \sigma = \pm \text{ or } \oplus, \ominus. \quad (27)$$

Physically, Eq. (27) expresses “microscopic” thermodynamic equilibrium between the process which takes  $\{N_{n\mathbf{k}} \rightarrow N_{n\mathbf{k}} + q, N_{n'\mathbf{k}'} \rightarrow N_{n'\mathbf{k}'} + q'\}$  to the “conjugate” process taking  $\{N_{n\mathbf{k}} \rightarrow N_{n\mathbf{k}} - q, N_{n'\mathbf{k}'} \rightarrow N_{n'\mathbf{k}'} - q'\}$ , with  $q, q' = \pm 1$ , leaving  $N_{n''\mathbf{k}''}$  unchanged for  $n''\mathbf{k}'' \notin \{n\mathbf{k}, n'\mathbf{k}'\}$ . Note that this is different from time-reversal symmetry which provides a relation between the processes acting on  $\{|n_l, \mathbf{k}_l\rangle\}$  phonons to the *same* processes acting on the  $\{|n_l, -\mathbf{k}_l\rangle\}$  phonons.

Moreover, since, by construction, the two-phonon scattering rates satisfy

$$\mathfrak{W}_{n\mathbf{k}n'\mathbf{k}'}^{\sigma, qq'} = \mathfrak{W}_{n'\mathbf{k}'n\mathbf{k}}^{\sigma, q'q}, \quad (28)$$

the following relations also hold:

$$\mathfrak{W}_{n'\mathbf{k}'n\mathbf{k}}^{\sigma, +-} = \sigma e^{\beta(\omega_{n\mathbf{k}} - \omega'_{n'\mathbf{k}'})} \mathfrak{W}_{n\mathbf{k}n'\mathbf{k}'}^{\sigma, +-}. \quad (29)$$

Together, these imply that there are only four independent such scattering rates between the  $|n, \mathbf{k}\rangle$  and  $|n', \mathbf{k}'\rangle$  phonons, namely  $\mathfrak{W}_{n\mathbf{k}, n'\mathbf{k}'}^{\sigma, ++}$  and  $\mathfrak{W}_{n\mathbf{k}, n'\mathbf{k}'}^{\sigma, +-}$  with  $\sigma = \oplus, \ominus$ .

As discussed at length, the first Born approximation alone does not lead to a nonzero thermal Hall effect, neither do those scattering rates which satisfy detailed balance as the latter imposes thermal equilibrium between “left” and “right” scattering. We find the kernels  $K^{L/H}$  defined in Eqs. (14,15) in terms of the  $\mathfrak{W}$  scattering rates:

$$K_{nk n' k'}^L = \frac{e^{\beta \hbar \omega_{nk}}}{D_{nk}} \left( \delta_{n, n'} \delta_{\mathbf{k}, \mathbf{k}'} + \frac{e^{\beta \hbar \omega_{n' k'}}}{2 N_{uc} D_{n' k'}} \sum_{q=\pm} e^{\frac{q-1}{2} \beta \hbar \omega_{n' k'}} \left\{ \mathfrak{W}_{nk, n' k'}^{\ominus, +, q} \left( q \coth\left(\frac{\beta \hbar \omega_{nk}}{2}\right) + \coth\left(\frac{\beta \hbar \omega_{n' k'}}{2}\right) \right) - 2 \mathfrak{W}_{nk, n' k'}^{\oplus, +, q} \right\} \right), \quad (30)$$

$$K_{nk n' k'}^H = \frac{e^{\beta \hbar \omega_{nk}} e^{\beta \hbar \omega_{n' k'}}}{2 N_{uc} D_{nk} D_{n' k'}} \sum_{q=\pm} \mathfrak{W}_{nk, n' k'}^{\ominus, +, q} e^{\frac{q-1}{2} \beta \hbar \omega_{n' k'}} \left( \coth\left(\frac{\beta \hbar \omega_{n' k'}}{2}\right) - q \coth\left(\frac{\beta \hbar \omega_{nk}}{2}\right) \right). \quad (31)$$

Incorporating the expression for  $D$  in the denominators of  $K^{L,H}$  provides an expansion up to  $O(\lambda^4)$  of the latter. We recover, as mentioned before, that the terms in  $\mathfrak{W}^{\oplus}$  do not contribute to  $K^H$  (they satisfy detailed-balance). The ‘‘anti-detailed-balance’’ relations satisfied by the  $\mathfrak{W}^{\ominus}$

terms do not however prohibit their contribution to  $K^L$ . See Sec. IV B for a discussion. Inserting Eq. (30) and Eq. (31) into Eq. (13), and after some algebra, one obtains the results for  $\kappa_{L,H}$ , respectively:

$$\begin{aligned} \kappa_L^{\mu\nu} = & \frac{\hbar^2}{k_B T^2} \frac{1}{V} \left\{ \sum_{nk} \frac{\omega_{nk}^2 v_{nk}^\mu v_{nk}^\nu}{4 D_{nk} \sinh^2(\beta \hbar \omega_{nk}/2)} \right. \\ & \left. + \sum_{nk n' k'} J_{nk}^\mu \frac{e^{\beta \omega_{nk}/2}}{D_{nk}} \left( \frac{1}{N_{uc}} \sum_{q=\pm} e^{\beta q \omega_{n' k'}/2} e^{\beta \omega_{nk}/2} \left\{ \mathfrak{W}_{nk n' k'}^{\ominus, +, q} \coth(\beta \omega_{n' k'}/2) - q \mathfrak{W}_{nk n' k'}^{\oplus, +, q} \right\} \right) \frac{e^{\beta \omega_{n' k'}/2}}{D_{n' k'}} J_{n' k'}^\nu \right\}, \end{aligned} \quad (32)$$

where the first term is the leading-order contribution and with  $J_{nk}^\mu = N_{nk}^{\text{eq}} \omega_{nk} v_{nk}^\mu$ , and

$$\kappa_H^{\mu\nu} = \frac{\hbar^2}{k_B T^2} \frac{1}{V} \sum_{nk n' k'} J_{nk}^\mu \frac{e^{\beta \hbar \omega_{nk}/2}}{D_{nk}} \left( \frac{1}{N_{uc}} \sum_{q=\pm} \frac{(e^{\beta \hbar \omega_{nk}} - e^{q \beta \hbar \omega_{n' k'}}) \mathfrak{W}_{nk, n' k'}^{\ominus, +, q}}{4 \sinh(\beta \hbar \omega_{nk}/2) \sinh(\beta \hbar \omega_{n' k'}/2)} \right) \frac{e^{\beta \hbar \omega_{n' k'}/2}}{D_{n' k'}} J_{n' k'}^\nu. \quad (33)$$

## D. The collision integral as correlation functions

### 1. Terms at $O(\lambda^2)$

The diagonal scattering rate  $D_{nk}^{(1)}$ , obtained by inserting  $T_{i \rightarrow f}^{[1]}$  from Eq. (18) into Eqs. (8-10), may now be cast into the form of a correlation function of  $Q$  operators. To do so, we first enforce the energy conservation  $\delta(E_f - E_i)$  by writing the latter as a time integral, i.e. use  $\int_{-\infty}^{+\infty} dt e^{i\omega t} = 2\pi \delta(\omega)$ ; we then identify  $A(t) = e^{+iHt} A e^{-iHt}$  and use the identity  $1 = \sum_{f_s} |f_s\rangle \langle f_s|$ . Taking the  $Q$ s in the initial state to be in thermal equilibrium  $p_{i_s} = Z_s^{-1} e^{-\beta E_{i_s}}$ , summing over  $|i_s\rangle$ , identifying  $\langle A \rangle_\beta = Z^{-1} \text{Tr}(e^{-\beta H} A)$ , summing over final phononic states  $f_p$  and taking the average over initial phononic

states  $i_p$ , we obtain the  $|T_{i \rightarrow f}^{[1]}|^2$  contribution of  $\Gamma^{\text{sc}}$ ,

$$D_{nk}^{(1)} = -\frac{1}{\hbar^2} \int dt e^{-i\omega_{nk} t} \langle [Q_{nk}(t), Q_{nk}^\dagger(0)] \rangle_\beta. \quad (34)$$

We now apply the same method to higher orders of the perturbative expansion.

### 2. Terms at $O(\lambda^4)$

We use the following time integral representation for the denominators appearing at second and higher Born orders (using a regularized definition of the sign function, i.e.  $\lim_{\eta \rightarrow 0} \text{sign}(t) e^{-\eta|t|} \rightarrow \text{sign}(t)$ ),

$$\begin{aligned} \frac{1}{x \pm i\eta} &= \text{PP} \frac{1}{x} \mp i\pi \delta(x) \\ &= \frac{1}{2i} \int_{-\infty}^{+\infty} dt_1 e^{it_1 x} (\text{sign}(t_1) \pm 1). \end{aligned} \quad (35)$$

Using Eqs. (19,20) and Eq. (22), we find the explicit expressions for the other semiclassical ( $\Gamma^{\text{sc}}$ ) scattering rates as correlation functions of the  $Q$  operators,

$$\mathfrak{W}_{nk'n'k'}^{\oplus,[2];[2],qq'} = \frac{2}{\hbar^4} \int_t \langle Q_{nk'n'k'}^{-q,-q'}(-t) Q_{nk'n'k'}^{q,q'}(0) \rangle, \quad (36)$$

$$\mathfrak{W}_{nk'n'k'}^{\ominus,[1,1];[1,1],qq'} = \frac{2}{\hbar^4} N_{\text{uc}} \Re \int_{t,t_1,t_2} \langle \llbracket Q_{nk}^{-q}(-t-t_2), Q_{n'k'}^{-q'}(-t+t_2) \rrbracket \{ Q_{n'k'}^{q'}(-t_1), Q_{nk}^q(t_1) \} \rangle, \quad (37)$$

$$\mathfrak{W}_{nk'n'k'}^{\oplus,[1,1];[1,1],qq'} = \frac{1}{\hbar^4} N_{\text{uc}} \int_{t,t_1,t_2} \langle \{ \cdot, \cdot \} \{ \cdot, \cdot \} - \llbracket \cdot, \cdot \rrbracket \llbracket \cdot, \cdot \rrbracket \rangle, \quad (38)$$

where we use the shorthand notation

$$\llbracket A(t_a), B(t_b) \rrbracket = \text{sign}(t_b - t_a) [A(t_a), B(t_b)], \quad (39)$$

and  $f_{t,\{t_j\}}$ ,  $j = 1, \dots, l$ , denotes the set of  $1 + l$  Fourier transforms evaluated once at  $\Sigma_{nkq}^{n'k'q'} = q\omega_{nk} + q'\omega_{n'k'}$  and  $l$  times at  $\Delta_{nkq}^{n'k'q'} = q\omega_{nk} - q'\omega_{n'k'}$ , i.e.  $f_{t,\{t_j\}} = \int dt dt_1 \dots dt_l e^{i\Sigma_{nkq}^{n'k'q'} t} e^{i\Delta_{nkq}^{n'k'q'}(t_1 + \dots + t_l)}$ . The symbols  $\cdot$  must be replaced by the same set of operators as the expression from the above. The commutators and anti-commutators ultimately capture antisymmetrization and symmetrization over the  $nkq \leftrightarrow n'k'q'$  indices. We provide expressions for  $\mathfrak{W}_{nk'n'k'}^{\ominus,[1,1];[2],qq'}$ ,  $\mathfrak{W}_{nk'n'k'}^{\oplus,[1,1];[2],qq'}$  (from  $\Gamma_{i \rightarrow f}^{\text{Q}2}$ ),  $\mathfrak{W}_{nk'n'k'}^{[1,2];[1],qq'}$  and  $\mathfrak{W}_{nk'n'k'}^{[1,1,1];[1],qq'}$  (from  $\Gamma_{i \rightarrow f}^{\text{Q}1}$ ) in Appendices C 4 d, C 5, Eqs. (C48, C49, C51, C56), respectively.

### 3. Scattering channels and conserving approximation

The above terms capture all contributions to the collision integral arising from the Born expansion of the transition amplitude, up to perturbative order  $\lambda^4$ . This gives, correspondingly, physical processes in the collision integral which contribute up to  $O(\lambda^4)$ .

In Eq. (21), while  $\Gamma_{i \rightarrow f}^{\text{SC}}$  and  $\Gamma_{i \rightarrow f}^{\text{Q}2}$  are “two-phonon” terms, the contribution from  $\Gamma_{i \rightarrow f}^{\text{Q}1}$  is a “one-phonon” term, i.e. one where the initial  $i$  and final  $f$  states differ by only one phonon  $|nk\rangle$ . Physically, this contributes to processes which create or annihilate a single phonon, in contrast with the  $O(\lambda^4)$  processes described so far, which create/annihilate two phonons with different quantum numbers. Because the single phonon process is physically distinct from the two-phonon ones, we expect that it is independent from the latter in the sense that the set of all the  $O(\lambda^4)$  single-phonon processes satisfies *independently* all physical constraints such as symmetries and conservation laws. Hence omitting these contributions is a “conserving approximation” in the traditional sense [14], and we will proceed with this omission for the most part in the following. We however include formal expressions for these terms in the appendices.

The remaining contributions in Eq. (21) are “two-phonon” terms, i.e. terms in which the initial  $i$  and final  $f$  states differ by two phonons  $|nk\rangle, |n'k'\rangle$ . The two-phonon,  $O(\lambda^4)$ , contributions to the  $\mathfrak{W}$  scattering rates

thus read

$$\mathfrak{W}_{nk,n'k'}^{\ominus,qq'} = \mathfrak{W}_{nk,n'k'}^{\ominus,[1,1];[2],qq'} + \mathfrak{W}_{nk,n'k'}^{\ominus,[1,1];[1,1],qq'}, \quad (40)$$

$$\mathfrak{W}_{nk,n'k'}^{\oplus,qq'} = \mathfrak{W}_{nk,n'k'}^{\oplus,[2];[2],qq'} + \mathfrak{W}_{nk,n'k'}^{\oplus,[1,1];[2],qq'} + \mathfrak{W}_{nk,n'k'}^{\oplus,[1,1];[1,1],qq'}.$$

Another physical distinction between the contributions in Eq. (21) can be made according to the “quantum” or semiclassical, nature of the terms. The one-phonon  $\Gamma_{i \rightarrow f}^{\text{Q}1}$  and two-phonon  $\Gamma_{i \rightarrow f}^{\text{Q}2}$  terms in Eq. (21) are “quantum” in the sense that the physical process corresponding to each contribution therein is an interference term between *distinct* scattering channels. In particular, in a “quantum” term, the number of scattering events in the two channels are different. On the contrary, each contribution in  $\Gamma_{i \rightarrow f}^{\text{SC}}$  is the probability amplitude of one given scattering channel, corresponding physically to the probability amplitude of a given scattering process, and in this respect is truly semiclassical. As a semiclassical approximation, we will neglect “quantum” contributions in the following; formal expressions for these terms are nonetheless included in the appendices. The only “semiclassical” contributions, up to  $O(\lambda^4)$ , to the collision integral are from the scattering rates shown in Eq. (36).

Upon applying our results to the case of a staggered antiferromagnet in Sec. V, we focus on the lowest-order contributions to  $K_{nk,n'k'}^L$  and  $K_{nk,n'k'}^H$ , which come from  $D_{nk}^{(1)}$  and  $\mathfrak{W}_{nk,n'k'}^{\ominus,qq'}$ , respectively. Therefore, in Sec. V, we consider only the lowest-order semiclassical contributions  $D_{nk} \approx D_{nk}^{(1)} + \check{D}_{nk}$  and  $\mathfrak{W}_{nk,n'k'}^{\ominus,qq'} \approx \mathfrak{W}_{nk,n'k'}^{\ominus,[1,1];[1,1],qq'}$ .

### 4. Physical interpretation

To leading order, the longitudinal conductivity is controlled by the diagonal scattering rate, whose main contribution occurs at order  $\lambda^2$ . The latter is given as the first term in Eq. (2), and is shown explicitly in Eq. (34). It is related to the Fourier transform of the commutator of two  $Q_{nk}$  operators at unequal times. The commutator structure identifies the phonon scattering rate  $D_{nk}^{(1)}$  with the spectral function of the  $Q_{nk}$  field at energy  $\omega_{nk}$ , i.e. it captures the proportion of the energy density contained in the  $Q_{nk}$  field located at  $\omega_{nk}$ , as expected from (lowest-order) linear response [15, 16].

As mentioned above, the first Born order transition matrices are hermitian. At second Born's order, the advanced/retarded Green's function,  $1/(E_{i/f} - E_m \pm i\eta)$ ,

appearing in  $T_{\mathbf{i} \rightarrow \mathbf{f}}$ , splits into on-shell and off-shell contributions, so that the scattering rate  $\propto |T_{\mathbf{i} \rightarrow \mathbf{f}}|^2$  then involves the product of two on-shell or two-offshell contributions, as well as the products of one on-shell and one off-shell one. Because of complex conjugation of one term upon taking the square modulus of the  $T$  matrix, the scattering rates which involve either two on-shell or two off-shell contributions are blind to the sign of  $\pm i\eta$ , i.e. to the advanced or retarded nature of the process, and enforce a detailed-balance relation, Eq. (27) with  $\sigma = \oplus$ . Therefore, the only scattering rates which can contribute to the Hall conductivity are those involving one on-shell (imaginary part) and one off-shell (real part) scattering event, which translates here into the product of a commutator and an anticommutator, Eq. (37).

#### IV. RELATIONS AND SYMMETRIES

In this section, we explore in more detail some physical relations verified by the scattering rates defined above, and their possible consequences on the longitudinal and Hall conductivities.

##### A. Time-reversal symmetry: reversal of the momenta

$Q$ operators	$\widehat{Q_{n\mathbf{k}}}^q = Q_{n,-\mathbf{k}}^q$
scattering rates	$\widehat{Q_{n\mathbf{k},n'\mathbf{k}'}^{qq'}}^{qq'} = Q_{n-\mathbf{k},n'-\mathbf{k}'}^{qq'}$ $D_{n,\mathbf{k}}^{(1)} = D_{n,-\mathbf{k}}^{(1)}$
conjugate process	$\mathfrak{W}_{n\mathbf{k},n'\mathbf{k}'}^{\sigma,qq'} = \sigma \mathfrak{W}_{n-\mathbf{k},n'-\mathbf{k}'}^{\sigma,qq'}$ $\frac{\mathfrak{W}^\sigma(\text{mr}[S])}{\mathfrak{W}^\sigma(S)} = e^{-\delta E_s^{(S)} \rightarrow p} \frac{\mathfrak{W}^\sigma(\text{pc}[S])}{\mathfrak{W}^\sigma(S)} = \sigma$
kernels	$K_{n\mathbf{k},n'\mathbf{k}'}^H = -K_{n-\mathbf{k},n'-\mathbf{k}'}^H$
conductivities	$\kappa_H = \mathbf{0}$

TABLE I: Relations which hold true in the presence of time-reversal *symmetry*. The phonon operator relation  $\widehat{a_{n\mathbf{k}}^q} = a_{n,-\mathbf{k}}^q$  holds true even when no time-reversal symmetry is present. See text for definitions and justifications.

We investigate the implications of time-reversal (TR) invariance on our results. In particular, we check explicitly that the Hall conductivity vanishes in a TR-symmetric system. It is important to note that, in a time-reversal invariant system, the scattering rates are a priori not time-reversal invariant themselves.

We denote with  $\widehat{Q}$  and  $|\widehat{\mathbf{n}}\rangle$  the time-reversed of operator  $Q$  and of state  $|\mathbf{n}\rangle$ , respectively. Then, because of the antiunitarity of the time-reversal operator, for any states  $\mathbf{n}, \mathbf{m}$  and any operator  $Q$ , we have  $\langle \widehat{\mathbf{n}} | Q^\dagger | \widehat{\mathbf{m}} \rangle = \langle \mathbf{m} | \widehat{Q} | \mathbf{n} \rangle$ .

Moreover, it is possible to choose a polarization index  $n$  invariant under TR, whence  $\widehat{a_{n\mathbf{k}}^q} = a_{n,-\mathbf{k}}^q$ .

Let us now consider what happens in a time-reversal-invariant system. In that case, the hamiltonian  $H'_{[1]} = \sum_{n\mathbf{k}q} Q_{n\mathbf{k}}^q a_{n\mathbf{k}}^q$  must be TR-invariant, so that  $\widehat{Q_{n\mathbf{k}}^q} = Q_{n,-\mathbf{k}}^q$ . Similarly, TR-invariance of  $H'_{[2]}$  (defined in Eq. (16)) entails  $\widehat{Q_{n\mathbf{k},n'\mathbf{k}'}^{qq'}} = Q_{n-\mathbf{k},n'-\mathbf{k}'}^{qq'}$ .

##### 1. Consequences for the scattering rates.

Following the same steps as those sketched in Sec. III D 1, and using the fact that  $E_{\widehat{\mathbf{m}}} = E_{\mathbf{m}}$  for any state  $\mathbf{m}$  of a TR-symmetric system, we can show explicitly that, *in a time-reversal-invariant system*, the following relations for the scattering rates exist:

$$D_{n,\mathbf{k}}^{(1)} = D_{n,-\mathbf{k}}^{(1)} \quad (41)$$

$$\mathfrak{W}_{n\mathbf{k},n'\mathbf{k}'}^{\sigma,qq'} = \sigma \mathfrak{W}_{n-\mathbf{k},n'-\mathbf{k}'}^{\sigma,qq'}. \quad (42)$$

The  $\sigma$  sign in the second relation can be understood as arising from two facts: (1) schematically,  $\mathfrak{W}^\sigma \sim \frac{1}{E_t - E_m + i\eta} \frac{1}{E_t - E_m - i\eta} + \sigma$  h.c. —which is reflected in the fact that  $\mathfrak{W}^\oplus$  (resp.  $\mathfrak{W}^\ominus$ ) expressed as an integral, Eqs. (36–38), contains an even (resp. odd) number of sign functions— and (2) an effect of time-reversal on the  $T$ -matrix is to exchange denominators  $\frac{1}{E_t - E_m + i\eta} \rightarrow \frac{1}{E_t - E_m - i\eta}$  (see Sec. III D 4 for an interpretation of the  $+i\eta$  regularization).

##### 2. Relation to detailed balance.

The decomposition of the scattering rate  $\mathfrak{W}_{n\mathbf{k},n'\mathbf{k}'}^{qq'}$  into odd and even terms under the “conjugation” (in the sense of detailed balance, i.e. thermodynamic equilibrium) of the associated scattering processes, is also that of its decomposition into terms, odd and even under the inversion of momentum, in the presence of time-reversal symmetry. Indeed, if a scattering process  $S = \left( \begin{smallmatrix} q \cdot n\mathbf{k} \\ q' \cdot n'\mathbf{k}' \end{smallmatrix} \right)$  transfers an energy  $\delta E_s^{(S)} = q\omega_{n\mathbf{k}} + q'\omega_{n'\mathbf{k}'}$  to the phonon system, (anti-)detailed balance with the “conjugate process”  $\text{pc}[S] = \left( \begin{smallmatrix} -q \cdot n\mathbf{k} \\ -q' \cdot n'\mathbf{k}' \end{smallmatrix} \right)$  reads  $\mathfrak{W}^\sigma(\text{pc}[S]) = \sigma e^{\delta E_s^{(S)} \rightarrow p} \mathfrak{W}^\sigma(S)$ . Meanwhile, in the presence of time-reversal symmetry, the momentum-reversal symmetry reads  $\mathfrak{W}^\sigma(\text{mr}[S]) = \sigma \mathfrak{W}^\sigma(S)$ , for the “momentum-reversed” process  $\text{mr}[S] = \left( \begin{smallmatrix} q \cdot n-\mathbf{k} \\ q' \cdot n'-\mathbf{k}' \end{smallmatrix} \right)$ . In other words, in a time-reversal invariant system, the scattering rate associated with the process “conjugate” of a given process  $S$  coincides (up to a Boltzmann weight)

with that of its momentum-reversed one:

$$\frac{\mathfrak{W}^\sigma(\text{mr}[S])}{\mathfrak{W}^\sigma(S)} = e^{-\delta E_{s \rightarrow p}^{(S)}} \frac{\mathfrak{W}^\sigma(\text{pc}[S])}{\mathfrak{W}^\sigma(S)} = \sigma. \quad (43)$$

Hence, while  $\sigma$  was defined as signature of the behavior of the scattering rates under “process conjugation,” it is *also* that of momentum reversal in a time-reversal invariant system. [17]

### 3. Consequences for the kernels.

How is this reflected in the kernels  $K^L, K^H$ ? Because the relation  $\mathbf{v}_{n\mathbf{k}} = \nabla_{\mathbf{k}} \omega_{n\mathbf{k}} = -\mathbf{v}_{n, -\mathbf{k}}$  holds, only that component of  $K^{L/H}$  which is even upon reversal of the momenta,  $\mathbf{k}^{(\prime)} \leftrightarrow -\mathbf{k}^{(\prime)}$ , has a non-vanishing contribution to the sum Eq. (13). A first consequence of this is that, in a TR-invariant system, the identity

$$K_{n\mathbf{k}, n'\mathbf{k}'}^H = -K_{n-\mathbf{k}, n'-\mathbf{k}'}^H \quad (44)$$

entails  $\kappa_H = \mathbf{0}$  – as per Onsager’s reciprocity relations stating that  $\kappa_H$  is TR-odd. Note that  $K^L$  in Eq. (30) involves both  $\mathfrak{W}^\ominus$  and  $\mathfrak{W}^\oplus$ . Therefore, there is no analog to Eq. (44) for  $K^L$ . However, in a TR-invariant system, the  $\mathfrak{W}^\ominus$  term in  $K^L$  does not contribute to  $\kappa_L$  – this is consistent with the Onsager-Casimir relations which state that  $\kappa_L$  is TR-even.

This indeed reflects the previous discussion as follows: when time reversal is preserved, TR-even  $\kappa_L$  gets contributions solely from “detailed-balance-even” and TR-even  $\mathfrak{W}^\oplus$ . On the other hand TR-odd  $\kappa_H$  gets contributions solely from “detailed-balance-odd” and TR-odd  $\mathfrak{W}^\ominus$ . Since the system is actually TR-even,  $\kappa_H$  vanishes.

## B. Point-group symmetries

Here we provide some sufficient (but non-necessary) conditions on  $K_{n\mathbf{k}n'\mathbf{k}'}^H$  under which the Hall conductivity vanishes.

### 1. Curie relations

From Fourier’s law  $j^\mu = -\kappa^{\mu\nu} \nabla_\nu T$ , the Curie and Onsager relations provide general constraints on the  $\kappa^{\mu\nu}$  coefficients, and in turn on its Hall component  $\kappa_H^{\mu\nu}$ . In Table II, we look at the  $D_{4h} = D_4 \times \mathbb{Z}_2$  point group—the largest tetragonal point group—with the associated axes aligned with the orthogonal basis  $(\mu, \nu, \rho)$  ( $\mu\nu$  is the basal plane and  $\rho$  the transverse direction). We can see that if the system is invariant under any one of the transformations  $g \in D_{4h}$  which are odd under the  $A_{2g}$  representation (i.e.  $C_2', C_2'', \sigma_v, \sigma_d$ ), the Hall conductivity must vanish.

$D_{4h}$	Id	$C_4$	$C_2$	$C_2'$	$C_2''$	inv	$S_4$	$\sigma_h$	$\sigma_v$	$\sigma_d$
$A_{2g}$	1	1	1	-1	-1	1	1	1	-1	-1
$\mu$	$\mu$	$\nu$	$-\mu$	$\pm\mu$	$\pm\nu$	$-\mu$	$\nu$	$\mu$	$\pm\mu$	$\pm\nu$
$\nu$	$\nu$	$-\mu$	$-\nu$	$\mp\nu$	$\pm\mu$	$-\nu$	$-\mu$	$\nu$	$\mp\nu$	$\pm\mu$
$\rho$	$\rho$	$\rho$	$\rho$	$-\rho$	$-\rho$	$-\rho$	$-\rho$	$-\rho$	$\rho$	$\rho$
$\kappa^{\mu\nu}$	$\kappa^{\mu\nu}$	$-\kappa^{\nu\mu}$	$\kappa^{\mu\nu}$	$-\kappa^{\mu\nu}$	$\kappa^{\nu\mu}$	$\kappa^{\mu\nu}$	$-\kappa^{\nu\mu}$	$\kappa^{\mu\nu}$	$-\kappa^{\mu\nu}$	$\kappa^{\nu\mu}$
$\kappa_H^{\mu\nu}$	$\kappa_H^{\mu\nu}$	$\kappa_H^{\mu\nu}$	$\kappa_H^{\mu\nu}$	$-\kappa_H^{\mu\nu}$	$-\kappa_H^{\mu\nu}$	$\kappa_H^{\mu\nu}$	$\kappa_H^{\mu\nu}$	$\kappa_H^{\mu\nu}$	$-\kappa_H^{\mu\nu}$	$-\kappa_H^{\mu\nu}$
cat	(a)	(d)	(a)	(b)	(c)	(a)	(d)	(a)	(b)	(c)

TABLE II: Elements of the  $D_{4h}$  point group aligned along the  $(\mu, \nu, \rho)$  basis (with  $\mu\nu$  the basal plane), their characters in the  $A_{2g}$  irrep (also labeled  $\Gamma_2^+$ ), and transformations of  $\mu, \nu, \rho, \kappa^{\mu\nu}, \kappa_H^{\mu\nu}$ . The lines for  $\kappa^{\mu\nu}$  and  $\kappa_H^{\mu\nu}$  hold true when the system is invariant under the corresponding  $D_{4h}$  operation (aligned with the  $\mu\nu\rho$  basis). The last line is the “category” (cat) to which the operation belongs, as defined in Sec. IV B 2. Here Id is the identity;  $C_4$  is the  $\pi/2$  rotation around the  $\rho$  axis;  $C_2, C_2'$  and  $C_2''$  are  $\pi$  rotations around the  $\rho$  axis,  $\mu$  or  $\nu$  axes, and in-plane directions bisecting the  $\mu, \nu$  axes, respectively; inv is inversion,  $S_4$  are  $\pi/2$  rotations around the  $\rho$  axis followed by a reflection through the basal  $\mu\nu$  plane;  $\sigma_h, \sigma_v$  and  $\sigma_d$  are reflections through the  $\mu\nu$  plane ( $\sigma_h$ ), through a plane containing  $\mu$  or  $\nu$  and the  $\rho$  direction ( $\sigma_v$ ), and through a plane containing the  $\rho$  direction and one bisecting the  $\mu, \nu$  directions ( $\sigma_d$ ), respectively.

### 2. Symmetry relations on $K^H$

We now turn to relations specific to the scattering situation, i.e. we analyze under which conditions on  $K_{n\mathbf{k}n'\mathbf{k}'}^H$  it befalls that  $\kappa_H^{\mu\nu} = 0$ . We start with the expression of  $\kappa_H^{\mu\nu}$  as a momentum integral, Eq. (13), i.e.  $\kappa_H^{\mu\nu} \propto \sum_{n\mathbf{k}n'\mathbf{k}'} J_{n\mathbf{k}}^\mu J_{n'\mathbf{k}'}^\nu K_{n\mathbf{k}n'\mathbf{k}'}^H$  and recall  $J_{n\mathbf{k}}^\mu = N_{n\mathbf{k}}^{\text{eq}} \omega_{n\mathbf{k}} \partial_{k^\mu} \omega_{n\mathbf{k}}$ .

If the *phonon* system is invariant under a unitary transformation  $g$ , then  $\omega_{n\mathbf{k}}$  is also invariant under this transformation. In turn only  $\mu$  in  $J_{n\mathbf{k}}^\mu$  transforms nontrivially under  $g$ . Therefore:

- If the phonon system is invariant under an operation  $g \in D_{4h}$  which leaves the  $\mu, \nu$  axes invariant, i.e.  $g = C_2, C_2', \text{inv}, \sigma_h, \sigma_v$ , and *if* one of the two following conditions, (a) under  $g$  the  $\mu\nu$  product is even (i.e.  $g = C_2, \text{inv}, \sigma_h$ ) and  $K_{n\mathbf{k}n'\mathbf{k}'}^H$  is odd, (b) under  $g$  the  $\mu\nu$  product is odd (i.e.  $g = C_2', \sigma_v$ ) and  $K_{n\mathbf{k}n'\mathbf{k}'}^H$  is even, is satisfied, *then* it follows that  $\kappa_H^{\mu\nu} = 0$ .
- Besides, recalling that by construction  $K_{n\mathbf{k}n'\mathbf{k}'}^H = -K_{n'\mathbf{k}'n\mathbf{k}}^H$ , *if* the system is invariant under an operation  $g \in D_{4h}$  which exchanges the  $\mu, \nu$  axes, i.e.  $g = C_4, C_2'', S_4, \sigma_d$ , and *if* one of the two following conditions, (c) under  $g$  the  $\mu\nu$  product is even (i.e.

$g = C_2''(\sigma_d)$  and  $K_{n\mathbf{k}n'\mathbf{k}'}^H$  is even, (d) under  $g$  the  $\mu\nu$  product is odd (i.e.  $g = C_4, S_4$ ) and  $K_{n\mathbf{k}n'\mathbf{k}'}^H$  is odd, is satisfied, then it follows that  $\kappa_H^{\mu\nu} = 0$ .

In terms of the behavior of  $K_{n\mathbf{k}n'\mathbf{k}'}^H$ , this analysis reduces to: if  $g \in D_{4h}$  is a symmetry of the phonon system, and if  $g : K_{n\mathbf{k}n'\mathbf{k}'}^H \mapsto -\chi_{A_{2g}}(g)K_{n\mathbf{k}n'\mathbf{k}'}^H$ , where  $\chi_{A_{2g}}(g)$  is the character of  $g$  in the  $A_{2g}$  representation of the  $D_{4h}$  point group, then  $\kappa_H^{\mu\nu} = 0$ . We emphasize that this analysis holds if the transformation  $g$  is a symmetry of the phonon system, and whether or not  $g$  is a symmetry of the whole system. For example, we will show explicitly in Sec. VC4 that there are cases where, under TR or  $\sigma_d$  the system is not invariant, but the kernel  $K_{n\mathbf{k},n'\mathbf{k}'}^H$  and the phonon system are, and so  $\kappa_H = 0$ .

Finally, note that the above analysis goes beyond the general predictions from Onsager, which tell us that  $\kappa_H$  vanishes in the presence of some symmetries of the whole system, namely  $C_2', C_2'', \sigma_v$  or  $\sigma_d$  (as well as time-reversal discussed in the previous subsection). Here, not only do we establish relations for the other symmetries in  $D_{4h}$  (as symmetries of the phonon subsystem only), we also show in which way  $\kappa_H$  vanishes, by inspecting the behavior of the kernels  $K_{n\mathbf{k},n'\mathbf{k}'}^H$  under those symmetry transformations. In turn, this may for example allow to gather information about the system—about  $K_{n\mathbf{k},n'\mathbf{k}'}^H$ —from the (non-)cancellation of  $\kappa_H$ .

## V. APPLICATION TO AN ORDERED MAGNET

We now turn to an application of these general results. There, we keep only the lowest-order terms in the expressions derived above, as described in Sec. IIID4, and we consider an interaction hamiltonian density which contains single-phonon interactions with a field  $Q$  (this is the first term in Eq. (1)) of the form

$$H' = \sum_{n\mathbf{k}} (a_{n\mathbf{k}}^\dagger Q_{n\mathbf{k}}^\dagger + a_{n\mathbf{k}} Q_{n\mathbf{k}}), \quad (45)$$

as obtained from the simplest case of linear coupling to the strain tensor.

We consider an ordered magnetic system, which we take to be a spin-orbit coupled Néel antiferromagnet with tetragonal symmetry. For concreteness, we treat the magnetism as purely two-dimensional, i.e. the full spin+phonon system is described by a stack of two dimensional antiferromagnets embedded into the three-dimension solid, so that in particular, we take, when going from the lattice to the continuum limit

$$\sum_{\mathbf{r}} \rightarrow \frac{1}{\mathbf{a}^2} \sum_z \int d^2x, \quad \sum_{\mathbf{k}} \rightarrow \frac{\mathbf{a}^2}{(2\pi)^2} \sum_{k_z} \int d^2k, \quad (46)$$

where  $\mathbf{a}$  is the in-plane lattice spacing.

## A. Magnon dynamics

### 1. Low-energy field-theoretical description

We consider a Néel antiferromagnet with a two-site magnetic unit cell, more precisely a bipartite lattice of spins such that the classical ground state is ordered in an antiferromagnetic configuration, with a local moment  $\mu_0$  oriented in the direction  $\mathbf{n}$ , i.e.  $\mathbf{n}$  is the Néel vector which has unit length in the ordered state at zero field. Within standard spin-wave theory,  $\mu_0 = S$  with  $S$  the spin value. For concreteness, we will choose the ordering axis at zero field to be aligned along the  $\hat{\mathbf{u}}_x$  axis (the set  $(\hat{\mathbf{u}}_x, \hat{\mathbf{u}}_y, \hat{\mathbf{u}}_z)$  is an orthonormal cartesian basis)—the results of this subsection hold regardless of this choice.

A general low energy spin configuration is described by two continuum fields: the aforementioned Néel vector  $\mathbf{n}(\mathbf{r})$  and a uniform magnetization density  $\mathbf{m}(\mathbf{r})$ , such that

$$\mathbf{S}_{\mathbf{r}} = (-1)^{\mathbf{r}} \mu_0 \mathbf{n}(\mathbf{r}) + \mathbf{a}^2 \mathbf{m}(\mathbf{r}). \quad (47)$$

where  $(-1)^{\mathbf{r}}$  is a sign which alternates between neighboring sites (recall we are considering a Néel antiferromagnet), and both continuum fields are assumed to be slowly-varying relative to the lattice spacing. Here  $\mathbf{a}$  is the 2d lattice spacing. We will assume the non-linear sigma model constraint that the spin length is fixed to  $\mu_0$ , which implies that

$$|\mathbf{n}|^2 + \frac{\mathbf{a}^4}{\mu_0^2} |\mathbf{m}|^2 = 1, \quad \mathbf{m} \cdot \mathbf{n} = 0. \quad (48)$$

The spin wave expansion consists of expanding these fields around the zero field ordered state, i.e.  $\mathbf{n}_{\text{ord}} = \hat{\mathbf{u}}_x, \mathbf{m}_{\text{ord}} = \mathbf{0}$ . To linear order around this state, we take  $\mathbf{n} = \hat{\mathbf{u}}_x + \mathbf{n}$  and  $\mathbf{m} = \mathbf{m}$ , where  $n_x = m_x = 0$ , leaving the remaining degrees of freedom  $n_y, n_z, m_y, m_z$ . In terms of the spins, this gives

$$\mathbf{S}_{\mathbf{r}} = (-1)^{\mathbf{r}} \mu_0 \hat{\mathbf{u}}_x + \sum_{a=y,z} ((-1)^{\mathbf{r}} \mu_0 n_a(\mathbf{r}) + \mathbf{a}^2 m_a(\mathbf{r})) \hat{\mathbf{u}}_a. \quad (49)$$

Because the local moment along the  $\hat{\mathbf{u}}_x$  axis is non-zero, the low energy fields satisfy the commutation relations  $[m_y(\mathbf{r}), n_z(\mathbf{r}')] = -[m_z(\mathbf{r}), n_y(\mathbf{r}')] = -i\delta(\mathbf{r} - \mathbf{r}')$ . The low energy continuum Hamiltonian density for these fields is

$$\mathcal{H}_{\text{NLS}} = \frac{\rho}{2} (|\nabla n_y|^2 + |\nabla n_z|^2) + \frac{1}{2\chi} (m_y^2 + m_z^2) + \sum_{a,b=y,z} \frac{\Gamma_{ab}}{2} n_a n_b, \quad (50)$$

where  $\rho$  is the spin stiffness constant,  $\chi$  is the spin susceptibility,  $\nabla = (\partial_x, \partial_y)$  denotes the in-plane gradient, and the  $\Gamma_{ab}$  are anisotropy coefficients which open a small spin wave gap (see App. F3). For an approximately Heisenberg system with isotropic exchange constant  $J$ ,

we have within spin wave theory that  $\chi^{-1} \approx 4J\mathbf{a}^2$ ,  $\rho \approx 2J\mu_0^2$ , while  $\Gamma_{ab}$  are determined by exchange anisotropies. The choice to normalize  $\mathbf{m}$  as a density while keeping  $\mathbf{n}$  dimensionless ensures that  $m_{y,z}$  fields are just the canonical momenta conjugate to the  $n_{z,y}$  fields, and hence Eq. (50) is just a Hamiltonian density of two free scalar boson fields.

The above description is appropriate to describe the ordered phase of the antiferromagnet, for any value of the spin, provided temperature is low compared to the Néel temperature and any applied magnetic fields are small compared to the saturation field. These conditions are well-satisfied in practice in experiments on many antiferromagnets. Specifically we will be interested in the case with an applied magnetic field perpendicular to the axis of the Néel vector (e.g. along  $z$  or  $y$ , given the choice in Eq. (49)). In general the field induces a non-zero uniform magnetization along its direction, e.g. for a  $z$ -axis field  $\langle m_z \rangle \neq 0$ . Such a “spin flop” configuration is favorable for an antiferromagnet in a field.

## 2. Symmetry considerations

Two symmetries clarify the calculations and provide physical insight. The first is the macroscopic time-reversal symmetry of the zero field state, which is what makes it an *anti*-ferromagnet. Specifically, the system in zero field is invariant under the combination of time-reversal symmetry TR and a translation  $T$ . Under this operation, we see that the continuum fields transform according to

$$\mathcal{T} = \text{TR} \times T : \quad m \rightarrow -m, \quad n \rightarrow n. \quad (51)$$

The presence of a staggered magnetization (with any orientation) does not break this symmetry, but a uniform magnetization does. Note that the *effective* quadratic low energy Hamiltonian, Eq. (50), is invariant under this symmetry. This is true even at non-zero fields, because the low energy Hamiltonian is quadratic. Thus effects of time-reversal symmetry breaking will become evident in terms beyond this form, notably in anharmonic corrections, and in the spin-lattice coupling itself. Specifically, we see that time-reversal symmetry will be effectively broken only by terms involving an odd number of powers of the  $m_a$  fields.

The second important symmetry is one which may be preserved not only by the underlying exchange Hamiltonian and crystal structure, but *also* by the applied field and the spontaneous ordered moments. In particular, the latter breaks the original translational symmetry of the square lattice by a single lattice spacing. However, a symmetry may be retained under such a simultaneous translation composed with a  $C_2$  spin rotation around the field axis. In the presence of spin-orbit coupling, generically the spin rotation must be accompanied by a spatial rotation, and the full combined operation is in fact nothing but a  $C_2$  rotation about an axis passing through the

mid-point of a bond of the square lattice. This of course requires the  $C_2$  rotation in question to be part of the lattice point group. In our problem, this is true when the field is along  $z$  or  $y$  (but not for a general orientation in the  $yz$  plane).

This odd symmetry is important for simplifying the magnon interactions. In particular, if the field axis is along  $z$ , then we see that  $m_z$  and  $n_y$  are both even under this operation, while  $m_y$  and  $n_z$  are odd under it (and vice versa if the field is along  $y$ ). Note that the fields within a canonically conjugate pair transform the same way under this symmetry. We take advantage of these facts in the following. In particular, only  $\Gamma_0 = \Gamma_{yy}$  and  $\Gamma_1 = \Gamma_{zz}$  do not vanish a priori, which ensures that the two valleys ( $\ell = 0, 1$ ) are exactly decoupled.

## 3. External magnetic field

At the lowest order, an applied external magnetic field  $\mathbf{h}$  couples solely to the  $\mathbf{m}$  field; this is already taken into account in Eq. (50) where the  $\mathbf{m}$  fields can acquire a (static) nonzero expectation value due to the spin alignment with the field.

Meanwhile, at higher orders the magnetic field also couples to the  $\mathbf{n}$  field; the main contribution comes from the square, isotropic coupling  $(\mathbf{n} \cdot \mathbf{h})^2$ . Due to the  $C_2$  symmetry around the field axis ( $y$  or  $z$ ), and since first-order terms of the form  $h_a n_b$  are forbidden by translational symmetry, this results in an additional term

$$\mathcal{H}_{\text{field}} = \frac{\chi}{2} \sum_{a=y,z} h_a^2 n_a^2. \quad (52)$$

Note this form is valid only when the field is along the  $y$  or  $z$  axis, not at other angles in the  $y-z$  plane (which would violate the  $C_2$  symmetry). The prefactor  $\chi/2$  is fixed to match the results obtained from microscopic calculations in Ref. [18], and we provide an alternative derivation in App. F3 as well as a more detailed derivation of the full form of the gap from a microscopic XXZ exchange model plus a Zeeman coupling to the field in App. F3.

## 4. Diagonalization

We proceed to diagonalize Eq. (50), supplemented by Eq. (52) following the discussion in Sec. V A 3, by introducing creation and annihilation operators in the standard way for free fields. We use the Fourier convention  $\phi_{\mathbf{k}} = \frac{1}{\sqrt{V}} \int d\mathbf{x} \phi(\mathbf{x}) e^{-i\mathbf{k} \cdot \mathbf{x}}$  for any continuum field



$\phi$ , where  $V$  is the volume of the system. Then

$$\begin{aligned} m_{\mathbf{k}}^y &= \sqrt{\frac{\chi\Omega_{\mathbf{k},0}}{2}} (b_{-\mathbf{k},0} + b_{\mathbf{k},0}^\dagger), \\ n_{\mathbf{k}}^z &= i \frac{1}{\sqrt{2\chi\Omega_{\mathbf{k},0}}} (b_{-\mathbf{k},0} - b_{\mathbf{k},0}^\dagger), \\ m_{\mathbf{k}}^z &= \sqrt{\frac{\chi\Omega_{\mathbf{k},1}}{2}} (b_{-\mathbf{k},1} + b_{\mathbf{k},1}^\dagger), \\ n_{\mathbf{k}}^y &= -i \frac{1}{\sqrt{2\chi\Omega_{\mathbf{k},1}}} (b_{-\mathbf{k},1} - b_{\mathbf{k},1}^\dagger), \end{aligned} \quad (53)$$

where

$$\Omega_{\mathbf{k},\ell} = \sqrt{v_m^2 \mathbf{k}^2 + \Delta_\ell^2}, \quad (54)$$

with  $v_m = \sqrt{\rho/\chi}$ . The magnon gaps depend on the applied (transverse) magnetic field in the form

$$\Delta_\ell = \sqrt{\Gamma_\ell/\chi + h_\ell^2}, \quad (55)$$

with valley index  $\ell = 0, 1$  and where we set  $h_0 = h_y$  and  $h_1 = h_z$ . This reflects the explicit breaking of  $O(3)$  rotational symmetry of the order parameter  $\mathbf{n}$  by the transverse field. With these definitions, we obtain

$$H_{\text{NLS}} + H_{\text{field}} = \sum_{\ell} \sum_{\mathbf{k}} \Omega_{\mathbf{k},\ell} b_{\mathbf{k},\ell}^\dagger b_{\mathbf{k},\ell}. \quad (56)$$

The  $b, b^\dagger$  fields with index  $\ell = 0$  have opposite  $C_2$  eigenvalue to those with  $\ell = 1$ . This guarantees that all terms preserving  $C_2$  symmetry must conserve the two boson flavors modulo 2.

## B. Formal couplings

### 1. Definitions

In general we can expand the operator  $Q_{n\mathbf{k}}$ , which couples to a single phonon, in powers of the magnon operators,

$$\begin{aligned} Q_{n\mathbf{k}}^q &= \sum_{\ell, q_1, z} \mathcal{A}_{\mathbf{k}}^{n, \ell | q_1 q} e^{ik_z z} b_{\ell, \mathbf{k}, z}^{q_1} \\ &+ \frac{1}{\sqrt{N_{\text{uc}}}} \sum_{\substack{\mathbf{p}, \ell, \ell' \\ q_1, q_2, z}} \mathcal{B}_{\mathbf{k}; \mathbf{p}}^{n, \ell_1, \ell_2 | q_1 q_2 q} e^{ik_z z} b_{\ell_1, \mathbf{p} + \frac{q}{2}\mathbf{k}, z}^{q_1} b_{\ell_2, -\mathbf{p} + \frac{q}{2}\mathbf{k}, z}^{q_2}. \end{aligned} \quad (57)$$

Note that while the phonons are three-dimensional excitations, and hence have a three-dimensional momentum  $\mathbf{k}$ , the spin operators (and hence magnons) only have two dimensional momenta. We will make use of the following:  $\mathbf{k} = \mathbf{k} + k_z \hat{\mathbf{u}}_z$ , where  $\mathbf{k}$  is the projection of  $\mathbf{k}$  onto the  $k_z = 0$  plane and  $\hat{\mathbf{u}}_z$  is the unit vector along  $z$ . A phonon is coupled to the sum of spin operators in all layers—we have here introduced the explicit label  $z$  for the layer. Because the spins in different layers are completely uncorrelated, there are however no cross-terms involving  $b$

operators from different layers, and in correlation functions the sums over  $z$  will collapse to independent correlators within each layer, which are all identical to one another. When possible, we will therefore take  $z = 0$  and suppress this index.

The naïve leading term in Eq. (57) is the single magnon one  $\mathcal{A}$ , linear in  $b_{\ell, \mathbf{k}}$  and  $b_{\ell, \mathbf{k}}^\dagger$  operators (notations defined below). This results in a quadratic mixing term in the Hamiltonian, hybridizing phonons and magnons. Being quadratic, it is trivially diagonalized, and has been considered by several authors. Generally, such coupling has little effect except when it is resonant, i.e. near a crossing point of the decoupled magnon and phonon bands. Since such a crossing is highly constrained by momentum and energy matching, it occurs in a narrow region of phase space, if at all, and is likely to be unimportant for transport. It in any case does not give rise to scattering, the focus of this work. We therefore henceforth neglect the  $\mathcal{A}$  contribution.

Non-trivial scattering processes arise from the second order term in the magnon field expansion of  $Q_{n\mathbf{k}}$ , parametrized by  $\mathcal{B}$ . Here as elsewhere we introduce particle-hole indices  $q_1, q_2 \in +, -$ , such that in particular

$$b_{\ell, \mathbf{p}, z}^+ = b_{\ell, \mathbf{p}, z}^\dagger, \quad b_{\ell, \mathbf{p}, z}^- = b_{\ell, -\mathbf{p}, z}. \quad (58)$$

Notice the minus sign in the momentum in the second relation. This means generally that

$$(b_{\ell, \mathbf{p}, z}^q)^\dagger = b_{\ell, -\mathbf{p}, z}^{-q}. \quad (59)$$

To make the coefficients unambiguous, we choose the symmetrized form

$$\mathcal{B}_{\mathbf{k}; \mathbf{p}}^{n, \ell_1, \ell_2 | q_1 q_2 q} = \mathcal{B}_{\mathbf{k}; -\mathbf{p}}^{n, \ell_2, \ell_1 | q_2 q_1 q}. \quad (60)$$

Demanding that  $Q_{n\mathbf{k}}^+ = (Q_{n\mathbf{k}}^-)^\dagger$  implies that

$$\mathcal{B}_{\mathbf{k}; \mathbf{p}}^{n, \ell_1, \ell_2 | q_1 q_2 +} = (\mathcal{B}_{\mathbf{k}; \mathbf{p}}^{n, \ell_2, \ell_1 | -q_2 -q_1 -})^*. \quad (61)$$

If the phonon mode  $n$  which  $Q_{n\mathbf{k}}^q$  is coupled to is  $C_2$  invariant, then only terms with  $\ell_1 = \ell_2$  are non-zero. In Sec. V C 1, we will introduce a concrete and general model of spin-lattice couplings, and see that within this model, almost all interactions obey this selection rule. In particular, off-diagonal terms with  $\ell_1 \neq \ell_2$  arise only from the  $\Lambda_{6,7}^{(\xi)}$  couplings defined in Eq. (70), which are furthermore smaller in magnitude than other couplings as they are related to magnetic anisotropy.

### 2. Diagonal scattering rate

Contributions to the first-order longitudinal scattering rate, Eq. (34), can be computed exactly using Wick's

theorem. To do so we use the free particle two point function, which in the notation of Eq. (58) is

$$\begin{aligned} \langle b_{\ell_1, \mathbf{p}_1, z_1}^{q_1}(t_1) b_{\ell_2, \mathbf{p}_2, z_2}^{q_2}(t_2) \rangle &= \delta_{\ell_1, \ell_2} \delta_{z_1, z_2} \delta_{q_1, -q_2} \delta_{\mathbf{p}_1 + \mathbf{p}_2, \mathbf{0}} \\ &\times f_{q_2}(\Omega_{\ell_1, \mathbf{p}_1}) e^{-iq_2 \Omega_{\ell_2, \mathbf{p}_2} (t_1 - t_2)}, \end{aligned} \quad (62)$$

where  $f_q(\Omega) = (1 + q)/2 + n_B(\Omega)$ , where  $n_B(\Omega)$  is the Bose distribution. One obtains two contributions,  $D_{\mathbf{nk}}^{(1)} = \sum_{s=\pm} D_{\mathbf{nk}}^{(1)s}$ , where  $D^{(1)+}$  corresponds to the emission of two magnons and  $D^{(1)-}$  corresponds to the scattering of a magnon from one state to another:

$$\begin{aligned} D_{\mathbf{nk}}^{(1)+} &= \frac{2\pi}{\hbar^2} \frac{1}{N_{\text{uc}}^{2d}} \sum_{\mathbf{p}, \ell, \ell'} \frac{\sinh(\frac{\beta}{2} \hbar \omega_{\mathbf{nk}})}{\sinh(\frac{\beta}{2} \hbar \Omega_{\ell, \mathbf{p} - \frac{\mathbf{k}}{2}}) \sinh(\frac{\beta}{2} \hbar \Omega_{\ell', -\mathbf{p} - \frac{\mathbf{k}}{2}})} \\ &\times \delta(\omega_{\mathbf{nk}} - \Omega_{\ell, \mathbf{p} - \frac{\mathbf{k}}{2}} - \Omega_{\ell', -\mathbf{p} - \frac{\mathbf{k}}{2}}) \left| \mathcal{B}_{\mathbf{k}; \mathbf{p}}^{n, \ell, \ell' | ++} \right|^2, \end{aligned} \quad (63)$$

and

$$\begin{aligned} D_{\mathbf{nk}}^{(1)-} &= \frac{4\pi}{\hbar^2} \frac{1}{N_{\text{uc}}^{2d}} \sum_{\mathbf{p}, \ell, \ell'} \frac{\sinh(\frac{\beta}{2} \hbar \omega_{\mathbf{nk}})}{\sinh(\frac{\beta}{2} \hbar \Omega_{\ell, \mathbf{p} - \frac{\mathbf{k}}{2}}) \sinh(\frac{\beta}{2} \hbar \Omega_{\ell', \mathbf{p} + \frac{\mathbf{k}}{2}})} \\ &\times \delta(\omega_{\mathbf{nk}} - \Omega_{\ell, \mathbf{p} - \frac{\mathbf{k}}{2}} + \Omega_{\ell', \mathbf{p} + \frac{\mathbf{k}}{2}}) \left| \mathcal{B}_{\mathbf{k}; \mathbf{p}}^{n, \ell, \ell' | +-} \right|^2. \end{aligned} \quad (64)$$

Note that the prefactor involves just the number of two-dimensional unit cells in a single layer,  $N_{\text{uc}}^{2d} = N_{\text{uc}}/N_{\text{layers}}$ , which results because a single sum over  $z$  gives a factor of the number of layers  $N_{\text{layers}}$ , converting the  $N_{\text{uc}}$  to  $N_{\text{uc}}^{2d}$ . One can compare the expressions in Eq. (63) and Eq. (64), and observe a difference of a factor 2 in the prefactor, the sign of the second  $\Omega$  frequency in the delta function, and that of the second to last index

in  $\mathcal{B}$ . The squared modulus  $|\dots|^2$  can be traced back to Fermi's golden rule, and the thermal  $\sinh(\dots)$  factors, which originate from Bose factors, fall off exponentially at large momenta. Energy conservation imposed by the delta functions strongly constrain these scattering rates. Specifically, if all magnons have the same velocity  $v_m$  and the phonons have an isotropic velocity  $v_{\text{ph}}$ , then we find that

$$\begin{aligned} \text{supp}(D_{\mathbf{nk}}^{(1)+}) &\subseteq \{(\mathbf{k}, k_z) | (v_{\text{ph}}^2 - v_m^2) |\mathbf{k}|^2 + v_{\text{ph}}^2 k_z^2 > 4\Delta^2\} \\ \text{supp}(D_{\mathbf{nk}}^{(1)-}) &\subseteq \{(\mathbf{k}, k_z) | (v_{\text{ph}}^2 - v_m^2) |\mathbf{k}|^2 + v_{\text{ph}}^2 k_z^2 < 0\}, \end{aligned} \quad (65)$$

where  $\Delta = \min(\Delta_0, \Delta_1)$  and  $\text{supp}(D)$  is the support of  $D$ . It follows that if  $v_m > v_{\text{ph}}$ ,  $D_{\mathbf{nk}}^{(1)+}$  is non-zero in two regions of large  $|k_z|$  bounded by hyperboloid surfaces tangent to the  $\left\{ \frac{k_z}{|\mathbf{k}|} = \frac{\sqrt{v_m^2 - v_{\text{ph}}^2}}{v_{\text{ph}}} \right\}$  cone, while  $D_{\mathbf{nk}}^{(1)-}$  is non-zero in the region outside the said cone, containing large  $|\mathbf{k}|$ . The two regions are mutually exclusive, i.e. for any given  $\mathbf{k}$  at most one of the two rates is non-zero. For  $v_m < v_{\text{ph}}$ , the constraints are even stronger, and  $D_{\mathbf{nk}}^{(1)-} = 0$  strictly vanishes, while  $D_{\mathbf{nk}}^{(1)+}$  is non-zero within an ellipsoid region containing  $\mathbf{k} = \mathbf{0}$ . The first and second scenarios are realized in  $\text{La}_2\text{CuO}_4$  [19], and in, e.g.,  $\text{FeCl}_2$  [20], respectively.

### 3. Off-diagonal scattering rate

Expanding each  $Q$  operator in terms of magnon operators in the four-point correlations, i.e. plugging in Eq. (57) into Eq. (37), one can obtain the Hall scattering rate using Wick's theorem. We find

$$\begin{aligned} \mathfrak{W}_{\mathbf{nk}, \mathbf{n}'\mathbf{k}'}^{\ominus, qq'} &= \frac{64\pi^2}{\hbar^4} \frac{1}{N_{\text{uc}}^{2d}} \sum_{\mathbf{p}} \sum_{\{\ell_i, q_i\}} \mathfrak{D}_{q\mathbf{k}q'\mathbf{k}', \mathbf{p}}^{nn' | q_1 q_2 q_3, \ell_1 \ell_2 \ell_3} \mathfrak{F}_{q\mathbf{k}q'\mathbf{k}', \mathbf{p}}^{q_1 q_2 q_4, \ell_1 \ell_2 \ell_3} \mathfrak{I} \mathfrak{m} \left\{ \mathcal{B}_{\mathbf{k}, \mathbf{p} + \frac{1}{2} q \mathbf{k} + q' \mathbf{k}'}^{n \ell_3 \ell_2 | q_2 q_3 q} \mathcal{B}_{\mathbf{k}', \mathbf{p} + \frac{1}{2} q' \mathbf{k}'}^{n' \ell_3 \ell_1 | -q_3 q_1 q'} \right. \\ &\times \text{PP} \left[ \frac{\mathcal{B}_{\mathbf{k}, \mathbf{p} + \frac{1}{2} q \mathbf{k}}^{n \ell_1 \ell_4 | -q_1 q_4 - q} \mathcal{B}_{\mathbf{k}', \mathbf{p} + q \mathbf{k} + \frac{1}{2} q' \mathbf{k}'}^{n' \ell_4 \ell_2 | -q_4 - q_2 - q'}}{\Delta_{\mathbf{nk}\mathbf{n}'\mathbf{k}'}^{qq'} + q_1 \Omega_{\mathbf{p}}^{\ell_1, -q_1} - q_2 \Omega_{\mathbf{p} + q \mathbf{k} + q' \mathbf{k}'}^{\ell_2, q_2} - 2q_4 \Omega_{\mathbf{p} + q \mathbf{k}}^{\ell_4, -q_4}} + \frac{\mathcal{B}_{\mathbf{k}', \mathbf{p} + \frac{1}{2} q' \mathbf{k}'}^{n' \ell_1 \ell_4 | -q_1 - q_4 - q'} \mathcal{B}_{\mathbf{k}, \mathbf{p} + \frac{1}{2} q \mathbf{k} + q' \mathbf{k}'}^{n \ell_4 \ell_2 | q_4 - q_2 - q}}{\Delta_{\mathbf{nk}\mathbf{n}'\mathbf{k}'}^{qq'} - q_1 \Omega_{\mathbf{p}}^{\ell_1, -q_1} + q_2 \Omega_{\mathbf{p} + q \mathbf{k} + q' \mathbf{k}'}^{\ell_2, q_2} - 2q_4 \Omega_{\mathbf{p} + q' \mathbf{k}'}^{\ell_4, q_4}} \right] \left. \right\}, \end{aligned} \quad (66)$$

where we defined  $\Omega_{\mathbf{p}}^{\ell, q} = \Omega_{\ell, q\mathbf{p}}$ , and the product of delta functions  $\mathfrak{D}$  and 'thermal factor'  $\mathfrak{F}$

$$\begin{aligned} \mathfrak{D}_{q\mathbf{k}q'\mathbf{k}', \mathbf{p}}^{nn' | q_1 q_2 q_3, \ell_1 \ell_2 \ell_3} &= \delta \left( \Sigma_{\mathbf{nk}\mathbf{n}'\mathbf{k}'}^{qq'} + q_1 \Omega_{\mathbf{p}}^{\ell_1, -q_1} + q_2 \Omega_{\mathbf{p} + q \mathbf{k} + q' \mathbf{k}'}^{\ell_2, q_2} \right) \\ \delta \left( \Delta_{\mathbf{nk}\mathbf{n}'\mathbf{k}'}^{qq'} + 2q_3 \Omega_{\mathbf{p} + q' \mathbf{k}'}^{\ell_3, -q_3} - q_1 \Omega_{\mathbf{p}}^{\ell_1, -q_1} + q_2 \Omega_{\mathbf{p} + q \mathbf{k} + q' \mathbf{k}'}^{\ell_2, q_2} \right), \\ \mathfrak{F}_{q\mathbf{k}q'\mathbf{k}', \mathbf{p}}^{q_1 q_2 q_4, \ell_1 \ell_2 \ell_3} &= q_4 \left( 2n_B(\Omega_{\mathbf{p} + q' \mathbf{k}'}^{\ell_3, -q_3}) + 1 \right) \\ &\left( 2n_B(\Omega_{\mathbf{p}}^{\ell_1, -q_1}) + q_1 + 1 \right) \left( 2n_B(\Omega_{\mathbf{p} + q \mathbf{k} + q' \mathbf{k}'}^{\ell_2, q_2}) + q_2 + 1 \right), \end{aligned} \quad (67)$$

and  $\Sigma_{\mathbf{nk}\mathbf{n}'\mathbf{k}'}^{q, q'} = q\omega_{\mathbf{nk}} + q'\omega_{\mathbf{n}'\mathbf{k}'}$ ,  $\Delta_{\mathbf{nk}\mathbf{n}'\mathbf{k}'}^{q, q'} = q\omega_{\mathbf{nk}} - q'\omega_{\mathbf{n}'\mathbf{k}'}$ . Note that while we described and will use below a continuum formulation of the spin wave theory in Sec. V A, the result in Eq. (66) is actually valid at the lattice level, i.e. when the full periodic band structure of the magnons is included, as it relies only upon the canonical commutation relations of the magnon operators, and their dispersions and couplings are taken completely arbitrary at this stage. Therefore this formula could be applied directly in many other circumstances.

We may understand the terms in Eq. (66) as follows: the second energy conservation delta function comes from Fermi's golden rule; the first delta function, and the denominator in the third line, come from  $\frac{1}{E_i - E_n + i\eta} = \text{PP} \frac{1}{E_i - E_n} - i\pi\delta(E_i - E_n)$ ; while the Bose factors appear when evaluating the thermal averages of magnon population numbers, and their product falls off exponentially at large momenta.  $\mathfrak{W}_{n\mathbf{k}n'\mathbf{k}'}$  may display divergences when the denominator vanishes. One can explicitly check that the detailed balance relation, Eq. (27), holds, using the properties of the  $\mathcal{B}$  coefficients, as well as  $\mathfrak{W}_{n\mathbf{k},n'\mathbf{k}'}^{\ominus,qq'} = \mathfrak{W}_{n'\mathbf{k}',n\mathbf{k}}^{\ominus,q'q}$ .

### C. Phenomenological coupling Hamiltonian

We now propose a symmetry-based phonon-magnon coupling Hamiltonian, Eq. (69), for the low-temperature ordered phase of a Néel antiferromagnet on lattice made of layers of square lattices, and, as above, we consider the layers to be *magnetically* decoupled. Moreover, for concreteness, we take the classical ground state to be Néel antiferromagnetic along the  $\hat{\mathbf{u}}_x$  axis, so that all the point-group symmetries of the crystal are preserved by the magnetic structure, up to a translation of half a magnetic unit cell. [21]

#### 1. Interaction Hamiltonian density

We consider the most general coupling between (1) the strain tensor,  $\mathcal{E}^{\alpha\beta} = \frac{1}{2}(\partial^\alpha u^\beta + \partial^\beta u^\alpha)$ , where  $\mathbf{u}$  is the lattice displacement field, and (2) spin bilinears in terms of the  $\mathbf{m}, \mathbf{n}$  fields, allowed by the symmetries of our tetragonal crystal in its paramagnetic phase, which has the largest symmetry group provided by the crystal structure (generated by mirror symmetries  $\mathcal{S}_x, \mathcal{S}_y, \mathcal{S}_z$ , fourfold rotational symmetry  $\mathcal{C}_4^{xy}$ , translation and time-reversal). Since we treat the magnetism as two dimensional, the coupling Hamiltonian is a sum over layers and an integral over two dimensional space,

$$H'_{\text{tetra}} = \sum_z \int d^2\mathbf{x} \mathcal{H}'_{\text{tetra}}(\mathbf{r}). \quad (68)$$

We use  $\mathbf{r} = (\mathbf{x}, z)$  to denote the three-dimensional coordinate. The corresponding local hamiltonian density reads, with all fields expressed in real space:

$$\mathcal{H}'_{\text{tetra}}(\mathbf{r}) = \sum_{\substack{\alpha,\beta \\ a,b=x,y,z}} \mathcal{E}_r^{\alpha\beta} \left( \Lambda_{ab}^{(n),\alpha\beta} n_a n_b + \frac{\Lambda_{ab}^{(m),\alpha\beta}}{n_0^2} m_a m_b \right) \Big|_{\mathbf{x},z}, \quad (69)$$

where  $n_0 = \mu_0/a^2$  is the ordered moment density. Here each  $\Lambda^{(\xi)}$  tensor, which we define to be symmetric in both

$ab$  and  $\alpha\beta$  variables, has seven independent coefficients, which we call

$$\begin{aligned} \Lambda_1^{(\xi)} &= \Lambda_{xx}^{(\xi),xx} = \Lambda_{yy}^{(\xi),yy}, \\ \Lambda_2^{(\xi)} &= \Lambda_{yy}^{(\xi),xx} = \Lambda_{xx}^{(\xi),yy}, \\ \Lambda_3^{(\xi)} &= \Lambda_{zz}^{(\xi),xx} = \Lambda_{zz}^{(\xi),yy}, \\ \Lambda_4^{(\xi)} &= \Lambda_{xx}^{(\xi),zz} = \Lambda_{yy}^{(\xi),zz}, \\ \Lambda_5^{(\xi)} &= \Lambda_{zz}^{(\xi),zz}, \\ \Lambda_6^{(\xi)} &= \Lambda_{xy}^{(\xi),xy} = \Lambda_{xy}^{(\xi),yx} = \Lambda_{yx}^{(\xi),yx} = \Lambda_{yx}^{(\xi),xy}, \\ \Lambda_7^{(\xi)} &= \Lambda_{xz}^{(\xi),xz} = \Lambda_{xz}^{(\xi),zx} = \Lambda_{zx}^{(\xi),zx} = \Lambda_{zx}^{(\xi),xz}, \\ &= \Lambda_{yz}^{(\xi),yz} = \Lambda_{yz}^{(\xi),zy} = \Lambda_{zy}^{(\xi),zy} = \Lambda_{zy}^{(\xi),yz}, \end{aligned} \quad (70)$$

and all other  $\Lambda_{ab}^{(\xi),\alpha\beta}$  are zero.

In Appendix F 1, we provide a microscopic derivation of these coupling constants starting from a spin hamiltonian  $H_{\text{spin}} = \sum_{\mathbf{r},\mathbf{r}'} S_{\mathbf{r}}^a J^{ab}(\mathbf{r} - \mathbf{r}') S_{\mathbf{r}'}^b$  on the *distorted* lattice, with  $\tilde{\mathbf{r}} = \mathbf{r} + \mathbf{u}(\mathbf{r})$  ( $J^{ab}$  is the exchange parameter between the  $a$  and  $b$  spin components, and depends a priori exponentially on the distance between the two sites). Expanding of the magnetic exchange at linear order in the displacement  $\mathbf{u}(\mathbf{r})$  (away from the position  $\mathbf{r}$  of the atoms in the absence of a phonon) results in a magnetoelastic coupling of the form Eq. (69), with coefficients  $\Lambda_{ab}^{(\xi),\alpha\beta}$  expressed in terms of spatial derivatives of the magnetic exchange  $J^{ab}$ .

Within this microscopic approach  $\Lambda_{6,7}^{(\xi)}$  are related to the spatial derivatives of symmetric off-diagonal exchange  $J^{xy}, J^{xz}, J^{yz}$ , while  $\Lambda_{1,2}^{(\xi)} - \Lambda_3^{(\xi)}$  and  $\Lambda_4^{(\xi)} - \Lambda_5^{(\xi)}$  are associated with the spatial derivatives of XXZ exchange anisotropy  $J^{xx,yy} - J^{zz}$ . Finally, note that in Eq. (69) bilinears of the  $m_a n_b$  kind, arising from e.g. alternating DM interactions  $J_{ij}^D$  i.e. such that  $J_{\mathbf{r},\mathbf{r}+\hat{\mathbf{u}}_a}^D = -J_{\mathbf{r}-\hat{\mathbf{u}}_a,\mathbf{r}}^D$  with  $a = x, y$ , could also contribute to the thermal Hall conductivity [22], but are not allowed in the single-site (paramagnetic) Bravais lattice we consider here.

#### 2. Expansion

We now carry out an expansion of the  $\mathbf{m}, \mathbf{n}$  fields in two steps. First we expand around the *zero-field, zero-net-magnetization* Néel-ordered configuration ( $\mathbf{n}_{\text{ord}} = \hat{\mathbf{u}}_x, \mathbf{m}_{\text{ord}} = \mathbf{0}$ ), assuming deviations are small and satisfy Eq. (48). One thereby expresses  $n_x$  and  $m_x$  in terms of the free fields  $m_{y/z}, n_{y/z}$  as, in real space:

$$\begin{aligned} n_x &= 1 - \frac{1}{2} \sum_{b=y,z} \left( n_b^2 + \frac{1}{n_0^2} m_b^2 \right), \\ m_x &= - \sum_{b=y,z} m_b n_b, \end{aligned} \quad (71)$$

which are correct to second order in the free fields (this constitutes a non-linear correction to Eq. (49)). In a second step, we include a net magnetization and expand  $\vec{\mathbf{n}}$

around it, i.e. write  $\mathbf{m}^\alpha = m_0^\alpha + m^\alpha$  where  $m_0^\alpha$  is the sum of both a possible spontaneous magnetization and response to the external magnetic field. This two-step expansion physically assumes  $m \ll m_0 \ll n_0$ . Using these forms in Eq. (69), we obtain the spin-lattice coupling to second order in the free field fluctuations:

$$\mathcal{H}'_{\text{tetra}}(\mathbf{r}) \approx \sum_{\alpha\beta} \mathcal{E}_{\mathbf{r}}^{\alpha\beta} \sum_{a,b=y,z} \sum_{\xi,\xi'=0,1} \lambda_{ab;\xi\xi'}^{\alpha\beta} n_0^{-\xi-\xi'} \eta_{a\xi\mathbf{r}} \eta_{b\xi'\mathbf{r}}, \quad (72)$$

where  $\eta_{a0} = n_a$  and  $\eta_{a1} = m_a$  and with

$$\begin{aligned} \lambda_{ab;\xi\xi'}^{\alpha\beta} &= \Lambda_{ab}^{(\xi),\alpha\beta} - \delta_{ab} \Lambda_{xx}^{(0),\alpha\beta}, \\ \lambda_{ab;01}^{\alpha\beta} &= \lambda_{ba;10}^{\alpha\beta} = \frac{-1}{n_0} \left[ m_0^a \Lambda_{bx}^{(1),\alpha\beta} + \delta_{ab} m_0^{\bar{a}} \Lambda_{ax}^{(1),\alpha\beta} + m_0^b \Lambda_{ax}^{(0),\alpha\beta} \right], \end{aligned} \quad (73)$$

with

where  $\bar{y} = z$ ,  $\bar{z} = y$  and we have associated  $\xi = n \Leftrightarrow \xi = 0$  and  $\xi = m \Leftrightarrow \xi = 1$  in  $\Lambda^{(\xi)}$ .

These relations are satisfied for any  $\Lambda_{ab}^{(\xi),\alpha\beta}$  in Eq. (69) (i.e. not necessarily satisfying the constraints Eq. (70)), but do assume a Néel moment along the  $x$  direction, and a net moment in the  $yz$  plane. Note that, while the bare (not linearized) interactions in Eq. (69) did not couple the  $n_a$  and  $m_b$  fields, such a coupling is present in the linearized  $\lambda_{ab;01}$  coefficient (i.e. that coupling  $n_a$  and  $m_b$ ). We can see immediately from Eq. (73) that this coupling vanishes in the absence of “anisotropic” couplings  $\Lambda_{6,7}^{(\xi)}$ . Importantly, it also vanishes in the absence of any uniform magnetization. This is a consequence of macroscopic time-reversal symmetry, Eq. (51). Conversely,  $\lambda_{ab;01}$  is the *only* term in our low energy description of the coupled spin-lattice system which is odd under this effective time-reversal symmetry. Consequently, time-reversal odd effects like skew scattering *must* involve

at least one factor of this coupling. This will appear explicitly at the end of the next subsection.

### 3. In terms of the eigenbosons, $b, b^\dagger$

We now seek to identify the  $\mathcal{B}$  coefficients as defined in Eq. (57) (with the convention Eq. (58)). To do so, we use the Eq. (53) representation of the  $m_a, n_a$  fields in terms of the  $b$  bosons, which diagonalize the pure magnetic Hamiltonian, and plug in their expressions into Eq. (72). This involves a unitary transformation which can be defined as (using  $a = 1 \Leftrightarrow a = y$  and  $a = 2 \Leftrightarrow a = z$ )

$$\eta_{a\xi\mathbf{r}} = \sum_{\mathbf{p}} \sum_{\ell=0,1} \sum_{q=\pm} U_{a\xi\ell q}(\mathbf{p}) b_{\ell\mathbf{p}}^q e^{i\mathbf{p}\cdot\mathbf{r}}, \quad (74)$$

$$U_{a\xi\ell q}(\mathbf{p}) = -\delta_{a-1,\ell-\bar{\xi} \bmod 2} F_{\xi q\ell}(\mathbf{p}), \quad (75)$$

$$F_{\xi q\ell}(\mathbf{p}) = (iq)^{\bar{\xi}} (-1)^{\bar{\xi}\ell} (\chi\Omega_{\ell\mathbf{p}})^{\xi-\frac{1}{2}}. \quad (76)$$

We defined  $\bar{\xi} = 1 - \xi$ , i.e.  $\bar{0} = 1, \bar{1} = 0$ , and  $\tilde{\xi} = 2\xi - 1$ , i.e.  $\tilde{0} = -1, \tilde{1} = 1$ . We also used relation for the valley  $\ell = \delta_{a-1,\xi}$ , and conversely  $a = 1 + \xi\ell + \bar{\xi}$ . Now inserting this expression into Eq. (72), and collapsing the  $a, b$  sums, we obtain

$$\begin{aligned} \mathcal{H}'_{\text{tetra}} &= \sum_{\alpha\beta} \sum_{\mathbf{p}_1, \mathbf{p}_2} \mathcal{E}_{\mathbf{r}}^{\alpha\beta} \sum_{q_1 q_2} \sum_{\ell_1 \ell_2=0,1} \sum_{\xi\xi'=0,1} n_0^{-\xi-\xi'} \lambda_{\ell_1-\bar{\xi}, \ell_2-\bar{\xi}'; \xi\xi'}^{\alpha\beta} \\ &F_{\xi q_1 \ell_1}(\mathbf{p}_1) F_{\xi' q_2 \ell_2}(\mathbf{p}_2) b_{\ell_1 \mathbf{p}_1}^{q_1} b_{\ell_2 \mathbf{p}_2}^{q_2} e^{i(\mathbf{p}_1 + \mathbf{p}_2)\cdot\mathbf{r}}. \end{aligned} \quad (77)$$

We similarly express the local strain in terms of its constituent Fourier modes, which are proportional to the phonon creation/annihilation operators, as discussed in detail in Appendix A. Putting in these two ingredients, some algebra (shown also in Appendix A) finally yields, if we define  $\hat{\lambda}_{\xi\xi'}^{\ell\ell';\alpha\beta} = \lambda_{\ell-\bar{\xi} \bmod 2, \ell'-\bar{\xi}' \bmod 2; \xi\xi'}^{\alpha\beta}$ ,

$$\mathcal{B}_{\mathbf{k};\mathbf{p}}^{n,\ell_1\ell_2|q_1q_2q} = \frac{iq}{2\sqrt{2M_{\text{uc}}}} \sum_{\xi\xi'} n_0^{-\xi-\xi'} \mathcal{L}_{\mathbf{nk};\xi\xi'}^{q,\ell_1,\ell_2} F_{\xi q_1 \ell_1} \left( \mathbf{p} + \frac{q}{2}\mathbf{k} \right) F_{\xi' q_2 \ell_2} \left( -\mathbf{p} + \frac{q}{2}\mathbf{k} \right) \quad (78)$$

where

$$\mathcal{L}_{\mathbf{nk};\xi\xi'}^{q,\ell_1,\ell_2} = \sum_{\alpha,\beta=x,y,z} \hat{\lambda}_{\xi\xi'}^{\ell_1\ell_2;\alpha\beta} \frac{k^\alpha (\varepsilon_{\mathbf{nk}}^\beta)^q + k^\beta (\varepsilon_{\mathbf{nk}}^\alpha)^q}{\sqrt{\omega_{\mathbf{nk}}}}. \quad (79)$$

Eq. (78) may now be inserted into Eq. (66). Note that  $i\bar{\xi}$  in  $F$  plays an important role as discussed in Sec. V C 4.

Finally, note that the only coefficients  $\lambda_{ab,\xi\xi'}$  which contribute to  $\mathcal{B}^{\ell_1\ell_2}$  with  $\ell_1 \neq \ell_2$  (i.e. to “intervalley hopping” recalling  $\mathcal{B}^{\ell_1\ell_2}$  is the coefficient of  $b_{\ell_1}^{q_1} b_{\ell_2}^{q_2}$  in  $Q^q$ ) are those which satisfy  $\delta_{ab} + \delta_{\xi\xi'} = 1$ —see App. F 2

for details. Such coefficients involve only the  $\Lambda_{6,7}^{(\xi)}$  couplings, which are typically much smaller than  $\Lambda_{1..5}^{(\xi)}$ . Therefore a good approximation is to consider only those contributions to the scattering rates Eqs. (63,64,66) with the smallest possible number of intervalley hoppings. Now, the forms  $D^{(1)} \sim \mathcal{B}^{\ell_1\ell_2} \mathcal{B}^{\ell_2\ell_1}$  and  $\mathfrak{W}^\ominus \sim \mathcal{B}^{\ell_1\ell_2} \mathcal{B}^{\ell_2\ell_3} \mathcal{B}^{\ell_3\ell_4} \mathcal{B}^{\ell_4\ell_1}$  impose that intervalley hopping can only happen an even number of times in  $D^{(1)}$  and  $\mathfrak{W}^\ominus$ . Because  $D_{\mathbf{nk}}^{(1)}$  is a priori nonzero even when  $\Lambda_{6,7} = 0$ , we discard the subdominant, of order  $\left(\frac{\Lambda_{6,7}}{\Lambda_{1..5}}\right)^2$ , contributions

from  $\ell_1 \neq \ell_2$  upon calculating  $D_{n\mathbf{k}}^{(1)}$ . On the other hand, a nonzero

$$\mathfrak{W}_{n\mathbf{k},n'\mathbf{k}'}^{\ominus,\text{eff},qq'} := \frac{1}{2} \left( \mathfrak{W}_{n\mathbf{k},n'\mathbf{k}'}^{\ominus,qq'} + \mathfrak{W}_{n-\mathbf{k},n'-\mathbf{k}'}^{\ominus,qq'} \right) \quad (80)$$

requires either (or both) nonzero  $\Lambda_{6,7}$ . The first nonzero term with  $\ell_1 = \ell_2 = \ell_3 = \ell_4$  in turn occurs at order  $\left(\frac{\Lambda_{6,7}}{\Lambda_{1..5}}\right)^1$ , and therefore corrections due to  $\ell_i \neq \ell_j$  are another order  $\left(\frac{\Lambda_{6,7}}{\Lambda_{1..5}}\right)^1$  smaller for  $\mathfrak{W}_{n\mathbf{k},n'\mathbf{k}'}^{\ominus,\text{eff},qq'}$ . We use this approximation in what follows, i.e. in Secs. VD and VF.

#### 4. Effective breaking of symmetries

(i). *Time reversal.* We now briefly comment on the relation between the “effective” time-reversal of the spin system  $\mathcal{T}$  and the transport properties of the phonon system. Indeed, it is obvious from Eqs. (63) and Eq. (66) that if all the  $\mathcal{B}$  coefficients satisfy

$$\mathcal{B}_{-\mathbf{k};-\mathbf{p}}^{n,\ell_1\ell_2|q_1q_2q} \stackrel{?}{=} \left( \mathcal{B}_{\mathbf{k};\mathbf{p}}^{n,\ell_1\ell_2|q_1q_2q} \right)^*, \quad (81)$$

then  $D_{n-\mathbf{k}}^{(1)} = D_{n\mathbf{k}}^{(1)}$  and  $\mathfrak{W}_{n-\mathbf{k},n'-\mathbf{k}'}^{\ominus,qq'} = -\mathfrak{W}_{n\mathbf{k},n'\mathbf{k}'}^{\ominus,qq'}$ , i.e. the phonon collision integral is effectively time-reversal symmetry preserving, as discussed in Sec. IV A. Therefore, no phonon Hall effect follows if the spin-phonon coupling satisfies Eq. (81).

Which terms in Eq. (72) are compatible with an effective time-reversal symmetry breaking? By direct inspection of Eq. (79), one finds that  $i\mathcal{L}_{n-\mathbf{k};\xi,\xi'}^{q,\ell_1,\ell_2} = \left( i\mathcal{L}_{n\mathbf{k};\xi,\xi'}^{q,\ell_1,\ell_2} \right)^*$ . Thus, only those terms in Eq. (78) with  $i^{\bar{\xi}+\xi'} = i$  may satisfy  $\mathcal{B}_{-\mathbf{k};-\mathbf{p}}^{n,\ell_1\ell_2|q_1q_2q} \neq \left( \mathcal{B}_{\mathbf{k};\mathbf{p}}^{n,\ell_1\ell_2|q_1q_2q} \right)^*$ . All others are such that  $\mathcal{B}_{-\mathbf{k};-\mathbf{p}}^{n,\ell_1\ell_2|q_1q_2q} = \left( \mathcal{B}_{\mathbf{k};\mathbf{p}}^{n,\ell_1\ell_2|q_1q_2q} \right)^*$ .

The breaking of effective time-reversal in the phonon system thus relies upon the presence of spin-phonon couplings where  $\xi' = \bar{\xi}$ , i.e.  $\lambda_{ab,01}$  and  $\lambda_{ab,10}$  (henceforth denoted “ $\lambda_{nm}$ ”) coefficients; this is consistent with the argument in Sec. VC2, based on macroscopic time-reversal  $\mathcal{T}$ , Eq. (51). Moreover, going back to Sec. IV B2, we see that if  $\mathbf{m}_0 \neq \mathbf{0}$  but  $\Lambda_6^{(\xi)} = 0 = \Lambda_7^{(\xi)}$ , then the kernel  $K_{n\mathbf{k},n'\mathbf{k}'}^H$  is invariant under momentum reversal; and so  $\kappa_H = 0$ , even though the system breaks  $\mathcal{T}$ .

(ii).  *$\sigma_d$  operation.* Here we briefly study the  $\sigma_d$  operation, i.e. a mirror transformation through the plane containing the  $\hat{z}$  and  $\frac{\hat{x}+\hat{y}}{\sqrt{2}}$  directions. The system, having antiferromagnetic ordering along the  $x$  axis as well as possibly  $m_0^y \neq 0$ , explicitly breaks this symmetry. However, if  $\Lambda_1^{(\xi)} = \Lambda_2^{(\xi)}$  and  $\Lambda_7^{(\xi)} = 0$ , then  $\sigma_d$  is preserved at the level of the kernel  $K_{n\mathbf{k},n'\mathbf{k}'}^H$ , whence  $\kappa_H = 0$ . This illustrates the importance of knowing the action of  $D_{4h}$  operations upon the kernels  $K_{n\mathbf{k},n'\mathbf{k}'}^H$ , because some symmetries which are explicitly broken globally might fail to be effectively broken in phonon scattering.

## D. Solutions of the delta functions

Each contribution to the scattering rate involves a momentum integral over an integrand which contains either a single delta function or a product of two delta functions. These express energy conservation constraints, which must be solved to carry out the integration. The argument of each delta function, which must be set to zero, is of the form

$$\varpi - \Omega_{\ell,\mathbf{p}} - s\Omega_{\ell,\mathbf{p}-\mathbf{k}} = 0, \quad (82)$$

where  $s = \pm 1$ . Using the continuum form of the magnon dispersion,  $\Omega_{\ell,\mathbf{p}} = \sqrt{v_m^2|\mathbf{p}|^2 + \Delta_\ell^2} = v_m\sqrt{|\mathbf{p}|^2 + \delta_\ell^2} = v_m\hat{\Omega}_{\ell,\mathbf{p}}$ , where  $\delta_\ell = \Delta_\ell/v_m$ , we can rewrite this as

$$\sqrt{|\mathbf{p}|^2 + \delta_\ell^2} + s\sqrt{|\mathbf{p}-\mathbf{k}|^2 + \delta_\ell^2} = a, \quad (83)$$

where  $a = \varpi/v_m$  and  $s = \pm 1$ .

The existence and type of solutions depend on the value of  $a^2 - \underline{k}^2$ , where  $\underline{k}^2 = k_x^2 + k_y^2$ . When they exist, the solutions are conics, as is summarized in Table III.

	$a^2 - \underline{k}^2 < 0$	$0 < a^2 - \underline{k}^2 < 4\delta_\ell^2$	$4\delta_\ell^2 < a^2 - \underline{k}^2$
$s = +$	no solutions	no solutions	ellipse
$s = -$	half-hyperbola	no solutions	no solutions

TABLE III: Solutions to a single delta function of the form  $\delta(\varpi - \Omega_{\ell,\mathbf{p}} - s\Omega_{\ell,\mathbf{p}-\mathbf{k}})$ , with  $s = \pm 1$ , as a function of the value of  $a^2 - \underline{k}^2$ , where  $a = \varpi/v_m$ ,  $\underline{k}^2 = k_x^2 + k_y^2$ , and  $\Omega_{\ell,\mathbf{p}} = v_m\sqrt{|\mathbf{p}|^2 + \delta_\ell^2}$ . The necessary existence conditions described in this Table are captured by the equation  $s(a^2 - \underline{k}^2) > 4\delta_\ell^2(s+1)/2$ .

It is then best to introduce coordinates  $p_{\parallel}, p_{\perp}$  which are along the principal axes of the hyperbola/ellipse:

$$\mathbf{p} = p_{\parallel}\hat{\mathbf{k}} + p_{\perp}\hat{\mathbf{z}} \times \hat{\mathbf{k}}, \quad (84)$$

where we define  $\hat{\mathbf{k}} = (k_x\hat{\mathbf{x}} + k_y\hat{\mathbf{y}})/\underline{k}$  (note the denominator  $\underline{k}$  which differs from  $k$  when  $k_z \neq 0$ ), and we can define the major  $\bar{a}$  and minor  $\bar{b}$  semi-axes, or conversely, of the conics:

$$\bar{a} = \frac{|a|}{2} \sqrt{1 - \frac{4\delta_\ell^2}{a^2 - \underline{k}^2}}, \quad \bar{b} = \frac{1}{2} \sqrt{|a^2 - \underline{k}^2 - \delta_\ell^2|}. \quad (85)$$

An immediate consequence is that, in the case of the ellipse  $-\bar{a} \leq p_{\parallel} - \frac{k}{2} \leq \bar{a}$  and  $-\bar{b} \leq p_{\perp} \leq \bar{b}$ , while in the case of the half-hyperbola:  $p_{\parallel} \geq \frac{k}{2} + \bar{a}$ .

Both Eq. (83) and a pair of such equations may be solved analytically, but the solutions are analytically complicated. We provide their details in Appendix E1, and give here only the final results.

## 1. Diagonal scattering rate

We have, in particular, the following compact form for  $D_{\mathbf{nk}}^{(1)|s}$ , with  $s = \pm$ ,

$$D_{\mathbf{nk}}^{(1)|s} = \frac{(3-s)\pi\mathbf{a}^2}{(2\pi)^2\hbar^2} \sum_{\ell,\ell'} \int d^2\mathbf{p} \frac{\sinh(\frac{\beta}{2}\hbar\omega_{\mathbf{nk}})}{\sinh(\frac{\beta}{2}\hbar\Omega_{\ell,\mathbf{p}}) \sinh(\frac{\beta}{2}\hbar\Omega_{\ell',\mathbf{p}-\mathbf{k}})} \delta(\omega_{\mathbf{nk}} - \Omega_{\ell,\mathbf{p}} - s\Omega_{\ell',\mathbf{p}-\mathbf{k}}) \left| \mathcal{B}_{\mathbf{k};-\mathbf{p}+\frac{\mathbf{k}}{2}}^{n,\ell,\ell'+s-} \right|^2, \quad (86)$$

where we converted the *two-dimensional* momentum sum to an integral using  $\sum_{\mathbf{p}} \rightarrow N_{\text{uc}}^{2\text{d}} \mathbf{a}^2 \int \frac{d^2\mathbf{p}}{(2\pi)^2}$ , where  $N_{\text{uc}}^{2\text{d}} \mathbf{a}^2$  is the area of the sample in the  $xy$  plane.

From now on, in this paragraph and the following, we make use of the approximation  $\mathcal{B}^{\ell \neq \ell'} \rightarrow 0$ , as explained previously. Then, collapsing the delta function (to avoid clutter, we identify  $y = p_{\perp}$ ):

$$D_{\mathbf{nk}}^{(1)|s} = \frac{(3-s)\mathbf{a}^2 \sinh(\frac{\beta}{2}\hbar\omega_{\mathbf{nk}})}{4\pi v_{\text{m}} \hbar^2} \int_{-\infty}^{+\infty} dy \sum_{\eta} f_{\eta}^s(y) J_{\eta}^s(y) \sum_{\ell} \frac{\left| \mathcal{B}_{\mathbf{k};-\mathbf{p}_{\ell,\mathbf{k}}^{(\eta)}(y)+\frac{\mathbf{k}}{2}}^{n,\ell,\ell'+s-} \right|^2}{\sinh(\frac{\beta}{2}\hbar\Omega_{\ell,\mathbf{p}_{\ell,\mathbf{k}}^{(\eta)}(y)}) \sinh(\frac{\beta}{2}\hbar\Omega_{\ell,\mathbf{p}_{\ell,\mathbf{k}}^{(\eta)}(y)-\mathbf{k}})}, \quad (87)$$

where

$$\begin{cases} f_{\eta}^{s=1}(y) = \Theta(\bar{b} - |y|) \Theta(a^2 - \underline{k}^2 - 4\delta_{\ell}^2) \\ f_{\eta}^{s=-1}(y) = \delta_{\eta,1} \Theta(\underline{k}^2 - a^2) \end{cases}, \quad (88)$$

where  $a = \omega_{\mathbf{nk}}/v_{\text{m}}$ ,  $\eta = \pm 1$  and

$$J_D^s(y) = \left| \sum_{r=\pm} \frac{s^{(r-1)/2} r c_r(y)}{\sqrt{c_r(y)^2 + y^2 + \delta_{\ell}^2}} \right|^{-1}, \quad (89)$$

with

$$c_{\eta}(y) = \frac{1}{2} \left( \underline{k} + \eta a \sqrt{1 - 4 \frac{\delta_{\ell}^2 + y^2}{a^2 - \underline{k}^2}} \right), \quad (90)$$

and

$$\mathbf{p}_{\ell,\mathbf{k}}^{(\eta)}(y) = c_{\eta}(y) \hat{\mathbf{k}} + y \hat{\mathbf{z}} \times \hat{\mathbf{k}}, \quad (91)$$

i.e. we identified  $p_{\parallel}$  and  $p_{\perp}$  in Eq. (84) with  $c_{\eta}(y)$  and  $y$ , respectively. At this point it may be comforting to check dimensions. Noting that  $y$  has dimensions of momentum, i.e. inverse length, and  $\mathcal{B}$  has dimensions of energy, i.e. inverse time, one can indeed see that  $D$  in Eq. (87) has proper dimensions of a rate.

## 2. Off-diagonal scattering rate

In this case, we must solve a *pair* of conic equations simultaneously, which takes the form:

$$\begin{cases} \varpi_1 - \Omega_{\ell,\mathbf{p}} - s_1 \Omega_{\ell,\mathbf{p}-\mathbf{k}_1} = 0 \\ \varpi_2 - \Omega_{\ell,\mathbf{p}} - s_2 \Omega_{\ell,\mathbf{p}-\mathbf{k}_2} = 0, \end{cases} \quad (92)$$

i.e.

$$\begin{cases} \sqrt{|\underline{\mathbf{p}}|^2 + \delta_{\ell}^2} + s_1 \sqrt{|\underline{\mathbf{p}} - \underline{\mathbf{k}}_1|^2 + \delta_{\ell}^2} = a_1 \\ \sqrt{|\underline{\mathbf{p}}|^2 + \delta_{\ell}^2} + s_2 \sqrt{|\underline{\mathbf{p}} - \underline{\mathbf{k}}_2|^2 + \delta_{\ell}^2} = a_2, \end{cases} \quad (93)$$

where  $a_i = \varpi_i/v_{\text{m}}$ . Indeed, the integrals which occur in the second order scattering rates involve pairs of delta functions, whose arguments are of the form considered above, with in Eq. (92),  $\varpi_1 = -q_1 \Sigma_{\mathbf{nk}_1 \mathbf{n}'\mathbf{k}'}^{qq'}$ ,  $\varpi_2 = -q_1 q' \omega_{\mathbf{n}'\mathbf{k}'}$ ,  $s_1 = q_1 q_2$ ,  $s_2 = -q_1 q_3$ ,  $\mathbf{k}_1 = -q \mathbf{k} - q' \mathbf{k}'$ ,  $\mathbf{k}_2 = -q' \mathbf{k}'$ ,  $\delta_{\ell} = \Delta_{\ell}/v_{\text{m}}$ . In this case, each of the two delta function constraints defines a half-hyperbola or an ellipse in the  $\mathbf{p}$  plane, and the integrand is confined to the intersections of these two curves. Consequently, the integral will be collapsed to a discrete set of points. It is straightforward to see geometrically that the intersection of two curves of these types is, except for the degenerate cases in which the two curves are identical, a set of at most four points. The two simultaneous equations can be solved analytically, but the solutions are algebraically complicated and we give here only the results and leave details to the Appendices.

Collapsing the delta functions as explained in Appendix E 1, we can write:

$$\mathfrak{W}_{n\mathbf{k},n'\mathbf{k}'}^{\ominus,qq'} = \frac{4\mathbf{a}^2}{v_m^3 \hbar^4} \sum_j \sum_{\ell, \{q_i\}} J_{\mathfrak{W}}(\mathbf{p}_j) \hat{\mathcal{F}}_{\mathbf{p}_j, q\mathbf{k}, q'\mathbf{k}'}^{\ell, \ell, \ell | q_4, q_1, q_2}$$

$$\mathfrak{Im} \left\{ \mathcal{B}_{\mathbf{k}, \mathbf{p}_j + \frac{1}{2}q\mathbf{k} + q'\mathbf{k}'}^{n\ell\ell | q_2 q_3 q} \mathcal{B}_{\mathbf{k}', \mathbf{p}_j + \frac{1}{2}q'\mathbf{k}'}^{n'\ell\ell | -q_3 q_1 q'} \text{PP} \left[ \frac{\mathcal{B}_{\mathbf{k}, \mathbf{p}_j + \frac{1}{2}q\mathbf{k}}^{n\ell\ell | -q_1 q_4 - q} \mathcal{B}_{\mathbf{k}', \mathbf{p}_j + q\mathbf{k} + \frac{1}{2}q'\mathbf{k}'}^{n'\ell\ell | -q_4 - q_2 - q'}}{v_m \frac{q_1 q \omega_{n\mathbf{k}}}{v_m} + \hat{\Omega}_{\ell, \mathbf{p}_j} - q_1 q_4 \hat{\Omega}_{\ell, \mathbf{p}_j + q\mathbf{k}}} + \frac{\mathcal{B}_{\mathbf{k}', \mathbf{p}_j + \frac{1}{2}q'\mathbf{k}'}^{n'\ell\ell | -q_1 - q_4 - q'} \mathcal{B}_{\mathbf{k}, \mathbf{p}_j + q'\mathbf{k}' + \frac{1}{2}q\mathbf{k}}^{n\ell\ell | q_4 - q_2 - q}}{v_m \frac{q_1 q' \omega_{n'\mathbf{k}'}}{v_m} + \hat{\Omega}_{\ell, \mathbf{p}_j} + q_1 q_4 \hat{\Omega}_{\ell, \mathbf{p}_j + q'\mathbf{k}'}} \right] \right\},$$

where  $\hat{\Omega} = \Omega/v_m$ , and

$$\hat{\mathcal{F}}_{\mathbf{p}, q\mathbf{k}, q'\mathbf{k}'}^{\ell_3, \ell_1, \ell_2 | q_4, q_1, q_2} = q_1 q_4 (2n_B(\Omega_{\ell_3, \mathbf{p}+q'\mathbf{k}'} + 1) (2n_B(\Omega_{\ell_1, \mathbf{p}} + q_1 + 1) (2n_B(\Omega_{\ell_2, \mathbf{p}+q\mathbf{k}+q'\mathbf{k}'} + q_2 + 1) \quad (94)$$

is a product of thermal factors and where, when they exist, the solutions,  $j = 0, \dots, 3$  take the form

$$\mathbf{p}_j = t_{\lfloor j/2 \rfloor} \mathbf{v}_{\lfloor j/2 \rfloor} + u_{\lfloor j/2 \rfloor}^{(j \bmod 2)} \mathbf{w}_{\lfloor j/2 \rfloor}, \quad (95)$$

where, for  $i = 0, 1$   $\mathbf{v}_i = a_2 \mathbf{k}_1 + (-1)^i a_1 \mathbf{k}_2$ ,  $\mathbf{w}_i = \hat{\mathbf{z}} \times \mathbf{v}_i$  (note that  $\mathbf{v}_i = \underline{\mathbf{v}}_i$ ,  $\mathbf{w}_i = \underline{\mathbf{w}}_i$  and  $\mathbf{p}_j = \underline{\mathbf{p}}_j$  are all in-plane vectors),  $t_i$  and  $u_i^{(\pm)}$  are given in Appendix E 1 (also recall we defined  $\tilde{0} = -1$ ,  $\tilde{1} = 1$ ,  $x \bmod 2$  is  $x \bmod 2$ , and  $\lfloor x \rfloor$  denotes the floor of  $x$ ), and

$$J_{\mathfrak{W}}(\mathbf{p}_j) = \left| s_1 \frac{\mathbf{k}_1 \wedge \underline{\mathbf{p}}_j}{\hat{\Omega}_{\ell, \mathbf{p}_j} \hat{\Omega}_{\ell, \mathbf{p}_j - \mathbf{k}_1}} + s_2 \frac{\underline{\mathbf{p}}_j \wedge \mathbf{k}_2}{\hat{\Omega}_{\ell, \mathbf{p}_j} \hat{\Omega}_{\ell, \mathbf{p}_j - \mathbf{k}_2}} + s_1 s_2 \frac{-\mathbf{k}_1 \wedge \mathbf{k}_2 + \underline{\mathbf{p}}_j \wedge \mathbf{k}_2 - \underline{\mathbf{p}}_j \wedge \mathbf{k}_1}{\hat{\Omega}_{\ell, \mathbf{p}_j - \mathbf{k}_1} \hat{\Omega}_{\ell, \mathbf{p}_j - \mathbf{k}_2}} \right|^{-1}, \quad (96)$$

where  $\underline{\mathbf{V}}_1 \wedge \underline{\mathbf{V}}_2 = V_1^x V_2^y - V_2^y V_1^x$  for any in-plane vectors  $\underline{\mathbf{V}}_{1,2}$ . Coefficients  $t_{0,1}$  are always well defined, but for each  $i$ ,  $u_i^{(\pm)}$  are the solutions to a quadratic equation which has zero, one or two solutions, whether the discriminant  $\mathbf{d}_{u,i}$  thereof is negative, zero, or positive.

Necessary (but not sufficient) conditions of existence of solutions are: (i) the existence of *both* conics, cf. Table III, (ii)  $\mathbf{d}_{u,0} \geq 0$  and/or  $\mathbf{d}_{u,1} \geq 0$ , (iii) when  $s_1$  and/or  $s_2$  is negative, the  $\mathbf{p}_j$  must lie on the  $\eta_{1,2} = 1$  branch of the 1 and/or 2 hyperbola. Even with these constraints, spurious solutions exist, so that one must check that the solutions Eq. (95) also satisfy the equations for the given values of  $a_1, a_2, \mathbf{k}_1, \mathbf{k}_2, q, q', q_i$ .

### E. Scaling and orders of magnitude

In this subsection, we discuss the temperature dependence and magnitude of the magnonic contributions to the different phonon scattering rates, which determine the phonon thermal conductivity and thermal diffusivity tensors. Since we consider a low-energy continuum theory (without a momentum cutoff) in which the dispersion of the phonons is linear, these hold only in the low-temperature limit, i.e. for  $T \ll \hbar v_{\text{ph}}/(\mathbf{a}k_B)$ . Similarly, we consider the low-energy dispersion of magnons, so our results are valid for  $T \ll \hbar v_m/(\mathbf{a}k_B) \sim J/k_B$ . In Table IV, we summarize some of the relations derived in this section.

quantity	$\tau^{-1}$	$\kappa_L$	$\mathfrak{W}^{\ominus}$	$\tau_{\text{skew}}^{-1}$	$\varrho_H$
T-scaling	$T^{d+2x}$	$T^{3-d-2x}$	$T^{d-1+3x}$	$T^{d+2+3x}$	$T^{d-1+3x}$
Eq. ref	(98)	(99)	(102)	(103)	(108)

TABLE IV: Scaling relations derived in Sec. V E and the corresponding equation number where they appear.

Note that these were obtained within a low-energy approach which omit in particular larger- $k$  deviations away from the acoustic phonon linear dispersion limit and other higher- $T$  effects such as Umklapp [23].

#### 1. Longitudinal scattering rate: Role of anisotropies and scaling exponent

First we consider the leading magnonic contributions to the longitudinal scattering rate,  $D_{n\mathbf{k}}^{(1)}$ . The typical magnitude of this quantity for  $|\mathbf{k}| \sim k_B T/v_{\text{ph}}$  sets the basic rate  $1/\tau$ . This rate has been studied previously in classic work on the phonon-magnon coupling in antiferromagnets. Reference [24] finds that  $1/\tau \sim T^5$  (for the moment we give only the  $T$  dependence under the above condition, and do not give the prefactor), for a model of exchange-striction in a Heisenberg antiferromagnet in three dimensions. This should be recovered from our formalism.

A general estimate can be obtained from Eqs. (63,64). To evaluate it requires, in addition to the dispersion relations, the phonon-magnon couplings  $\mathcal{B}$ , which are given in Eq. (78). At the level of temperature scaling for typ-

ical thermal momenta, for temperatures well above the magnon gap,  $v_m k \gg \Delta$ , we may replace  $k \sim k_B T / v_{\text{ph}}$ ,  $\omega \sim v_{\text{ph}} k \sim k_B T$  and  $\Omega \sim k_B T$  (the latter is true if the ratio between  $v_m$  and  $v_{\text{ph}}$  is order one). Noting that  $\tilde{\xi}$  and  $\tilde{\xi}'$  in Eq. (78) equal  $\pm 1$ , we see that a general phonon-magnon coupling is a sum of three contributions,

$$\mathcal{B} \sim \left( \frac{k_B T}{M v_{\text{ph}}^2} \right)^{\frac{1}{2}} n_0^{-1} \left( \lambda_{mm} \frac{\chi k_B T}{n_0} + \lambda_{mn} + \lambda_{nn} \frac{n_0}{\chi k_B T} \right). \quad (97)$$

Here, as above, we label generic Néel-Néel vector couplings  $\lambda_{nn} \equiv \lambda_{ab,00}$ , net magnetization-magnetization couplings  $\lambda_{mm} \equiv \lambda_{ab,11}$  and “cross” Néel-magnetization couplings  $\lambda_{mn} \equiv \lambda_{ab,10}$ .

Depending upon which of these terms is dominant, the temperature dependence of  $\mathcal{B} \sim T^{1/2+x}$ , with  $x = -1, 0, 1$  corresponding to the  $\lambda_{nn}$ ,  $\lambda_{mn}$  and  $\lambda_{mm}$  terms, respectively. We can then estimate the scattering rate by converting the momentum sum over  $\mathbf{p}$  to a  $d$ -dimensional integral ( $d$  is the spin-exchange dimensionality) and recalling  $|p| \sim T$ . We see therefore that

$$\frac{1}{\tau} \sim T^{d-1} |\mathcal{B}|^2 \sim T^{d+2x}. \quad (98)$$

A priori, the dominant contributions would arise from terms with  $x = -1$ , which have the smallest power of temperature, which would give  $1/\tau \sim T^{d-2} \sim T$  in  $d = 3$  dimensions. This *does not* agree with Ref. [24]. Instead, one notices that what one might expect to be the subdominant contribution from  $x = +1$ , which gives  $1/\tau \sim T^{d+2}$  in general dimensions, does agree with the classic theory for  $d = 3$ .

Why is this the case? The resolution lies in the fact that Ref. [24] assumes isotropic Heisenberg interactions, and is carried out in zero magnetic field. As a consequence, the Hamiltonian has SU(2) symmetry, and Goldstone’s theorem protects the gaplessness of the magnon modes *even in the presence of strain*. In particular, because even an arbitrarily strained lattice must preserve the gapless magnons in this case, the spin-lattice coupling, Eq. (69) must be spin-rotationally invariant, and moreover its quadratic expansion, Eq. (72), must vanish for a magnon configuration which is a small rotation of the Néel order, which corresponds to either  $n_y$  or  $n_z$  non-zero and spatially constant. This means that the non-zero terms in Eq. (72) involve only  $\xi, \xi' = m$  and not  $n$  (in a treatment including higher order terms, spatial gradients  $\nabla n$  would appear, but these scale in the same manner as  $m$ ). One can indeed check in Eq. (73) that when the interactions  $\Lambda_{ab}^{(m/n),\alpha\beta}$  are isotropic ( $\propto \delta_{ab}$ ),  $\lambda_{nn}$  vanishes, and  $\lambda_{mn}$  vanishes at zero field when the uniform magnetization  $m_0^a = 0$ . Taking the  $\lambda_{mm}$  contribution in Eq. (97) gives  $x = +1$  in Eq. (98) as needed for agreement with earlier work.

What is the physics of the different values of  $x$ ? We see that stronger effects (smaller powers of temperature) arise from coupling to  $n$  than to  $m$ . This is a fundamental property of antiferromagnets: fluctuations of the

order parameter  $n$  are stronger and more long-ranged than those of the uniform magnetization  $m$ , which is naturally suppressed when antiferromagnetic interactions dominate. Thus larger effects would be expected from coupling of strain to the staggered magnetization than to the uniform one, as the formula indeed shows.

How is this reflected in  $\kappa_L(T)$ ? The last step from the scattering time  $\tau$  to the longitudinal conductivity  $\kappa_L$  is a standard one [23, 25]. The sum over phonon momentum  $\mathbf{k}$  in the first term of Eq. (32) is converted to a three-dimensional integral (the *magnon* momentum integral was  $d$ -dimensional, with  $d = 2$  in the case of a layered antiferromagnet).

For temperatures  $k_B T \gg \Delta$ , the scaling for the temperature dependence of the longitudinal conductivity is

$$\kappa_L \sim T^{3-d-2x}. \quad (99)$$

As can be seen from Eq. (97), a crossover between the low-temperature  $x = -1$  and the high-temperature  $x = +1$  behaviors occurs at  $T_\lambda^*$ ,

$$k_B T_\lambda^* \sim \frac{n_0}{\chi} \sqrt{\frac{\lambda_{nn}}{\lambda_{mm}}}. \quad (100)$$

Eq. (100) assumes that the intermediate behavior  $x = 0$ , due to the  $\lambda_{mn}$  coupling which is proportional to both anisotropic exchanges and the net magnetization, is negligible; this is consistent with our numerical results shown in Sec. VF 4. The above results, Eqs. (99,100), also assume that  $D_{n\mathbf{k}}^{(1)}$  is the dominant scattering rate contributing to the longitudinal inverse scattering time  $D_{n\mathbf{k}}$ . (The role of  $\check{D}_{n\mathbf{k}}$  is considered in more detail in Sec. VF 4.) However, many more scattering processes, such as boundary or impurity scattering, which in Eq. (2) are encompassed as  $\check{D}_{n\mathbf{k}}$ , contribute (through Matthiessen’s rule) to the phonon relaxation. Thus,  $\kappa_L$  should be considered a probe of the *full*  $D_{n\mathbf{k}}$ .

## 2. Longitudinal scattering rate: Role of the gap and magnetic field dependence

Since we have seen that the assumption of isotropic interactions suppresses the coupling to the staggered magnetization, this discussion suggests that breaking of spin-rotation symmetry should greatly enhance phonon scattering. While this may indeed be the case, we should note a subtlety: although spin anisotropy indeed allows such coupling, it also allows the formation of a magnon gap —enlarged by the presence of an external magnetic field,  $\Delta_\ell = \sqrt{\Gamma_\ell/\chi + h_\ell^2}$ . Which behavior should be expected from the combination of these two effects?

Regardless of the form of coupling (scaling exponent  $x$ ), if  $k_B T \ll \Delta$ , magnon-phonon scattering will become energetically unavailable. More precisely,  $D^{(1)+}$ , corresponding to the process whereby a phonon excites



two magnons, is exponentially suppressed due to the required rest energy  $2\Delta$ , while  $D^{(1)-}$ , corresponding to the process whereby a phonon scatters a magnon, is exponentially suppressed due to the exponential decrease of all magnon populations at temperatures below the gap. Therefore  $D^{(1)}$  as a whole is exponentially suppressed if  $k_B T \ll \Delta$ ; We check this behavior numerically in Sec. VF 6.

Thus, a crossover in the behavior of  $\kappa_L(T)$  occurs at temperature  $T_\Delta^* \sim \Delta/k_B$ . Below  $T_\Delta^*$ , the phonon thermal conductivity is mostly due to *other* scattering effects, which are captured by  $\check{D}_{n\mathbf{k}}$  in this work. For constant  $\check{D}_{n\mathbf{k}}$ , this yields  $\kappa_L \sim T^3$ . Above  $T_\Delta^*$ , phonon-magnon scattering becomes available, and is enhanced by anisotropic coupling; provided this is the dominant effect, the resulting thermal conductivity behavior is  $\kappa_L \sim T^{3-d-2x}$  with  $x = -1$  which, for  $d = 2$  (two-dimensional magnons), is the *same power* of temperature as that obtained with only constant  $\check{D}_{n\mathbf{k}}$ . However, the proportionality constant is larger with phonon-magnon scattering than without, which, for sufficiently strong anisotropic couplings (i.e. sufficiently large  $\lambda_{nn}$ ), may lead to a ‘‘bump’’ in  $\kappa_L(T)$ , as we indeed numerically see in Sec. VF 4.

Remarkably, this effect depends on the external magnetic field through the width of the magnon gap (recall the latter is field dependent), and may be an important feature of  $\kappa_L(\mathbf{h}, T) - \kappa_L(\mathbf{0}, T)$ . For the sake of completeness, we note that types of dependences on the magnetic field may arise at temperatures where the scaling exponent  $x = 0$  plays a role, because the  $\lambda_{mn}$  coupling depends explicitly on the net magnetization  $m_0$  in (see Eq. (73)). It is however not clear how this contribution could become non-negligible in any range of temperatures, and the gap dependence  $\Delta(\mathbf{h})$  is arguably the main culprit as regards the dependence on  $\mathbf{h}$  of the longitudinal conductivity.

### 3. Transverse scattering: scaling exponent

We can now apply similar reasoning to the transverse/Hall scattering rate  $\mathfrak{W}^\ominus$  from Eq. (66). Obviously if temperature is sufficiently low, i.e. below magnon gaps, the result will be exponentially suppressed. Of greater interest is the energy regime above the magnon gaps, in which we may assume acoustic linearly dispersing magnons (and phonons). We proceed by counting the obvious factors of momentum and energy, and by assuming the relevant momentum scales are set by dimensional analysis, i.e.  $\mathbf{k}, \mathbf{k}' \sim k_B T/v_m$  etc. Inspection of Eq. (66) shows one sum over magnon momentum  $\mathbf{p}$ , which converts to an integration in the thermodynamic limit, two energy delta functions, and one energy denominator, which, using the aforementioned momentum scaling implies that

$$\mathfrak{W}^\ominus \sim T^{d-3} \mathcal{B}^4. \quad (101)$$

Here we considered the *magnon* momentum integration as  $d$ -dimensional, as in the previous discussion of longitudinal scattering rates.

Now to proceed we must estimate the contribution of the four  $\mathcal{B}$  factors. To do so, we need to consider the effective time-reversal symmetry  $\mathcal{T}$ . This symmetry must be broken to obtain a non-zero effective skew-scattering rate,  $\mathfrak{W}_{n\mathbf{k}, n'\mathbf{k}'}^{\ominus, \text{eff}, qq'}$ , which in particular is odd under  $\mathcal{T}$ . As discussed in Secs. VC 2 and VC 3, under  $\mathcal{T}$  the  $\lambda_{mm}$  and  $\lambda_{nn}$  couplings are even while only the  $\lambda_{mn}$  couplings are odd; therefore  $\mathfrak{W}^{\ominus, \text{eff}}$  must contain an odd number of factors of  $\lambda_{mn}$ . Furthermore, in the low field regime we consider here,  $\mathcal{T}$  symmetry breaking happens through the development of a small uniform magnetization, hence  $\lambda_{mn} \propto m_0$ , which in turn is linearly proportional to the applied field (see Eq. (73)). Consequently, to obtain the linear-in-field Hall scattering rate, we should keep just one (and not three, the other available odd number) factors of  $\lambda_{mn}$ . Therefore, we may use Eq. (97) to estimate

$$\mathfrak{W}^{\ominus, \text{eff}} \sim T^{d-1} \lambda_{mn} (\lambda_{mm} T + \lambda_{nn} T^{-1})^3 \sim T^{d-1+3x}. \quad (102)$$

Here, as in Sec. VE 1,  $x = +1$  obtains in a large parameter region where  $\frac{\lambda_{mm}}{\lambda_{nn}} \ll \left(\frac{n_0}{\chi k_B T}\right)^2$ , while  $x = -1$  results if  $\lambda_{nn}$  is non-zero and dominant in a low-temperature regime where the magnon gap remains negligible.

It is by no means clear *how* the latter regime would be achieved, and if we assume that the  $x = +1$  case dominates, then it is interesting to see that  $\mathfrak{W}^{\ominus, \text{eff}}$  in Eq. (102) scales like  $T^{d+2}$ , which is the *same power* of temperature as the magnon contribution to the longitudinal scattering rate in Eq. (98).

This scaling is a bit surprising, as we should expect that the transverse is smaller than the longitudinal scattering, since it comes from a higher order term. To resolve this, we should consider more carefully the relationship of  $\mathfrak{W}^{\ominus, \text{eff}}$  to a ‘‘skew scattering rate’’. In particular, one should note that  $\mathfrak{W}_{n\mathbf{k}n\mathbf{k}'}^{\ominus, \text{eff}}$  enters the collision term via a *sum* over  $\mathbf{k}'$ , which converts to an integral over  $\mathbf{k}'$  in the thermodynamic limit. Therefore the measure of this integral, which is expected to be dominated by  $|\mathbf{k}'| \sim k_B T/v_m, k_B T/v_{\text{ph}}$ , contributes an additional factor of  $T^3$  (since phonons are always three-dimensional). Thus it would be more correct to estimate the skew scattering rate as

$$\frac{1}{\tau_{\text{skew}}} \sim T^3 \mathfrak{W}^{\ominus, \text{eff}} \sim T^{d+2+3x}. \quad (103)$$

For  $x = 1$  and  $d = 2$ , this scales as  $T^7$  which is indeed small compared to the  $T^4$  predicted in the same regime for the longitudinal scattering.

Additionally, we highlight in Sec. VF 7, through numerical evaluations, the strong momentum-orientation dependence of  $\mathfrak{W}^\ominus$ .

#### 4. Transverse scattering: thermal Hall resistivity

We would like to emphasize that within any scattering mechanism of phonon thermal Hall effect, the skew scattering rate is a more fundamental measure of chirality of the phonons than the thermal Hall *conductivity*. This is because the Hall conductivity inevitably involves the combination of the skew and longitudinal scattering rates (in the form  $\tau^2/\tau_{\text{skew}}$ ), and the longitudinal scattering rate of phonons has many other contributions that do not probe chirality, and may have complex dependence on temperature and other parameters that obscure the skew scattering. The scaling of the temperature dependence of  $1/\tau_{\text{skew}}$  given above is a much more reliable prediction than any corresponding one made for  $\kappa_H$  for this reason, and we do not quote the latter here. Instead, to extract the skew scattering rate, one should look at the thermal Hall *resistivity*,  $\varrho_H$ , which is simply proportional to  $1/\tau_{\text{skew}}$ , at least in the simplest view where the angle-dependence of the longitudinal scattering does not spoil its cancellation.

We define the thermal Hall resistivity tensor as usual by the matrix inverse,  $\varrho = \kappa^{-1}$ . In particular, considering the simplest case of isotropic  $\kappa^{\mu\mu} \rightarrow \kappa_L$  and  $\kappa_L \gg \kappa^{\mu \neq \nu}$ , one thus has

$$\varrho_H^{\mu\nu} = \frac{\varrho_{\mu\nu} - \varrho_{\nu\mu}}{2} \approx \frac{-\kappa_{\mu\nu} + \kappa_{\nu\mu}}{2\kappa_L^2} = -\frac{\kappa_H^{\mu\nu}}{\kappa_L^2}. \quad (104)$$

The quantity  $\varrho_H^{\mu\nu}$  is independent of the scale of the longitudinal scattering, in the sense that under a rescaling  $D_{n\mathbf{k}} \rightarrow \zeta D_{n\mathbf{k}}$ , then  $\varrho_H^{\mu\nu}$  is unchanged (see indeed Eqs. (32,33) for an explicit check at leading perturbative order).

As explained before, let us further assume that  $D_{n\mathbf{k}} = 1/\tau$  is  $(n, \mathbf{k})$ -independent, e.g. as if the case if dominated by some extrinsic effects. In that case, we can extract the longitudinal dependence from the transverse conductivity kernel, and redefine  $\tilde{K}_{n\mathbf{k}n'\mathbf{k}'}^H = \tau^{-2} K_{n\mathbf{k}n'\mathbf{k}'}^H$  which is now independent of the longitudinal scattering rate  $\tau^{-1}$ . Besides, to leading order one has simply  $K_{n\mathbf{k}n'\mathbf{k}'}^L = \tau e^{\beta\hbar\omega_{n\mathbf{k}}} \delta_{nn'} \delta_{\mathbf{k}\mathbf{k}'}$ , from which, assuming  $\omega_{n\mathbf{k}} = v_{\text{ph}}|\mathbf{k}|$  and  $N^{\text{eq}} = n_B$ , we have simply

$$\kappa_L = \tau \frac{\hbar^2}{k_B T^2} \frac{1}{V} \sum_{n\mathbf{k}} e^{\beta\hbar\omega_{n\mathbf{k}}} (J_{n\mathbf{k}}^\alpha)^2 = \tau c_v \frac{v_{\text{ph}}^2}{3}, \quad (105)$$

where by construction the result does not depend on the chosen direction  $\alpha$  of the current (for instance  $\alpha = x, y, z$ ). This is the well-known relation between the thermal conductivity  $\kappa_L$  and the thermal capacity

$$c_v = \frac{\partial}{\partial T} \left[ \frac{1}{V} \sum_{n\mathbf{k}} N_{n\mathbf{k}}^{\text{eq}} \hbar\omega_{n\mathbf{k}} \right] = k_B \frac{2\pi^2}{5} \left( \frac{k_B T}{\hbar v_{\text{ph}}} \right)^3 \quad (106)$$

of the phonon gas. Consequently, Eq. (104) evaluates to

$$\varrho_H^{\mu\nu} = -k_B^{-1} \left( \frac{15v_{\text{ph}}}{2\pi^2} \right)^2 \left( \frac{\hbar}{k_B T} \right)^8 \times \frac{V}{(2\pi)^6} \sum_{n\mathbf{k}n'\mathbf{k}'} J_{n\mathbf{k}}^\mu \tilde{K}_{n\mathbf{k}n'\mathbf{k}'}^H J_{n'\mathbf{k}'}^\nu. \quad (107)$$

This expression does not depend on  $\tau$ , which justifies studying  $\varrho_H$  instead of  $\kappa_H$ . From it and Eq. (31), one can readily derive the scaling relation

$$\varrho_H \sim \mathfrak{W}^{\ominus, \text{eff}} \sim T^{d-1+3x}, \quad (108)$$

which we check numerically in Sec. V F 5.

#### 5. Detailed scaling analysis of the longitudinal conductivity

The scaling with temperature described above, obtained by replacing every momentum scale  $\hbar v_{\text{m,ph}} k$ ,  $\hbar v_{\text{m,ph}} \underline{k}$ ,  $\hbar v_{\text{m,ph}} p$  by that of the temperature,  $k_B T$ , are expected to be valid for  $v = v_{\text{m}}/v_{\text{ph}}$  of ‘‘order one’’. Here we investigate more carefully the dependence of these quantities on  $v$  when the latter becomes large. Surprisingly, we show below that the prediction of Eq. (99) for the high temperature scaling of  $\kappa_L$  breaks down already for  $v > 3$ , giving way to a continuously variable power law exponent. For the thermal Hall resistivity, we find that the temperature exponent, Eq. (108), remains independent of the velocity ratio.

To obtain these results, we analyze the full integral expressions directly, distinguishing momentum and temperature dependencies. Various technical details are provided in Appendix E 4.

To analyze  $\kappa_L$ , we start by writing the expression for the diagonal scattering rate, Eq. (87), in dimensionless form, in terms of a scaling parameter  $\varkappa$  and dimensionless variable  $\tilde{y}$ ,

$$\varkappa = \frac{\hbar v_{\text{ph}} k}{k_B T}, \quad \tilde{y} = y/k. \quad (109)$$

We assume the relevant momentum and energy scales are large compared to any gaps,  $\delta_\ell \ll k, k_B T/v_{\text{m}}$ , and therefore in the following set  $\delta_\ell \rightarrow 0$ . Then we can obtain scaling forms,

$$c_\eta(y) = k \tilde{c}_\eta(\tilde{y}), \quad (110)$$

$$\Omega_{\ell, \mathbf{p}_{\ell, \mathbf{k}}^{(\eta)}(y)}, \Omega_{\ell, \mathbf{p}_{\ell, \mathbf{k}}^{(\eta)}(y) - \mathbf{k}} = v_{\text{m}} k \tilde{\Omega}_\ell^{\pm\eta}(\tilde{y}),$$

$$\mathcal{B}_{\mathbf{k}; -\mathbf{p}+\mathbf{k}/2}^{n, \ell, \ell+s-} = k^{3/2} \tilde{\mathcal{B}}_{mm}(\tilde{y}) + k^{1/2} \tilde{\mathcal{B}}_{mn}(\tilde{y}) + k^{-1/2} \tilde{\mathcal{B}}_{nn}(\tilde{y}),$$

and the precise functional forms of  $\tilde{c}_\eta(\tilde{y})$ ,  $\tilde{\Omega}_\ell^{\pm\eta}(\tilde{y})$  and  $\tilde{\mathcal{B}}_{\xi\xi'}$  are given in Appendix E 4, Eqs. (E20-E25). We find, after making the change of variables in the integral of Eq. (87) from  $y$  to  $\tilde{y}$ ,

$$D_{n\mathbf{k}}^{(s)}(T) = \sum_{x=-1}^1 k^{2+2x} \mathbb{F}_x^{(s)}(\varkappa, v, \theta), \quad (111)$$

where the scaling functions  $F_x^{(s)}(\varkappa, v, \theta)$  are

$$F_x^{(s)}(\varkappa, v, \theta) = \frac{(3-s)\alpha^2 \sinh(\varkappa/2)}{4\pi v_m \hbar^2} \int_{-\infty}^{+\infty} d\tilde{y} \sum_{\eta} \tilde{f}_{\eta}^s(\tilde{y}) \tilde{J}_{\tilde{D}}^s(\tilde{y}) \\ \times \sum_{\ell} \frac{\tilde{C}_x(\tilde{y})}{\sinh(\frac{v\varkappa}{2}\tilde{\Omega}_{\ell}^{+\eta}(\tilde{y})) \sinh(\frac{v\varkappa}{2}\tilde{\Omega}_{\ell}^{-\eta}(\tilde{y}))}. \quad (112)$$

Here  $\tilde{C}_x(\tilde{y})$  are quadratic combinations of the original  $\tilde{B}_{mm}, \tilde{B}_{mn},$  and  $\tilde{B}_{nn}$  coefficients given in Appendix E4. Eq. (111) agrees with the scaling behavior given in Eq. (98) (with  $d = 2$ ). In Appendix E4 we derive the behavior of the scaling functions  $F_x^{(s)}$  at small and large  $\varkappa$ , which will be useful in the following.

The scaling form of the scattering rate is input to the thermal conductivity. To see the implication, we presume for simplicity the total scattering rate  $D_{nk} = \sum_s D_{nk}^{(s)} + \check{D}$  is dominated by a single value of  $x$ . We note in passing that when the gaps are zero, only one value of  $s$  contributes here:  $s = -1$  for  $v > 1$  (the case of most interest), and  $s = 1$  for  $v < 1$ . Then

$$D_{nk} = \left( \frac{k_B T}{\hbar v_{\text{ph}}} \right)^{2+2x} \left( \varkappa^{2+2x} F_x(\varkappa) + \check{D}(T) \right). \quad (113)$$

Here we defined  $\check{D}(T) = \left( \frac{\hbar v_{\text{ph}}}{k_B T} \right)^{2+2x} \check{D}$ , which is temperature-dependent. In particular for  $x = 0, 1$ , it becomes very small at high temperature. Inserting this into Eq. (32), turning the sum over  $\mathbf{k}$  into an integral, and using spherical coordinates, we obtain

$$\kappa_L^{\mu\mu} \sim \frac{k_B}{\hbar^2} \left( \frac{\hbar v_{\text{ph}}}{k_B T} \right)^{2x-1} \\ \int_0^{+\infty} d\varkappa \int_0^{\pi} d\theta \int_0^{2\pi} d\phi \frac{\hat{k}^{\mu} \hat{k}^{\mu} \sin \theta \varkappa^4 \sinh^{-2}(\varkappa/2)}{\varkappa^{2x+2} F_x(\varkappa, v, \theta) + \check{D}(T)}. \quad (114)$$

Now we are in a position to investigate the temperature dependence of the conductivity. To simplify the discussion, we restrict the remainder of this section to the case  $x = 1$ , since  $F_1$  is the largest contribution when spin-orbit coupling is weak, and is also enhanced at high temperature. First consider the low temperature limit. Then  $\check{D}(T)$  becomes large at low  $T$ , and we can simply replace the denominator of the integrand in Eq. (114) by  $\check{D}(T)$ . This is just the extrinsic limit in which the constant  $\check{D}$  scattering dominates and one recovers the  $T^3$  dependence of the thermal conductivity arising from the phonon heat capacity.

Next we turn to the higher temperature limit. There, the parameter  $\check{D}(T)$  becomes small, and might naively be neglected. Dropping this term in Eq. (114), the sole remaining temperature dependence is in the prefactor, and agrees with what was found earlier in Eq. (99) (for  $d = 2$ ). This procedure is valid provided the integral in Eq. (114) converges for  $\check{D}(T) = 0$ . To check this, we must consider the potential divergences at small and large  $\varkappa$ . At small  $\varkappa$ , the integrand behaves like  $1/(\varkappa^2 F_1(\varkappa))$ . As shown

in Sec. E4,  $F_1(\varkappa)$  grows as small  $\varkappa$  (see Eq. (E29)), ensuring there is no divergence. The large  $\varkappa$  limit is more problematic. This is because although the  $\sinh^{-2}(\varkappa/2)$  factor decays exponentially, the factor  $F_x$  in the denominator also decays exponentially. Specifically, we show in Sec. E4 that Eq. (112) implies

$$F_x(\varkappa, v, \theta) \underset{\varkappa \gg 1}{\sim} \bar{F}(v, \theta) e^{-\alpha(v, \theta)\varkappa}, \quad (115)$$

where the function  $\alpha(v, \theta) = \frac{1}{2}(v|\sin \theta| - 1)$  (see Eq. (E27)), and  $\bar{F}(v, \theta)$  a constant. This implies an exponential *growth* of  $1/F_x$  with  $\varkappa$  when  $\check{D}$  is neglected. For  $v > 3$ , the integral becomes divergent for  $\check{D} = 0$ , and the naïve scaling fails.

To see what happens for  $v > 3$ , we deduce from the above discussion that the integral in Eq. (114) becomes dominated in this case by large  $\varkappa \gg 1$ . Then we approximate  $\sinh \frac{\varkappa}{2} \sim e^{\varkappa/2}$ , and use the asymptotic form of  $F_x$  in Eq. (115). We must then distinguish two cases. If  $\alpha < 1$ , the  $\varkappa$  integral converges, even for  $\check{D}(T) \rightarrow 0$ , and we obtain, in the latter limit,  $\kappa_L \sim T^{-1}$ . When  $\alpha > 1$ , we must be more careful. Successively performing the changes of variables  $u = e^{-\varkappa}$ ,  $u = v\check{D}(T)^{\alpha(v, \theta)^{-1}}$  and  $v = w[-\alpha(v, \theta)^{-1} \ln \check{D}(T)]^{-\alpha(v, \theta)^{-1}}$ , and a saddle-point procedure assuming  $\alpha > 1$ , we arrive at (see Appendix E4)

$$\kappa_L \sim \frac{1}{T} \check{D}(T)^{\alpha_0^{-1}-1} \left( -\alpha_0^{-1} \ln \check{D}(T) \right)^{4-\alpha_0^{-1}} I_0(v) \quad (116)$$

where  $\alpha_0(v) = \alpha(v, 0) = (v-1)/2 > 1$ ,  $I_0(v) = \int_0^{+\infty} dw \frac{1}{w^{\alpha_0} F_0(v, 0) + 1}$ . This entails, up to logarithmic corrections, the result quoted in Eq. (5),

$$\kappa_L \sim \begin{cases} T^{-1} & \text{for } v < 3 \\ T^{3-8(v-1)^{-1}} & \text{for } v > 3 \end{cases}. \quad (117)$$

We see that the  $1/T$  high-temperature behavior of  $\kappa_L$  changes for  $v > 3$  to a power law with an exponent that continuously depends upon  $v$ , and even changes sign: for  $v > 11/3$ , the conductivity *increases* with increasing temperature at high  $T$ . We indeed recover this nontrivial feature numerically, see Fig. 1.

Note that this behavior is all obtained within the linearized phonon and magnon models, and thus eventually changes when the temperature exceeds for example the Debye energy.

## F. Numerical results

### 1. Implementation

Details about the numerical implementation are given in Appendix E3. In short, we use C together with (i) the Cubature library to perform the one-dimensional momentum integrals (appearing in the definitions of

$D_{n\mathbf{k}}^{(1)|s}$ , Eq. (87)), (ii) the Cuba library [26] to perform multi-dimensional integrals (three-dimensional for  $\kappa_L^{\mu\mu}$ , first term in Eq. (32), and in six-dimensional for  $\varrho_H^{\mu\nu}$ , Eq. (107)).

## 2. Choice of parameters

(i). *Polarization vectors* In Eq. (79),  $\mathcal{L}$  is the trace over the product of the coupling matrix  $\lambda$ , with matrix elements  $\lambda^{\alpha\beta}$ , and that,  $\mathcal{S}$ , which determines the structure of the strain tensor and has matrix elements

$$\mathcal{S}_{n\mathbf{k}}^{q;\alpha\beta} = \frac{k^\alpha (\varepsilon_{n\mathbf{k}}^\beta)^q + k^\beta (\varepsilon_{n\mathbf{k}}^\alpha)^q}{\sqrt{\omega_{n\mathbf{k}}}}. \quad (118)$$

Values of  $(n, \mathbf{k})$  such that this factor vanishes correspond to phonons which are not coupled to the magnons, and whose longitudinal conductivity is solely driven by  $\check{D}_{n\mathbf{k}}$ , i.e. other scattering effects. While this may indeed happen in practice, to highlight the effects of phonon-magnon scattering we choose a basis of polarization vectors  $(\varepsilon_{0,\mathbf{k}}, \varepsilon_{1,\mathbf{k}}, \varepsilon_{2,\mathbf{k}})$  such that this is never the case (at least for  $\alpha = \beta$ , as with  $\Lambda_{1..5}$  which are much larger than  $\Lambda_{6,7}$ ).

These polarization vectors enforce  $\varepsilon_{n,-\mathbf{k}} = \varepsilon_{n\mathbf{k}}^* = -\varepsilon_{n\mathbf{k}}$  (so that  $\mathcal{S}_{n,-\mathbf{k}}^{q;\alpha\beta} = \mathcal{S}_{n\mathbf{k}}^{q;\alpha\beta} = -\mathcal{S}_{n\mathbf{k}}^{-q;\alpha\beta}$ ) as well as the tetragonal symmetry of the crystal, as required by the general theory of elasticity [27]; explicit expressions are given in App. E 2 b.

(ii). *Extrinsic phonon scattering rate* For similar reasons, the extrinsic phonon scattering rate is taken to be  $\check{D}_{n\mathbf{k}} \rightarrow \gamma_{\text{ext}}$ , a constant independent of  $(n, \mathbf{k})$  and small compared with the typical  $D_{n\mathbf{k}}$  as soon as  $T > T_\Delta^*$  (see Sec. V E 2). In very clean monocrystals and in the absence of any other phonon scattering events,  $\gamma_{\text{ext}} \sim v_{\text{ph}}/L$  reduces to the rate at which phonons bounce off the boundaries of the sample (of size  $L$ ).

(iii). *Phonon dispersion* The phonon dispersion relation is chosen linear,  $n$ -independent and isotropic,  $\omega_{n\mathbf{k}} = v_{\text{ph}}|\mathbf{k}|$ , so that the different regimes of scaling exponents  $x$  appear clearly.

## 3. Units and numerical values

We express our numerical results in units where  $\hbar^{\text{code}} = 1$ ,  $k_B^{\text{code}} = 1$ ,  $v_{\text{ph}}^{\text{code}} = 1$  and with unit lattice spacing  $\mathbf{a}^{\text{code}}$ . Then, the mass of the unit cell  $M_{\text{uc}}$  is expressed in units of  $M_0 = \frac{\hbar}{v_{\text{ph}}\mathbf{a}}$  and is typically large—of the order  $M_{\text{uc}} \sim 10^4 M_0$ .  $T$  is expressed in units of  $T_0 = \frac{\hbar v_{\text{ph}}}{\mathbf{a}k_B}$  and should verify  $T/T_0 \lesssim 1$  so that the assumption of linearly dispersing phonons is correct. Correspondingly, we can define an energy  $\epsilon_0 = k_B T_0$ , and the isotropic part of the exchange  $J$  is expressed in units of  $\epsilon_0$ .

The magnon velocity is fixed according to linear spin wave theory, which gives  $v_m = 2\sqrt{d}JS\mathbf{a}/\hbar$ , with  $J$  the

isotropic magnetic exchange constant. We take  $d = 2$  and  $S = 1/2$ ; moreover, it is known that for  $S = 1/2$  there is a renormalization factor  $Z \approx 1.2$  enhancing the velocity, so that  $v_m/v_{\text{ph}} = \sqrt{2}ZJ/\epsilon_0 \approx 1.7J/\epsilon_0$  in our units. Since, for isotropic exchange,  $\chi = \frac{1}{4\mathbf{a}^2 J}$ , we also take  $\chi_{\text{code}}^{-1} = 4(J/\epsilon_0)$ .

Spin-phonon couplings  $\Lambda_{1..7}$  are expressed in units of  $\epsilon_0/\mathbf{a} = \hbar v_{\text{ph}}/\mathbf{a}^2$ . We describe a possible microscopic mechanism for spin-strain coupling in App. F 1, where we show that  $\Lambda_{1..5}$  typically arise as derivatives of the isotropic magnetic exchange constants. Since the latter ultimately arises from the overlap of atomic wavefunctions, which vary over distances of the order  $a_B$  the Bohr radius, we expect  $\Lambda_{1..5} \sim J/a_B$ . Meanwhile  $\Lambda_{6,7}$  come from anisotropic exchanges and are thus expected to be considerably smaller.

Since the differences  $\Lambda_{1,2}^{(\xi)} - \Lambda_3^{(\xi)}$  and  $\Lambda_4^{(\xi)} - \Lambda_5^{(\xi)}$  are due to anisotropic exchanges, they are chosen a fraction of a  $\Lambda_{1..5}^{(\xi)}$ . Since these magnetoelastic couplings typically arise as derivatives of magnetic exchange, we also take  $\Lambda_i^{(m)} \approx -\Lambda_i^{(n)}$  for  $i = 1..7$ ; see App. F 1 for a detailed derivation.

Scattering rates  $D_{n\mathbf{k}}$  and  $\gamma_{\text{ext}}$  are expressed in units of  $\gamma_0 = v_{\text{ph}}/\mathbf{a}$ , and we assume  $\gamma_{\text{ext}}$  to be small, of the order of  $1/L$  with  $L$  the size of the sample—typically  $\gamma_{\text{ext}} \sim 10^{-7} v_{\text{ph}}/\mathbf{a}$ . Finally, thermal conductivities are expressed in units of  $\kappa_0 = k_B v_{\text{ph}}/\mathbf{a}^2$ .

For numerical calculations, we kept most dimensionless materials parameters (e.g. the ratio of  $v_m$  and  $v_{\text{ph}}$ ) fixed and constant, with the values given in Table VI. Those parameters for which we explore a given range of values are given in the captions of the figures in the following subsections. The fixed values are loosely inspired by Copper Deuterioformate Tetradeuterate (CFTD), a square lattice  $S=1/2$  antiferromagnet which has been intensively studied via neutron scattering [28–30] due to its convenient scale of exchange which suits such measurements. For our purposes, CFTD has the desirable attribute that the magnon and phonon velocities are comparable (based on an estimate of the sound velocity from the corresponding hydrate [31]), which creates a significant phase space for magnon-phonon scattering. By contrast, in  $\text{La}_2\text{CuO}_4$ ,  $v_m$  is much larger than  $v_{\text{ph}}$ .

$v_0$	$\mathbf{a}_0$	$\gamma_0$	$M_0$	$T_0$	$\epsilon_0$	$\chi_0^{-1}$	$\Lambda_0$	$\kappa_0$
$v_{\text{ph}}$	$\mathbf{a}$	$\frac{v_{\text{ph}}}{\mathbf{a}}$	$\frac{\hbar}{v_{\text{ph}}\mathbf{a}}$	$\frac{\hbar v_{\text{ph}}}{\mathbf{a}k_B}$	$k_B T_0$	$\epsilon_0 \mathbf{a}^2$	$\frac{\epsilon_0}{\mathbf{a}}$	$\frac{k_B v_{\text{ph}}}{\mathbf{a}^2}$

TABLE V: Table of units of velocity  $v_0$ , distance  $\mathbf{a}_0$ , rate  $\gamma_0$ , mass  $M_0$ , temperature  $T_0$ , energy  $\epsilon_0$ , inverse susceptibility  $\chi_0^{-1}$ , coupling  $\Lambda_0$  and thermal conductivity  $\kappa_0$  used in Table VI.

Finally, note that the following scaling relations for  $\kappa_L$ ,

$$\kappa_L \left( \{ \Lambda_{1..7}^{(\xi)} \}, \gamma_{\text{ext}} \right) = \zeta_0^2 \kappa_L \left( \{ \zeta_0 \Lambda_{1..7}^{(\xi)} \}, \zeta_0^2 \gamma_{\text{ext}} \right), \quad (119)$$

$v_m$	$v_{ph}$	$\chi^{-1}$	$n_0$	$\alpha$	$M_{uc}$	$m_0^x$	$m_0^y$	$m_0^z$	$\Delta_0$	$\Delta_1$
$v$	1.0	$2.08v$	1/2	1.0	$8 \cdot 10^3$	0	0.0	0.05	0.2	0.04
							0.05	0.0		

$\xi$	$\Lambda_1^{(\xi)}$	$\Lambda_2^{(\xi)}$	$\Lambda_3^{(\xi)}$	$\Lambda_4^{(\xi)}$	$\Lambda_5^{(\xi)}$	$\Lambda_6^{(\xi)}$	$\Lambda_7^{(\xi)}$
$n = 0$	$4.8v$	$4.0v$	$5.6v$	$4.0v$	$4.8v$	$0.24v$	$0.32v$
$m = 1$	$-4.0v$	$-4.8v$	$-5.6v$	$-4.8v$	$-4.0v$	$-0.32v$	$-0.24v$

TABLE VI: Numerical values of the fixed parameters used in all numerical evaluations, expressed in the units given in Table V. The upper and lower entries for  $m_0^y$  and  $m_0^z$  correspond to the two cases for calculating  $\varrho_H^{xy}$  and  $\varrho_H^{zz}$ , respectively.  $v = v_m/v_{ph}$  is a dimensionless multiplier used to reproduce the effect of a varying magnetic exchange scale, which mainly impacts  $v_m, \chi, \Lambda_i^\xi$ . In the plots, we use the values  $v = 2.5, 5, 10$ .

and for  $\varrho_H$ ,

$$\begin{aligned} \varrho_H \left( \{\Lambda_{1,\dots,5}^{(\xi)}\}, \{\Lambda_{6,7}^{(\xi)}\}, m_0^{y,z} \right) \\ = \zeta_1^{-3} \zeta_2^{-1} \zeta_3^{-1} \varrho_H \left( \{\zeta_1 \Lambda_{1,\dots,5}^{(\xi)}\}, \{\zeta_2 \Lambda_{6,7}^{(\xi)}\}, \zeta_3 m_0^{y,z} \right) \\ + O \left( (m_0^{y,z})^3 (\Lambda_{6,7}^{(\xi)})^3 \right), \end{aligned} \quad (120)$$

hold for any rescaling factors  $\zeta_{0,\dots,3}$ . Eqs. (119,120) make it possible to extrapolate results from our calculations for values of the parameters which are not explicitly explored in Table VI and Figs. 4(a), 4(b), 2(a), and 2(b).

#### 4. Results for $\kappa_L$

Numerical results for  $\kappa_L(T)$  are displayed in Figs. 2(a), 2(b) at fixed  $v = v_m/v_{ph} = 2.5$ .

Fig. 2(a) shows plots of  $\kappa_L(T)$  for several values of the extrinsic scattering  $\gamma_{ext}$  and fixed  $v = v_m/v_{ph} = 2.5$ . This figure exhibits all the behaviors described in Secs. VE1, VE2, with the extra feature that here there are two crossover temperatures,  $T_{\Delta,0}^*$  and  $T_{\Delta,1}^*$  defined by the two different magnon gaps  $\Delta_0, \Delta_1$  whose values we give in Tab. VI. These are more clearly visible in Fig. 2(b), where we show  $\kappa_L(T)$  in a small window of low temperatures and for smaller values of  $\gamma_{ext}$ .

Four scaling regimes can then be identified:

(i). For  $T \lesssim T_{\Delta,1}^*$ , only extrinsic scattering contributes to the full phonon scattering rate, and  $\kappa_L \propto T^3/\gamma_{ext}$ .

(ii). For  $T_{\Delta,1}^* \lesssim T \lesssim T_{\Delta,0}^*$ , both the extrinsic and the  $x = -1$  phonon-magnon (only in the  $\ell = 1$  valley) scattering rates contribute with the same scaling exponent, yielding  $\kappa_L \propto T^3$  with a smaller proportionality coefficient than in the first regime.

(iii). For  $T_{\Delta,0}^* \lesssim T \lesssim T_\lambda^*$ , both the extrinsic and the  $x = -1$  phonon-magnon (now in both valleys) scattering rates contribute with the same scaling exponent,

yielding  $\kappa_L \propto T^3$  with yet a smaller proportionality coefficient.

(iv). For  $T > T_\lambda^*$ , the  $x = +1$  phonon-magnon scattering rate is dominant and yields  $\kappa_L \propto T^{-1}$ . Note that  $T_\lambda^*$  is defined in Eq. (100) in the  $\check{D}_{n\mathbf{k}} = 0$  case; here by  $T_\lambda^*$  we mean the more general crossover temperature in the presence of a finite  $\check{D}_{n\mathbf{k}} = \gamma_{ext}$ .

The exponents quoted above are found with very good accuracy from a log-log scale plot (see inset of Fig. 2(a) and Appendices), regardless of the value of  $\gamma_{ext}$ ; in that sense these exponents are universal. The influence of (non-universal)  $\gamma_{ext}$  on the results of Fig. 2(a) is essentially threefold:

- Since the full phonon scattering rate is  $D_{n\mathbf{k}} = \gamma_{ext} + D_{n\mathbf{k}}^{(1)}$ , unsurprisingly  $\kappa_L(T)$  is always a decreasing function of  $\gamma_{ext}$ .
- The ‘‘bumps’’ at  $T \sim T_{\Delta,\ell}^*$  come from the fact that the  $x = -1$  phonon-magnon scattering rate is much larger than  $\gamma_{ext}$  as soon as the gap permits this scattering process; therefore, for large enough  $\gamma_{ext}$ , this feature disappears. More precisely, one should compare  $\gamma_{ext}$  with  $D_{nn,\ell} := \eta^2 f^2 \Delta_\ell / M_{uc}$ , where the dimensionless parameters  $\eta, f$  are defined by  $\lambda_{nn} \simeq \eta \lambda_{mm}$  and  $\Lambda_{1..5} \simeq fJ/\alpha$ . The first bump is noticeable iff  $\gamma_{ext} \lesssim D_{nn,1}$ , and the second bump is noticeable iff  $\max(\gamma_{ext}, D_{nn,1}) \lesssim D_{nn,0}$ .
- Since  $\gamma_{ext}$  and the  $\lambda_{nn}$  coupling lead to the same scaling exponent, the  $T \sim T_\lambda^*$  crossover results from a competition between  $\lambda_{mm}$  on the one hand and  $(\gamma_{ext}, \lambda_{nn})$  on the other; thus the larger  $\gamma_{ext}$ , the greater the dependence of  $T_\lambda^*$  on  $\gamma_{ext}$ , and  $T_\lambda^*(\gamma_{ext})$  is an increasing function of  $\gamma_{ext}$ .

Finally, Fig. 1 shows plots of  $\kappa_L(T)$  for several values of the velocity ratio  $v_m/v_{ph} = v$  at fixed  $\gamma_{ext} = 10^{-6}$ . In particular, we recover, at  $T \gg T_\lambda^*$ , the particularly non-trivial behavior described in Sec. VE5; namely that for all  $v$  values greater than  $v = 3$  the high-temperature behavior of  $\kappa_L$  goes like  $T^{3-8(v-1)^{-1}}$  (Eq. (117)) and the exponent indeed changes signs at  $v = 11/3$ , i.e. the conductivity *increases* with increasing temperature for  $v > 11/3$ .

#### 5. Results for $\varrho_H$

We evaluated numerically  $\varrho_H^{\mu\nu}$  for both  $\mu\nu = xy$  and  $xz$ , in both cases with a net magnetization  $\mathbf{m}_0$  oriented along  $\rho$ , the axis perpendicular to the Hall plane  $\mu\nu$ . Results are presented in Fig. 3. Here the dashed straight lines on the double logarithmic scale indicate the expected  $T^4$  scaling.

This behavior is consistent with the arguments given in Sec. VE4, especially Eq. (108), with  $d = 2$ -dimensional magnons and scaling exponent  $x = +1$ , corresponding to

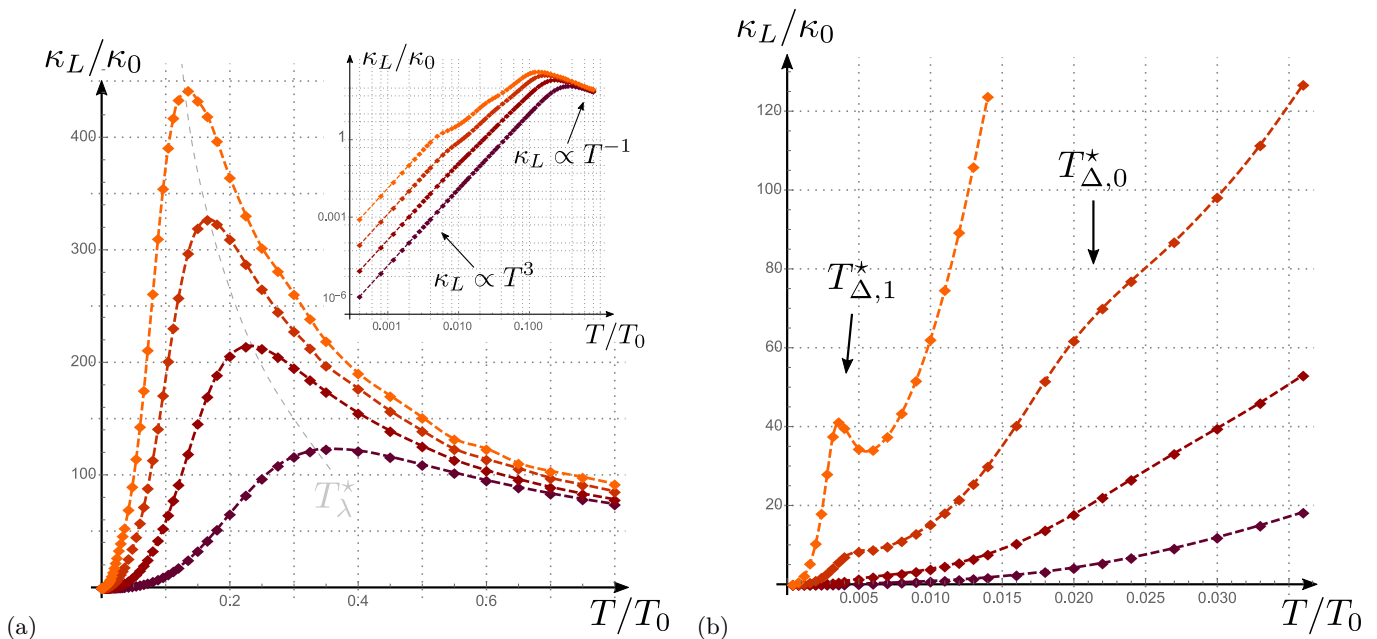


FIG. 2: Longitudinal thermal conductivity  $\kappa_L$  (in units of  $\kappa_0 = \kappa_B v_{\text{ph}}/a^2$ ) with respect to temperature  $T$  (in units of  $T_0 = \hbar v_{\text{ph}}/(ak_B)$ ), for four different values of  $\gamma_{\text{ext}}$ . (a)  $\gamma_{\text{ext}} = 1 \cdot 10^{-z} (v_{\text{ph}}/a)$ ,  $z \in [4, 7]$ , from darker ( $z = 4$ ) to lighter ( $z = 7$ ) shade. The dashed gray line indicates the evolution of the crossover temperature  $T_\lambda^*$  as a function of  $\gamma_{\text{ext}}$ . Inset: log-log plot; the scaling behaviors are consistent with the analysis presented in the text. The inset is reproduced in App. G. (b)  $\gamma_{\text{ext}} = 1 \cdot 10^{-z} (v_{\text{ph}}/a)$ ,  $z \in [6, 9]$ , from darker ( $z = 6$ ) to lighter ( $z = 9$ ) shade. The two crossover temperatures  $T_{\Delta,1}^*$  and  $T_{\Delta,0}^*$  are defined in the text up to a prefactor; here we identify the corresponding features in  $\kappa_L$  but do not indicate specific values of  $T$ . See App. G for a log-log plot.

the temperature regime where isotropic exchange dominates over the phonon-magnon coupling. We expect from Eq. (102) that deviations from this scaling behavior would be observed at lower temperatures, not investigated here.

We emphasize that the numerical values of  $\varrho_H^{xy}$  and  $\varrho_H^{zx}$  are of the same order of magnitude. This is remarkable in a layered system which has entirely different magnon dynamics in the  $xy$  and  $xz$  planes, in this case where magnons are explicitly two-dimensional, carrying energy only within  $xy$  layers. It can be understood from the fact that here *phonons* are isotropic, carrying energy in all three directions, and that *including*  $\mathcal{T}$ -odd scattering exists in all directions, therefore allowing a Hall effect in both the  $xy$  and  $xz$  directions.

Numerically evaluating the dependence on  $v = v_m/v_{\text{ph}}$  of  $\varrho_H$ , we find that  $|\varrho_H^{xy}/\varrho_H^{xz}| < 1$  for all the values of  $v$  studied, and that the prefactors of  $\varrho_H^{xy}, \varrho_H^{xz}$  are rapidly suppressed for large  $v$ , as shown in Fig. 3. From a simple analysis, we expect  $|\varrho_H^{xy}/\varrho_H^{xz}| \propto 1/v$  for large  $v$ . The reason for the overall suppression of the Hall resistivity with increasing  $v$  is also clearly due to the diminishing phase space for scattering, but we have not obtained the exact dependence analytically.

Finally, we note that for our *choice* of antiferromagnetic order along the  $\hat{x}$ -axis in this model and within linearized spin-wave theory,  $\varrho_H^{yz} = 0$ .

## 6. Results for $D_{n\mathbf{k}}$

Fig. 4(a) shows the angular dependence of  $D_{n\mathbf{k}}$ . Throughout this section, we use  $\mathbf{k} = k(\cos \phi \hat{\mathbf{u}}_x + \sin \phi \hat{\mathbf{u}}_y)$ , with  $\phi \in [0, 2\pi[$ , and  $k_z = k \cos \theta$  with  $\theta \in [0, \pi]$ . Note that, in turn,  $k^2 = k^2 \sin^2 \theta$ . Also, since all the results are invariant under  $k_z \rightarrow -k_z$  i.e.  $\theta \rightarrow \pi - \theta$ , we plot results for  $\theta \in [0, \pi/2]$  only.

(i). *In-plane  $\phi(\mathbf{k})$  angular dependence.* We see from Fig. 4(a) that phonon-magnon scattering is typically larger for values of  $\phi(\mathbf{k})$  associated with high-symmetry axes of the system, i.e.  $\phi = 0 \text{ mod}[\pi/2]$ . This is inherited from the structure of  $\mathcal{L} = \text{Tr}[\boldsymbol{\lambda}^T \boldsymbol{\mathcal{S}}]$  in Eq. (79), which enters the magnetoelastic coupling, Eq. (69). The latter is by definition invariant under all symmetries of the crystal, so that components of the strain tensor couple to functions of the magnetization fields  $\mathbf{m}, \mathbf{n}$  with the same symmetries.

Now, while the symmetry group of the crystal structure is tetragonal, the  $C_4$  symmetry is spontaneously broken by the antiferromagnetic order along the  $x$  axis, while the  $C_2$  and mirror symmetries are preserved when the magnetic field is along the  $z$  axis. More precisely, *how* does the  $C_4$  symmetry (as acting on the  $\alpha, \beta$  indices) break? Since the  $\boldsymbol{\mathcal{S}}$  factor in Eq. (79) has the same structure as the strain tensor itself, it preserves  $C_4$ ; therefore the latter can only be broken in the  $\boldsymbol{\lambda}$  factor.

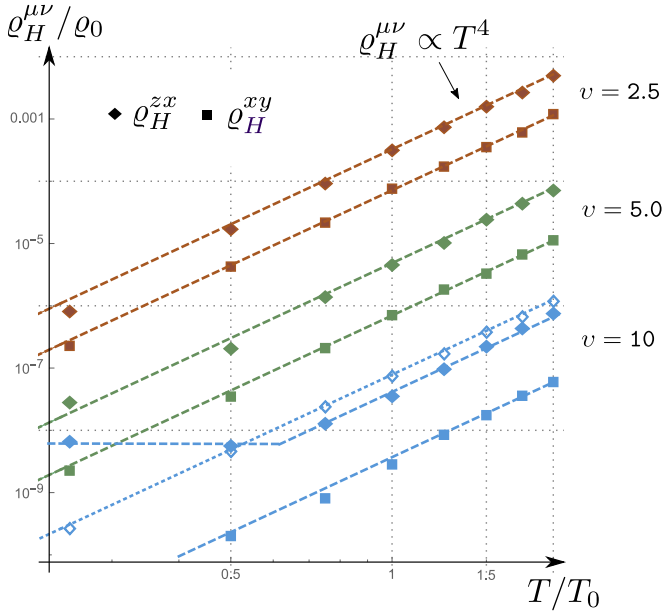


FIG. 3: Hall resistivities  $\varrho_H^{xy}(T)/\varrho_0$  and  $\varrho_H^{zx}(T)/\varrho_0$  for three values of  $v = v_m/v_{ph}$ . The low temperature saturation of  $\varrho_H^{zx}(T)/\varrho_0$  observed for  $v = 10$  is due to the non-negligible contributions of the  $\lambda_{nn}$  term in that range. This is confirmed by the data shown in empty blue diamonds, which is the result of calculations at the same value of  $v_m/v_{ph} = 10$  and approximately the same coupling constants as the full blue diamonds, except that  $\lambda_{nn} = 0$  there (the values of  $\lambda_{mm}$  are also slightly different but, importantly, the values of  $\lambda_{mn}$  are unchanged).

Let us focus on the  $\lambda_{mm}, \lambda_{nn}$  cases, since these coefficients can be nonzero in the absence of a net magnetization  $m_0$ . A broken  $C_4$  symmetry then means that  $0 \neq \lambda'_{\xi,a} := \lambda'_{aa;\xi\xi} - \lambda'_{aa;\xi\xi}$ . By inspection of Eqs. (70) and (73), one sees that there are two ways the latter can be nonzero: (1) in the ( $\xi = n$ ) channel,  $\lambda'_{n,a}$  is proportional to anisotropic exchanges; and (2) in the ( $\xi = m$ ) channel,  $\lambda'_{m,a}$  contains both isotropic and anisotropic exchange constants, and is consequently much larger than  $\lambda'_{n,a}$ . From this analysis, it follows that the deviation from  $C_4$  symmetry as captured in  $D_{n\mathbf{k}}^{(1)}$  by  $\lambda'_{\xi,a}$  is largest for values of  $|\mathbf{k}|$  where the  $\lambda_{mm}$  contributions dominate over the  $\lambda_{nn}$  ones, i.e. at large  $|\mathbf{k}|$  (recall Eq. (97)). One can check that this is indeed the case, as is shown in Appendix G.

(ii). *Out-of-plane  $\theta(\mathbf{k})$  angular dependence.* The out-of-plane angular dependence illustrates quite clearly the dynamical constraints satisfied by  $D_{n\mathbf{k}}$ , as outlined

in Sec. VB 2. By inspection of Eq. (65), we define

$$\theta_- = \arctan\left(v_{ph}^{-1} \sqrt{v_{ph}^2 - v_m^2}\right), \quad (121)$$

$$\theta_+^{(1)}(|\mathbf{k}|) = \arcsin\left(v_m^{-1} \sqrt{v_{ph}^2 - 4\Delta'/|\mathbf{k}|^2}\right), \quad (122)$$

$$\theta_+^{(2)}(|\mathbf{k}|) = \arcsin\left(v_m^{-1} \sqrt{v_{ph}^2 - 4\Delta/|\mathbf{k}|^2}\right), \quad (123)$$

where  $\Delta' = \max(\Delta_0, \Delta_1)$ . Note that outside the domain of definition of  $\sqrt{\dots}$ , by continuity one fixes  $\theta_+^{(1,2)} := 0$ . The figure Fig. 4(a) can then be divided in four areas as follows:

- The vertical black band at angles  $\theta(\mathbf{k}) \in [\theta_+^{(1)}(|\mathbf{k}|), \theta_-]$  corresponds to values of  $(k_z, |\mathbf{k}|)$  such that energy and momentum conservation cannot be satisfied simultaneously because of the magnon gap  $\Delta$ ; therefore  $D_{n\mathbf{k}}^+ = 0 = D_{n\mathbf{k}}^-$ .
- For angles  $\theta(\mathbf{k}) > \theta_-$ , scattering of the “ph+m  $\rightarrow$  m” type becomes possible, i.e.  $D^- > 0$ . Meanwhile, following Eq. (65),  $D^+ = 0$ .
- Conversely, for  $\theta(\mathbf{k}) < \theta_+^{(2)}(|\mathbf{k}|)$ , scattering of the “ph  $\rightarrow$  m+m” type becomes possible, i.e.  $D^+ > 0$ , while  $D^- = 0$ .
- For  $\theta \in [\theta_+^{(2)}, \theta_+^{(1)}]$ , scattering of the “ph  $\rightarrow$  m+m” type is possible only in the valley with the smallest gap, while in the other no scattering can happen; therefore, in that region  $D^+ > 0$  but its value drops (without vanishing a priori) at the interface  $\theta(\mathbf{k}) = \theta_+^{(2)}(|\mathbf{k}|)$ .

(iii). *Dependence on  $|\mathbf{k}|$ .* In Fig. 4(b), we show the dependence of  $D_{n\mathbf{k}}$  as a function of the norm  $|\mathbf{k}|$  and the out-of-plane angle  $\theta$ . This plot displays divergences near the singular lines  $\theta_+^{(1,2)}, \theta_-$ , which can be attributed to the thresholds for magnon scattering just above the gaps.

The angular width  $\delta\theta(\mathbf{k})$  of the two black and darker regions bounded from the right by  $\theta_-$ , where scattering is forbidden in at least one of the two valleys, varies with  $|\mathbf{k}|$ . From Eq. (65), we see that this width scales like  $\delta\theta \sim (\Delta_\ell/v_{ph}|\mathbf{k}|)^2$ . These regions extend down to  $|\mathbf{k}| = 0$ , reflecting the fact that phonons with too little energy are unable to excite magnon pairs. The momentum magnitude thresholds for the excitation of magnon pairs are naturally given by  $k_1 = 2\Delta/v_{ph}$  and  $k_2 = 2\Delta'/v_{ph}$ .

## 7. Results for $\mathfrak{W}_{n\mathbf{k}n'\mathbf{k}'}^\ominus$

Although the angular dependences of the  $\mathfrak{W}_{n\mathbf{k}n'\mathbf{k}'}^{\ominus,qq'}$  skew-scattering rates are more intricate than those of  $D_{n\mathbf{k}}$ , a few general remarks can be made. In particular, in Fig. 5, where we plot  $\mathfrak{W}^{\ominus,-+}$  as a function of  $\theta$  and  $\varphi$  at fixed  $|\mathbf{k}'| = 0.8/a$ ,  $k_x = 0.2/a$ ,  $k_y = 0$ ,  $k_z = 0.1/a$  (and temperature  $T = 0.5T_0$ ), we have:



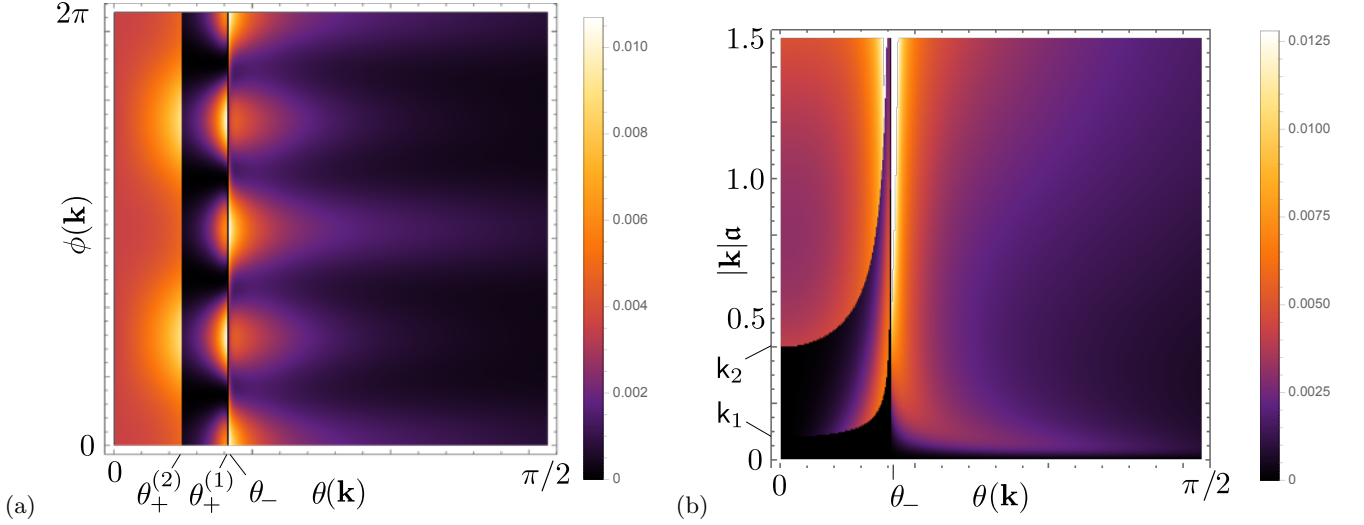


FIG. 4: Diagonal scattering rate  $D_{n\mathbf{k}}^{(1)}/\gamma_0$  at fixed temperature  $T = 0.5T_0$  and in polarization  $n = 0$ . (a) as a function of  $\theta(\mathbf{k}) = \arccos(k_z/|\mathbf{k}|) \in [0, \pi/2]$  (horizontal axis) and  $\phi(\mathbf{k}) = \text{Arg}(k_x + ik_y) \in [0, 2\pi]$  (vertical axis) for fixed  $|\mathbf{k}| = 0.5/a$ . (b) as a function of  $\theta(\mathbf{k}) = \arccos(k_z/|\mathbf{k}|) \in [0, \pi/2]$  (horizontal axis) and  $|\mathbf{k}|a$  (vertical axis) for fixed  $\phi(\mathbf{k}) = 0$ . Other parameter values are explored in App. G.

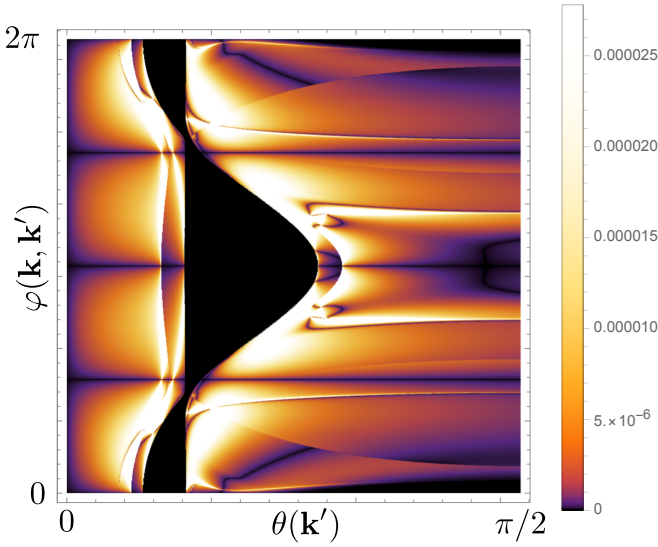


FIG. 5: Skew-scattering rate  $\mathfrak{W}_{n\mathbf{k}n'\mathbf{k}'}^{\ominus,--}/\gamma_0$  as a function of  $\theta(\mathbf{k}') \in [0, \pi/2]$  (horizontal axis) and  $\varphi(\mathbf{k}, \mathbf{k}') = \phi(\mathbf{k}') - \phi(\mathbf{k})$  (vertical axis) for fixed  $|\mathbf{k}'| = 0.8/a$ ,  $k_x = 0$ ,  $k_y = 0.2/a$ ,  $k_z = 0.1/a$ ,  $\mathbf{m}_0 = 0.05 \hat{z}$  and temperature  $T = 0.5 T_0$ . Other parameter values are explored in App. G. Note that the colorbar is not scaled linearly.

- Although  $k_z \neq 0$ , we can still take advantage of the  $k'_z \leftrightarrow -k'_z$  symmetry, and it is sufficient to consider  $\theta(\mathbf{k}') \in [0, \pi/2]$ . This comes from the fact that, for purely planar magnons, the phonon momenta  $k_z, k'_z$  are not coupled. Meanwhile there is a priori no  $\varphi(\mathbf{k}, \mathbf{k}') \leftrightarrow -\varphi(\mathbf{k}, \mathbf{k}')$  symmetry except when

$\mathbf{k}$  is along one of the high-symmetry axes of the crystal, as is the case here (cf.  $k_y = 0$ ).

- The vertical black line at  $\theta(\mathbf{k}') = \theta_-$  can still be identified, and corresponds to magnons being gapped as in  $D_{n\mathbf{k}}^{(1)}$ . However, in  $\mathfrak{W}^{\ominus}$ , the width and position of the gapped (black) zone now depend also on  $\varphi(\mathbf{k}, \mathbf{k}')$ , due to the second energy conservation constraint in  $\mathfrak{W}^{\ominus}$  (a feature absent in  $D^{(1)}$  where there is only one energy constraint).
- In Appendix G, we explore other orientations of in-plane  $(k_x, k_y)$ , and show that the features of  $\mathfrak{W}_{n\mathbf{k}n'\mathbf{k}'}^{\ominus,qq'}$  quoted above still hold. This is consistent with the above observations being consequences of the energy conservation constraints, which depend only of the *relative* angle  $\phi(\mathbf{k}) - \phi(\mathbf{k}')$  since both phonon and magnon dispersions are isotropic in the  $xy$  plane.
- In Fig. 5,  $\mathfrak{W}_{n\mathbf{k}n'\mathbf{k}'}^{\ominus,-+}$  also seems to vanish along certain special lines, especially those located at  $\varphi(\mathbf{k}, \mathbf{k}') = 0, \pi/2, \pi, 3\pi/2, 2\pi$ . These features are *not* independent of the orientation  $\phi(\mathbf{k})$ ; in fact they are salient features of the in-plane momenta being along the high-symmetry axes of the crystal. Thus, they do not result from energy conservation constraints, but from subtle effects in the structure of Eq. (66).

Finally, we point out that the values of  $\mathfrak{W}^{\ominus}$  in Fig. 5 are small compared to the values of  $D^{(1)}$  obtained for similar values of momenta. This can be understood from the combination of (1) the anti-detailed-balance structure of  $\mathfrak{W}^{\ominus}$ , from which it follows that  $\mathfrak{W}_{n\mathbf{k},n'\mathbf{k}'}^{\ominus,qq'} + \mathfrak{W}_{n-\mathbf{k},n'-\mathbf{k}'}^{\ominus,qq'} =$



$O(\mathbf{m}_0)$  as shown in Sec. IV A, and (2) the  $C_2$  symmetry of the system around the  $\hat{z}$  axis, which (since for planar magnons  $k_z \leftrightarrow -k_z$  is a symmetry) entails  $\mathfrak{W}_{n\mathbf{k},n'\mathbf{k}'}^{\ominus,qq'} = \mathfrak{W}_{n-\mathbf{k},n'-\mathbf{k}'}^{\ominus,qq'}$ . Thus  $\mathfrak{W}_{n\mathbf{k},n'\mathbf{k}'}^{\ominus,qq'} = O(\mathbf{m}_0)$  itself. This, together with the analysis given in Sec. V C 4 showing that terms which are odd in  $\mathbf{m}_0$  are also proportional to anisotropic couplings, implies that  $\mathfrak{W}_{n\mathbf{k},n'\mathbf{k}'}^{\ominus,qq'}$  is indeed typically much smaller than  $D_{n\mathbf{k}}^{(1)}$ .

### G. Discussion of the results in absolute scales

Here we discuss the absolute scales of  $\kappa_L$ ,  $\varrho_H$  and  $\kappa_H$  we obtain using the parameter values from Table VI and those in the figure captions. First it is instructive to estimate the basic scales for thermal conductivity and temperature derived from phonons, which define the scales for our numerical plots. Using the phonon velocity for CFTD,  $v_{\text{ph}}^{\text{CFTD}} = 4 \cdot 10^3 \text{ m}\cdot\text{s}^{-1}$  and its in-plane lattice parameter  $\mathbf{a}^{\text{CFTD}} = 5.7 \cdot 10^{-10} \text{ m}$ , we find (see Table V),

- $\kappa_0^{\text{CFTD}} = 0.17 \text{ W}\cdot\text{K}^{-1}\cdot\text{m}^{-1}$ ,
- $T_0^{\text{CFTD}} = 54 \text{ K}$ ,
- $\gamma_0 = 7.0 \cdot 10^{12} \text{ Hz}$ .

Note that these scales do not vary greatly for many materials. For example, in  $\text{La}_2\text{CuO}_4$ , we find  $\kappa_0^{\text{LCO}} = 0.38 \text{ W}\cdot\text{K}^{-1}\cdot\text{m}^{-1}$  and  $T_0^{\text{LCO}} = 80 \text{ K}$ . Importantly, the scale  $\kappa_0$  is order one in SI units, which allows a roughly direct comparison with most data.

Next we can use the actual computed values to see what this mechanism predicts for the “test” material CFTD. We have at  $T \approx 0.5T_0 \approx 27 \text{ K}$ ,

- $\kappa_L^{\text{CFTD}} \approx 125\kappa_0 \approx 22 \text{ W}\cdot\text{K}^{-1}\cdot\text{m}^{-1}$  for any of the  $\gamma_{\text{ext}}$  values presented in Fig. 2(a),
- for  $\gamma_{\text{ext}} = 10^{-4}\gamma_0 = 7.0 \cdot 10^8 \text{ Hz}$ ,  $T_\lambda^{*,\text{CFTD}} \approx 0.3T_0 \approx 16 \text{ K}$ ,
- for  $\gamma_{\text{ext}} = 10^{-7}\gamma_0 = 7.0 \cdot 10^5 \text{ Hz}$ ,  $T_\lambda^{*,\text{CFTD}} \approx 0.1T_0 \approx 5.4 \text{ K}$ ,
- $\varrho_H^{\text{CFTD}} \approx 2 \cdot 10^{-5}\varrho_0 \approx 1.2 \cdot 10^{-4} \text{ K}\cdot\text{m}\cdot\text{W}^{-1}$ ,
- $|\theta_H^{\text{CFTD}}| \approx 2.6 \cdot 10^{-3}$ ,
- $|\kappa_H^{\text{CFTD}}| \approx 5.8 \cdot 10^{-2} \text{ W}\cdot\text{K}^{-1}\cdot\text{m}^{-1}$ .

Note that  $\kappa_L$ ,  $\kappa_H$  and  $\theta_H$  all depend on the choice of values for  $\gamma_{\text{ext}}$ .

## VI. CONCLUSIONS

### A. Summary of results and method

In this paper, we studied the problem of scattering of phonons due to a weak *intrinsic* (i.e. without disorder)

coupling to a fluctuating field  $Q$ , which is itself a quantum mechanical degree of freedom. Using the T-matrix formalism, we derived the scattering rates of phonons up to fourth order in coupling. The result is expressed generally, without any assumptions on the nature of the fluctuating field (i.e. it can be highly non-Gaussian), in terms of correlation functions of  $Q$ . Using these scattering rates in the Boltzmann equation leads to general expressions for the thermal conductivity tensor, and, when symmetry allows, a non-vanishing thermal Hall effect. A central result is that the skew scattering of phonons (which we define sharply as a scattering component which obeys an *anti*-detailed balance relation), and hence the thermal Hall conductivity, is proportional to a four-point correlation function of  $Q$ , which we give explicitly. We highlight throughout the various constraints due to symmetry (both exact and approximate), unitarity, and thermal equilibrium.

As an illustration of the method, we applied these results to the case where the fluctuating field  $Q$  arises from spin wave (magnon) excitations of an ordered two-sublattice antiferromagnet. We model the latter via standard spin wave theory, for which phase space constraints imply that the dominant contribution arises from bilinears in the creation/annihilation operators of the spin waves. We obtain a general formula for the second order and fourth order scattering rates in terms of the dispersion of phonons and magnons, and the spin-lattice coupling constants. To obtain concrete results, we focus in particular on the limit in which the relevant magnons are acoustic, and we assume tetragonal symmetry and two-dimensionality of the magnons (but we retain the three dimensionality of the phonons). Under these assumptions we obtain all the (seven) symmetry-allowed spin-lattice coupling interactions, and calculate the second order and fourth order scattering rates, and thereby the thermal conductivity, including a phenomenological parallel scattering rate of phonons due to other mechanisms, e.g. boundary and impurity scattering. The final formulae are evaluated via numerical integration for representative model parameters. We observe a number of distinct scattering regimes, which we identify with features in the longitudinal thermal conductivity. We obtain a non-vanishing thermal Hall effect, in agreement with general symmetry arguments. Please see Sec. V for details.

### B. About (anti-)detailed balance

The detailed-balance and anti-detailed-balance relations, Eq. (4), played an important role in our discussion of the thermal Hall effect. A few comments on their nature and implications are appropriate.

*Quasi-equilibrium assumption:* These detailed-balance relations arise (as generalizations of the Kubo-Martin-Schwinger relations [32]) from the assumption that the  $Q$  fields relax to equilibrium between two scattering events.

This is typical in a linear response regime, when transport is dominated by the contribution of well-defined quasiparticles and drag effects are negligible.

*Role of the self-energy:* Within our treatment, the relations we obtain rely on the fact that, *at the order considered*, the equilibrium phonon distribution is the unperturbed one (this is shown in particular in Appendix C 3). At a general order in perturbation theory, this is not guaranteed a priori, because the phonons are renormalized by an interaction-induced self-energy whose real part shifts the dispersion relation and hence the equilibrium populations. However, within the quasi-particle picture, it seems likely that this assumption of a preserved spectrum of bare phonons is not necessary, and the (anti-)detailed-balance relations should hold for the *renormalized* phonon quasiparticles.

*No two-point contributions to the Hall effect:* The detailed-balance relations enforce that all terms involved in the calculation of the thermal Hall conductivity which contain two-point correlation functions of the  $Q$  fields cancel each other and therefore provide no contributions to  $\kappa_H$ . This relies on the linear-response limit: the cancellation occurs when we expand the collision integral to linear order in the  $\delta N$  out-of-equilibrium populations.

### C. Relation to other work

While we are not aware of any general results on the intrinsic phonon Hall conductivity due to scattering, there are a number of complementary theoretical papers as well as some prior work which overlap a small part of our results. The specific problem of phonons scattering from magnons was studied long ago to the leading second order in the coupling by Cottam [24]. That work, which assumed the isotropic SU(2) invariant limit, agrees with our calculations when these assumptions are imposed. The complementary mechanism of intrinsic phonon Hall effect due to phonon Berry curvature was studied by many authors [10, 33–35], including how the phonon Berry curvature is induced by spin-lattice coupling in Ref. [11]. The majority of recent theoretical work has concentrated on *extrinsic* effects due to scattering of phonons by defects [36–39]. The pioneering paper of Mori *et al.* [9] in particular recognized the importance of higher order contributions to scattering for the Hall effect, and is in some ways a predecessor to our work.

### D. General observations

While often times scattering is regarded as a process which destroys coherence and suppresses interesting dynamical phenomena, our work reveals that higher order scattering probes highly non-trivial structure of correlations. Due to the constraints of detailed balance, the skew scattering, appropriately defined, contains only contributions of  $O(Q^4)$  and no terms of lower order in  $Q$ ,

and so can in principle directly reveal subtle structures in the quantum correlations, without a need for subtraction. Measurements of such skew scattering of phonons—which *a priori* include but are not limited to the thermal Hall effect—might therefore be considered a probe of the quantum material hosting those phonons. Taking advantage of this potential opportunity is a challenge to experiment, as well as to theory, which should interpret the results and predict systems to maximize the effects.

We would like to comment on the analysis of thermal Hall effect experiments in quantum materials. As is well-known, thermal Hall conductivity is generally a small effect. In particular, the dimensionless measure of the Hall angle,  $\theta_H = \tan^{-1}(\kappa_H^{xy}/\kappa_H^{xx})$  is always much less than  $\pi/2$  by two or more orders of magnitude, even in systems where thermal Hall effect is lauded as “huge”. (An actually large thermal Hall angle ( $\theta_H = O(1)$ ) is obtained only the quantum thermal Hall regime when phonons are ballistic and edge states dominate over the bulk phonon contributions, which is extraordinarily difficult to achieve.) For small  $\theta_H$ , the skew scattering contributions are perturbative to the thermal conductivity, i.e. proportional to the latter rate  $1/\tau_{\text{skew}}$ . Dimensional reasoning implies that therefore  $\kappa_H \sim \tau^2/\tau_{\text{skew}}$ , where  $\tau$  is the standard, non-skew scattering time. This means that the thermal Hall *conductivity* has a very strong dependence on  $\tau$ , which is often sample-dependent and of course grows with sample quality, implying that the thermal Hall conductivity is larger in cleaner samples.

This dependence also means that  $\kappa_H$  itself, as well as the dimensionless Hall angle  $\theta_H \sim \kappa_H/\kappa_L$  depend not only on the skew scattering but also the ordinary scattering. Since the latter receives contributions from many different mechanisms, which may themselves have strong temperature and field dependence, neither  $\kappa_H$  itself nor  $\kappa_H/\kappa_L$  are ideal quantities to examine to probe the physics of skew scattering. Instead, we suggest that the thermal Hall *resistivity*,  $\varrho_H \equiv -\kappa_H/\kappa_L^2$ , is the quantity which is most easily interpreted physically. This quantity is independent of the non-skew scattering, at least when the latter is largely momentum-independent, and is always independent of the overall scale of non-skew scattering. The temperature and field dependence of  $\varrho_H$  is generally expected to be simpler than that of the other quantities, at least when phonon skew scattering is the dominant mechanism for the Hall effect. This expectation is true not only when the skew scattering is intrinsic, as studied here, but also for extrinsic skew scattering due to defects.

### E. Future directions

Our general formalism can be applied very broadly. In particular, because it does not require any assumptions on the nature of the  $Q$  correlations, it may be applied directly to exotic states, to quantum or classical critical points, or to situations in which the  $Q$  field is a compos-

ite operator. We will present an application to fermionic systems, including the spinon Fermi surface spin liquid, in an upcoming paper. Apart from other specific applications which may be easily imagined, it would also be interesting to explore further how general properties of four-point correlations of  $Q$  may be detected via phonon skew scattering. In particular, the correlations which enter the scattering rates are not obviously time-ordered, and we wonder if these might contain some information on many-body chaos (Ref. [4]).

Despite the generality of our formulation, it is still specialized in several ways. We consider only scattering contributions to the phonon Boltzmann equation. In general the interactions with fields  $Q$  will both induce scattering and modify the dynamics of the phonons in a non-dissipative way, e.g. induce phonon Berry phases [11]. While we believe it is usually the case that scattering is dominant, a more complete treatment including both effects would be of interest. Furthermore, in this paper we fully “integrate out” the electronic degrees of freedom, and follow the distribution function of the phonons only. More generally, there are coupled modes of phonons and electronic states, and one can consider the distributions for these coupled modes. One expects such effects are important largely when there are reso-

nances between phonons and electronic excitations. All these problems could be addressed via a Keldysh treatment of coupled quantum kinetic equations, which is an interesting subject for future work.

## ACKNOWLEDGMENTS

We thank Mengxing Ye for valuable discussions, as well as Xiao Chen and Jason Iaconis for a collaboration on a related topic. We also sincerely acknowledge Roser Valentí for her encouragements and enthusiasm. The premises of this project were funded by the Agence Nationale de la Recherche through Grant ANR-18-ERC2-0003-01 (QUANTEM). The bulk of this project was funded by the European Research Council (ERC) under the European Union’s Horizon 2020 research and innovation program (Grant agreement No. 853116, acronym TRANSPORT). L.B. was supported by the DOE, Office of Science, Basic Energy Sciences under Award No. DE-FG02-08ER46524. It befits us to acknowledge the hospitality of the KITP, where part of this project was carried out, funded under NSF Grant NSF PHY-1748958.

- 
- [1] Léo Mangeolle, Leon Balents, and Lucile Savary, “Phonon thermal hall conductivity from scattering with collective fluctuations,” to appear (2022).
- [2] J. M. Luttinger, “Theory of thermal transport coefficients,” *Phys. Rev.* **135**, A1505–A1514 (1964).
- [3] Xiao Chen, Jason Iaconis, Leon Balents, and Lucile Savary, “Scaling and methodology for thermal conductivity in quantum magnets,” to appear.
- [4] Brian Swingle, “Unscrambling the physics of out-of-time-order correlators,” *Nature Phys* **14**, 988–990 (2018).
- [5] Yuan Wan and N. P. Armitage, “Resolving continua of fractional excitations by spinon echo in THz 2D coherent spectroscopy,” *Phys. Rev. Lett.* **122**, 257401 (2019).
- [6] L. J. P. Ament, M. van Veenendaal, T. P. Devereaux, J. P. Hill, and J. van den Brink, “Resonant inelastic x-ray scattering studies of elementary excitations,” *Rev. Mod. Phys.* **83**, 705–767 (2011).
- [7] Lucile Savary and T. Senthil, “Probing hidden orders with resonant inelastic x-ray scattering,” arXiv:1506.04752 (2015), arXiv:1506.04752 [cond-mat.str-el].
- [8] Lev Davidovich Landau and Evgenii Mikhailovich Lifshitz, *Quantum mechanics: non-relativistic theory*, Vol. 3 (Elsevier, 2013).
- [9] Michiyasu Mori, Alexander Spencer-Smith, Oleg P. Sushkov, and Sadamichi Maekawa, “Origin of the phonon Hall effect in rare-earth garnets,” *Phys. Rev. Lett.* **113**, 265901 (2014).
- [10] Tao Qin, Jianhui Zhou, and Junren Shi, “Berry curvature and the phonon hall effect,” *Phys. Rev. B* **86**, 104305 (2012).
- [11] Mengxing Ye, Lucile Savary, and Leon Balents, “Phonon Hall viscosity in magnetic insulators,” arXiv:2103.04223 (2021), arXiv:2103.04223 [cond-mat.str-el].
- [12] L. Sheng, D. N. Sheng, and C. S. Ting, “Theory of the phonon Hall effect in paramagnetic dielectrics,” *Phys. Rev. Lett.* **96**, 155901 (2006).
- [13] Yu. Kagan and L. A. Maksimov, “Anomalous hall effect for the phonon heat conductivity in paramagnetic dielectrics,” *Phys. Rev. Lett.* **100**, 145902 (2008).
- [14] Gordon Baym and Leo P. Kadanoff, “Conservation laws and correlation functions,” *Phys. Rev.* **124**, 287–299 (1961).
- [15] Henrik Bruus and Karsten Flensberg, *Many-Body Quantum Theory in Condensed Matter Physics* (Oxford Graduate Texts, 2004).
- [16] Suhas Gangadharaiah, A. L. Chernyshev, and Wolfram Brenig, “Thermal drag revisited: Boltzmann versus Kubo,” *Phys. Rev. B* **82**, 134421 (2010).
- [17] Notice, however, that this coincidence does not survive the breaking of time reversal symmetry.
- [18] L. Benfatto and M. B. Silva Neto, “Field dependence of the magnetic spectrum in anisotropic and dzyaloshinskii-moriya antiferromagnets. i. theory,” *Phys. Rev. B* **74**, 024415 (2006).
- [19] A.V. Bazhenov, C.B. Rezchikov, and I.S. Smirnova, “Lattice dynamics of the  $\text{La}_2\text{CuO}_4$  cmca orthorhombic phase at  $\kappa = 0$ ,” *Physica C: Superconductivity* **273**, 9–20 (1996).
- [20] G. Laurence and D. Petitgrand, “Thermal conductivity and magnon-phonon resonant interaction in antiferromagnetic  $\text{FeCl}_2$ ,” *Phys. Rev. B* **8**, 2130–2138 (1973).

- [21] In the absence of a magnetic field, and an “alternating” Dzyaloshinskii-Moriya (DM) interaction which we do not consider here.
- [22] Xiaou Zhang, Yinhan Zhang, Satoshi Okamoto, and Di Xiao, “Thermal Hall effect induced by magnon-phonon interactions,” *Phys. Rev. Lett.* **123**, 167202 (2019).
- [23] T. M. Tritt, *Thermal conductivity* (Kluwer Academic Plenum Publishers, 2004).
- [24] M G Cottam, “Spin-phonon interactions in a Heisenberg antiferromagnet. II. The phonon spectrum and spin-lattice relaxation rate,” *Journal of Physics C: Solid State Physics* **7**, 2919–2932 (1974).
- [25] Peter Carruthers, “Theory of thermal conductivity of solids at low temperatures,” *Rev. Mod. Phys.* **33**, 92–138 (1961).
- [26] T. Hahn, “Cuba—a library for multidimensional numerical integration,” *Computer Physics Communications* **168**, 78–95 (2005).
- [27] A. A. Maradudin and S. H. Vosko, “Symmetry properties of the normal vibrations of a crystal,” *Rev. Mod. Phys.* **40**, 1–37 (1968).
- [28] N. B. Christensen, H. M. Rønnow, D. F. McMorrow, A. Harrison, T. G. Perring, M. Enderle, R. Coldea, L. P. Regnault, and G. Aeppli, “Quantum dynamics and entanglement of spins on a square lattice,” *Proceedings of the National Academy of Sciences* **104**, 15264–15269 (2007), <https://www.pnas.org/doi/pdf/10.1073/pnas.0703293104>.
- [29] Bastien Dalla Piazza, M Mourigal, Niels Bech Christensen, GJ Nilsen, P Tregenna-Piggott, TG Perring, Mechtild Enderle, Desmond Francis McMorrow, DA Ivanov, and Henrik Moodysson Rønnow, “Fractional excitations in the square-lattice quantum antiferromagnet,” *Nature Physics* **11**, 62–68 (2015).
- [30] H. M. Rønnow, D. F. McMorrow, R. Coldea, A. Harrison, I. D. Youngson, T. G. Perring, G. Aeppli, O. Syljuåsen, K. Lefmann, and C. Rischel, “Spin dynamics of the 2d spin  $\frac{1}{2}$  quantum antiferromagnet Copper Deuterioformate Tetrahydrate (CFTD),” *Phys. Rev. Lett.* **87**, 037202 (2001).
- [31] Hiroshi Kameyama, Yoshihiro Ishibashi, and Yutaka Yakagi, “Elastic constants in cupric formate tetrahydrate single crystals,” *Journal of the Physical Society of Japan* **35**, 1450–1455 (1973).
- [32] Paul C Martin and Julian Schwinger, “Theory of many-particle systems. i,” *Physical Review* **115**, 1342 (1959).
- [33] Takuma Saito, Kou Misaki, Hiroaki Ishizuka, and Naoto Nagaosa, “Berry phase of phonons and thermal Hall effect in nonmagnetic insulators,” *Phys. Rev. Lett.* **123**, 255901 (2019).
- [34] Lifa Zhang, Jie Ren, Jian-Sheng Wang, and Baowen Li, “Topological nature of the phonon Hall effect,” *Phys. Rev. Lett.* **105**, 225901 (2010).
- [35] Yunchao Zhang, Yanting Teng, Rhine Samajdar, Subir Sachdev, and Mathias S. Scheurer, “Phonon Hall viscosity from phonon-spinon interactions,” *Phys. Rev. B* **104**, 035103 (2021).
- [36] Xiao-Qi Sun, Jing-Yuan Chen, and Steven A Kivelson, “Large extrinsic phonon thermal Hall effect from resonant scattering,” arXiv preprint arXiv:2109.12117 (2021).
- [37] Haoyu Guo and Subir Sachdev, “Extrinsic phonon thermal Hall transport from Hall viscosity,” *Phys. Rev. B* **103**, 205115 (2021).
- [38] Haoyu Guo, Darshan G Joshi, and Subir Sachdev, “Resonant side-jump thermal Hall effect of phonons coupled to dynamical defects,” arXiv preprint arXiv:2201.11681 (2022).
- [39] Benedetta Flebus and AH MacDonald, “Charged defects and phonon Hall effects in ionic crystals,” arXiv preprint arXiv:2106.13889 (2021).

## Appendix A: Strain tensor

In Sec. V C we employ a continuum model of the spin-phonon system. The phonons themselves correspondingly derive from the theory of continuum elasticity, which has the Hamiltonian density

$$\mathcal{H}_{\text{el}} = \frac{1}{2\rho}\Pi_{\mu}^2 + \frac{1}{2}C_{\alpha\beta\gamma\delta}\mathcal{E}^{\alpha\beta}\mathcal{E}^{\gamma\delta}. \quad (\text{A1})$$

Within this appendix,  $\rho$  is the mass density (we will take  $\rho V = M_{\text{uc}}N_{\text{uc}}$ ) and  $C_{\alpha\beta\gamma\delta}$  is a rank four tensor of elastic constants, which can be taken to satisfy  $C_{\alpha\beta\gamma\delta} = C_{\beta\alpha\gamma\delta} = C_{\alpha\beta\delta\gamma} = C_{\gamma\delta\alpha\beta}$ . The canonical variables of this classical field theory are the displacement field  $u_{\mu}$  and its canonically conjugate momentum  $\Pi_{\mu}$ . Due to translational and rotational symmetry, the Hookian potential energy is expressed solely through the strain tensor,

$$\mathcal{E}^{\alpha\beta}(\mathbf{R}) = \frac{1}{2}(\partial_{\alpha}u_{\beta} + \partial_{\beta}u_{\alpha}). \quad (\text{A2})$$

By construction the strain is a symmetric tensor in its two indices, i.e.  $\mathcal{E}^T = \mathcal{E}$ . Define the Fourier transforms

$$u_{\mu}(\mathbf{x}) = \frac{1}{\sqrt{V}} \sum_{\mathbf{k}} e^{i\mathbf{k}\cdot\mathbf{x}} u_{\mu,\mathbf{k}}, \quad \Pi_{\mu}(\mathbf{x}) = \frac{1}{\sqrt{V}} \sum_{\mathbf{k}} e^{i\mathbf{k}\cdot\mathbf{x}} \Pi_{\mu,\mathbf{k}}. \quad (\text{A3})$$

Here since  $u_{\mu}(\mathbf{x})$  and  $\Pi_{\mu}(\mathbf{x})$  are real fields, we have  $u_{n,-\mathbf{k}} = u_{n\mathbf{k}}^*$  and  $\Pi_{n,-\mathbf{k}} = \Pi_{n\mathbf{k}}^*$ . The Fourier space fields satisfy the commutation relations

$$[\Pi_{\mu,\mathbf{k}}, u_{\nu,\mathbf{k}'}] = i\delta_{\mu\nu}\delta_{\mathbf{k}+\mathbf{k}',\mathbf{0}}. \quad (\text{A4})$$

We obtain

$$H_{\text{el}} = \sum_{\mathbf{k}} \left\{ \frac{1}{2\rho}\Pi_{\mu,-\mathbf{k}}\Pi_{\mu,\mathbf{k}} + \frac{1}{2}\mathcal{K}_{\alpha\beta}(\mathbf{k})u_{\alpha,-\mathbf{k}}u_{\beta,\mathbf{k}} \right\}, \quad (\text{A5})$$

with

$$\mathcal{K}_{\alpha\beta}(\mathbf{k}) = C_{\alpha\gamma\beta\delta}k_{\gamma}k_{\delta}. \quad (\text{A6})$$

The matrix  $\mathcal{K}_{\alpha\beta}$  is by construction real and symmetric, and hence has real eigenvalues  $\mathcal{K}_n$ , which additionally must be positive for stability. We define the eigenvalues and eigenvectors  $\varepsilon_n^{\alpha}$  via

$$\mathcal{K}_{\alpha\beta}(\mathbf{k})\varepsilon_n^{\beta}(\mathbf{k}) = \mathcal{K}_n(\mathbf{k})\varepsilon_n^{\alpha}(\mathbf{k}), \quad (\text{A7})$$

with  $\varepsilon_n^\alpha(-\mathbf{k}) = (\varepsilon_n^\alpha(\mathbf{k}))^*$  and the standard normalization  $\sum_\alpha (\varepsilon_n^\alpha(\mathbf{k}))^* \varepsilon_{n'}^\alpha(\mathbf{k}) = \delta_{nn'}$ . Now we make the change of basis

$$u_{\mu\mathbf{k}} = \sum_n \varepsilon_n^\mu(\mathbf{k}) u_{n\mathbf{k}}, \quad \Pi_{\mu\mathbf{k}} = \sum_n \varepsilon_n^\mu(\mathbf{k}) \Pi_{n\mathbf{k}}, \quad (\text{A8})$$

which gives

$$[\Pi_{n\mathbf{k}}, u_{n'\mathbf{k}'}] = i\delta_{nn'}\delta_{\mathbf{k}+\mathbf{k}',\mathbf{0}}, \quad (\text{A9})$$

and

$$H_{\text{el}} = \sum_{n,\mathbf{k}} \left\{ \frac{1}{2\rho} \Pi_{n,-\mathbf{k}} \Pi_{n,\mathbf{k}} + \frac{1}{2} \mathcal{K}_n(\mathbf{k}) u_{n,-\mathbf{k}} u_{n,\mathbf{k}} \right\}. \quad (\text{A10})$$

Now we can finally define creation/annihilation operators

$$\begin{aligned} u_{n\mathbf{k}} &= \frac{1}{\sqrt{2}} \frac{1}{(\rho\mathcal{K}_n)^{1/4}} (a_{n\mathbf{k}} + a_{n,-\mathbf{k}}^\dagger), \\ \Pi_{n\mathbf{k}} &= i \frac{1}{\sqrt{2}} (\rho\mathcal{K}_n)^{1/4} (a_{n\mathbf{k}} - a_{n,-\mathbf{k}}^\dagger), \end{aligned} \quad (\text{A11})$$

with canonical boson operators

$$[a_{n\mathbf{k}}, a_{n'\mathbf{k}'}^\dagger] = \delta_{nn'}\delta_{\mathbf{k},\mathbf{k}'}, \quad (\text{A12})$$

and the Hamiltonian

$$H_{\text{el}} = \sum_{n\mathbf{k}} \omega_{n\mathbf{k}} a_{n\mathbf{k}}^\dagger a_{n\mathbf{k}}, \quad (\text{A13})$$

and

$$\omega_{n\mathbf{k}} = \sqrt{\frac{\mathcal{K}_n(\mathbf{k})}{\rho}}. \quad (\text{A14})$$

Having finally arrived at the canonical phonon operators, we recombine the several steps of the above procedure to obtain the expression for the displacement field,

$$u_\mu(\mathbf{x}) = \frac{1}{\sqrt{V}} \sum_{n\mathbf{k}} \frac{1}{\sqrt{2\rho\omega_{n\mathbf{k}}}} (a_{n\mathbf{k}} + a_{n,-\mathbf{k}}^\dagger) \varepsilon_{n\mathbf{k}}^\mu e^{i\mathbf{k}\cdot\mathbf{x}}. \quad (\text{A15})$$

Now we can use the definition in Eq. (71) of the strain to obtain

$$\mathcal{E}^{\mu\nu}(\mathbf{x}) = \quad (\text{A16})$$

$$\frac{1}{\sqrt{V}} \sum_{n\mathbf{k}} \frac{1}{\sqrt{2\rho\omega_{n\mathbf{k}}}} (a_{n\mathbf{k}} + a_{n,-\mathbf{k}}^\dagger) \frac{i}{2} (k^\mu \varepsilon_{n\mathbf{k}}^\nu + k^\nu \varepsilon_{n\mathbf{k}}^\mu) e^{i\mathbf{k}\cdot\mathbf{x}}. \quad (\text{A17})$$

Now let us consider the coupling of the strain to the continuum spin fluctuations, Eq. (72) of the main text. The full spin-lattice coupling in three dimensions is written as

$$H'_{s-1} = \sum_z \int dxdy \mathcal{E}^{\alpha\beta}(\mathbf{x}) \lambda_{ab;\xi\xi'}^{\alpha\beta} n_0^{-\xi-\xi'} \eta_{a\xi\mathbf{x}} \eta_{b\xi'\mathbf{x}}. \quad (\text{A18})$$

Note the sum over discrete 2d layers. We now insert the Fourier expansion of the strain from Eq. (A16) and the corresponding Fourier expansion of the magnetic fluctuations, which we repeat here:

$$\eta_{a\xi\mathbf{x}} = \frac{1}{\sqrt{A_{2d}}} \sum_{\mathbf{q}} \eta_{a\xi\mathbf{q},z} e^{i\mathbf{q}\cdot\mathbf{x}}. \quad (\text{A19})$$

In this equation, and in the rest of this section, we are careful to denote two-dimensional vectors with an underline. Since magnetic fluctuations in different layers are taken as independent, we do not introduce a  $z$ -component of the wavevector for the magnons, and simply leave  $z$  explicitly as a layer index for these fields. Note also the prefactor Eq. (A19) therefore involves the square root of the two dimensional area of a single plane,  $A_{2d}$ .

With this in mind, we obtain from Eq. (A18)

$$\begin{aligned} H'_{s-1} &= \frac{1}{\sqrt{V}} \sum_z \sum_{\mathbf{k},\mathbf{p}} \lambda_{ab;\xi\xi'}^{\mu\nu} n_0^{-\xi-\xi'} \frac{1}{\sqrt{2\rho\omega_{n\mathbf{k}}}} e^{ik_z z} \quad (\text{A20}) \\ &\times \frac{i}{2} (k^\mu \varepsilon_{n\mathbf{k}}^\nu + k^\nu \varepsilon_{n\mathbf{k}}^\mu) (a_{n\mathbf{k}} + a_{n,-\mathbf{k}}^\dagger) \eta_{a\xi,\underline{\mathbf{p}}-\frac{1}{2}\mathbf{k},z} \eta_{b\xi',-\underline{\mathbf{p}}-\frac{1}{2}\mathbf{k},z}. \end{aligned}$$

From here we can see that

$$\begin{aligned} Q_{n\mathbf{k}} &= \frac{i}{2\sqrt{V}} \frac{(k^\mu \varepsilon_{n\mathbf{k}}^\nu + k^\nu \varepsilon_{n\mathbf{k}}^\mu)}{\sqrt{2\rho\omega_{n\mathbf{k}}}} \sum_{\xi\xi',ab} \lambda_{ab;\xi\xi'}^{\mu\nu} n_0^{-\xi-\xi'} \\ &\times \sum_z \sum_{\underline{\mathbf{p}}} e^{ik_z z} \eta_{a\xi,\underline{\mathbf{p}}-\frac{1}{2}\mathbf{k},z} \eta_{b\xi',-\underline{\mathbf{p}}-\frac{1}{2}\mathbf{k},z}. \end{aligned} \quad (\text{A21})$$

Next we use Eq. (74) to express this in terms of canonical bosons:

$$Q_{n\mathbf{k}} = \frac{i(k^\mu \varepsilon_{n\mathbf{k}}^\nu + k^\nu \varepsilon_{n\mathbf{k}}^\mu)}{4\sqrt{2V}\rho\omega_{n\mathbf{k}}} \sum_z \sum_{\mathbf{p}} \sum_{qq'} \sum_{\xi\xi'ab} \lambda_{ab;\xi\xi'}^{\mu\nu} n_0^{-\xi-\xi'} e^{ik_z z} (-1)^{\bar{\xi}(\delta_{a-1,\xi} + \frac{1+q}{2}) + \bar{\xi}'(\delta_{b-1,\xi'} + \frac{1+q'}{2})} i^{\bar{\xi} + \bar{\xi}'} \\ \times (\chi\Omega_{\delta_{a-1,\xi},\mathbf{p}-\frac{1}{2}\mathbf{k}})^{\bar{\xi}/2} (\chi\Omega_{\delta_{b-1,\xi'},-\mathbf{p}-\frac{1}{2}\mathbf{k}})^{\bar{\xi}'/2} b_{\mathbf{p}-\frac{1}{2}\mathbf{k},\delta_{a-1,\xi},z}^{q'} b_{-\mathbf{p}-\frac{1}{2}\mathbf{k},\delta_{b-1,\xi'},z}^{q'}. \quad (\text{A22})$$

We now define  $\ell_1 = \delta_{a-1,\xi} = 0, 1$  and  $\ell_2 = \delta_{b-1,\xi'}$ , which is inverted by  $a = 1 + \bar{\xi}\ell_1 + \bar{\xi}$  and  $b = 1 + \bar{\xi}'\ell_2 + \bar{\xi}'$ . This gives

$$Q_{n\mathbf{k}} = \frac{i(k^\mu \varepsilon_{n\mathbf{k}}^\nu + k^\nu \varepsilon_{n\mathbf{k}}^\mu)}{4\sqrt{2V}\rho\omega_{n\mathbf{k}}} \sum_z \sum_{\mathbf{p}} \sum_{qq'} \sum_{\xi\xi'\ell_1\ell_2} \lambda_{\xi\ell_1 + \bar{\xi} + 1, \xi'\ell_2 + \bar{\xi}' + 1; \xi, \xi'}^{\mu\nu} n_0^{-\xi-\xi'} e^{ik_z z} (-1)^{\bar{\xi}(\ell_1 + \frac{1+q}{2}) + \bar{\xi}'(\ell_2 + \frac{1+q'}{2})} i^{\bar{\xi} + \bar{\xi}'} \\ \times (\chi\Omega_{\ell_1, \mathbf{p}-\frac{1}{2}\mathbf{k}})^{\bar{\xi}/2} (\chi\Omega_{\ell_2, -\mathbf{p}-\frac{1}{2}\mathbf{k}})^{\bar{\xi}'/2} b_{\mathbf{p}-\frac{1}{2}\mathbf{k}, \ell_1, z}^{q'} b_{-\mathbf{p}-\frac{1}{2}\mathbf{k}, \ell_2, z}^{q'}. \quad (\text{A23})$$

From here, we recognize that  $Q_{n\mathbf{k}} = Q_{n\mathbf{k}}^-$  in Eq. (57), and thereby extract  $\mathcal{B}$ . We use  $V\rho = N_{\text{uc}}M_{\text{uc}}$ .

## Appendix B: General hydrodynamics of phonons

Our goal is to derive the thermal current carried by the phonons,

$$j^\mu = \frac{1}{V} \sum_{n\mathbf{k}} \bar{N}_{n\mathbf{k}} v_{n\mathbf{k}}^\mu \omega_{n\mathbf{k}}, \quad (\text{B1})$$

in order to extract the thermal conductivity tensor. This requires knowledge of the average phonon populations  $\bar{N}_{n\mathbf{k}}$ , which, in presence of a gradient of temperature, differ from their equilibrium values. These populations can be obtained by solving Boltzmann's equation

$$\partial_t \bar{N}_{n\mathbf{k}} + \mathbf{v}_{n\mathbf{k}} \cdot \nabla_{\mathbf{r}} \bar{N}_{n\mathbf{k}} = \mathcal{C}_{n\mathbf{k}}[\{\bar{N}_{n'\mathbf{k}'}\}], \quad (\text{B2})$$

where the collision integral  $\mathcal{C}_{n\mathbf{k}}[\{\bar{N}_{n'\mathbf{k}'}\}]$  depends on the populations in *all* ( $n', \mathbf{k}'$ ) states. To solve this equation, we expand the out-of-equilibrium populations around their equilibrium value as  $\bar{N}_{n\mathbf{k}} = N_{n\mathbf{k}}^{\text{eq}} + \delta\bar{N}_{n\mathbf{k}}$ . Within linear response, the perturbations can be considered small and we may expand the collision integral

$$\mathcal{C}_{n\mathbf{k}}[\{\bar{N}_{n'\mathbf{k}'}\}] = O_{n\mathbf{k}} + \sum_{n'\mathbf{k}'} \mathcal{C}_{n\mathbf{k}n'\mathbf{k}'} \delta\bar{N}_{n'\mathbf{k}'} + O(\delta\bar{N}^2), \quad (\text{B3})$$

around its value  $O_{n\mathbf{k}}$  in equilibrium. Since the thermal current must vanish in equilibrium,  $O_{n\mathbf{k}}$  must be zero (we go back to this statement in Sec. C 2 c). In Eq. (B3), the ‘‘collision matrix’’  $\mathcal{C}_{n\mathbf{k}n'\mathbf{k}'}$  is defined as the first-order Taylor coefficient, and one neglects the quadratic order in the perturbation. Formally inverting the collision matrix in the stationary Boltzmann equation (i.e. Eq. (B1) with  $\partial_t \bar{N} = 0$ ) leads to

$$\delta\bar{N}_{n\mathbf{k}} = C_{n\mathbf{k}n'\mathbf{k}'}^{-1} \frac{\omega_{n'\mathbf{k}'}}{k_B T^2} (N_{n'\mathbf{k}'}^{\text{eq}})^2 v_{n'\mathbf{k}'}^\nu \partial_\nu T. \quad (\text{B4})$$

From Eq. (B4) and Fourier's law, we can identify the components of the thermal conductivity tensor:

$$\frac{\kappa^{\mu\nu} \pm \kappa^{\nu\mu}}{2} = -\frac{1}{2k_B T^2} \frac{1}{V} \sum_{n\mathbf{k}n'\mathbf{k}'} \omega_{n\mathbf{k}} \omega_{n'\mathbf{k}'} v_{n\mathbf{k}}^\mu v_{n'\mathbf{k}'}^\nu \quad (\text{B5}) \\ \cdot \left( C_{n\mathbf{k},n'\mathbf{k}'}^{-1} e^{\beta\omega_{n'\mathbf{k}'}} (N_{n'\mathbf{k}'}^{\text{eq}})^2 \pm (n\mathbf{k} \leftrightarrow n'\mathbf{k}') \right).$$

This expression shows that a nonzero phonon Hall conductivity requires the factor in the second line to be nonzero, which is equivalent to

$$C_{n\mathbf{k},n'\mathbf{k}'} e^{\beta\omega_{n'\mathbf{k}'}} (N_{n'\mathbf{k}'}^{\text{eq}})^2 \neq C_{n'\mathbf{k}',n\mathbf{k}} e^{\beta\omega_{n\mathbf{k}}} (N_{n\mathbf{k}}^{\text{eq}})^2, \quad (\text{B6})$$

where the constraint is now on  $C_{n\mathbf{k},n'\mathbf{k}'}$  instead of its inverse. In other words, only the antisymmetric in  $n\mathbf{k} \leftrightarrow n'\mathbf{k}'$  part of  $C_{n\mathbf{k},n'\mathbf{k}'} e^{\beta\omega_{n'\mathbf{k}'}} (N_{n'\mathbf{k}'}^{\text{eq}})^2$  contributes to the Hall conductivity.

In order to proceed further analytically, and invert the scattering matrix, we separate diagonal from the off-diagonal parts in  $C_{n\mathbf{k}n'\mathbf{k}'} = -\delta_{nn'} \delta_{\mathbf{k},\mathbf{k}'} D_{n\mathbf{k}} + M_{n\mathbf{k}n'\mathbf{k}'}$ , and assume that  $D_{n\mathbf{k}} \gg \sum_{n'\mathbf{k}'} M_{n\mathbf{k}n'\mathbf{k}'}$ . This ought to be the case whenever the interactions are small, and/or if other damping processes are large. Then,  $C_{n\mathbf{k}n'\mathbf{k}'}^{-1} \approx -\delta_{nn'} \delta_{\mathbf{k},\mathbf{k}'} D_{n\mathbf{k}}^{-1} - M_{n\mathbf{k}n'\mathbf{k}'} D_{n\mathbf{k}}^{-1} D_{n'\mathbf{k}'}^{-1}$ . The antisymmetry in  $n\mathbf{k} \leftrightarrow n'\mathbf{k}'$  condition for the Hall conductivity mentioned above leads to the fact that the diagonal term contributes to the longitudinal conductivity, but not to the Hall part, and translates into

$$\frac{\kappa^{\mu\nu} - \kappa^{\nu\mu}}{2} =: \frac{1}{2k_B T^2} \frac{1}{V} \sum_{n\mathbf{k}n'\mathbf{k}'} \frac{\omega_{n\mathbf{k}} v_{n\mathbf{k}}^\mu}{D_{n\mathbf{k}}} \frac{\omega_{n'\mathbf{k}'} v_{n'\mathbf{k}'}^\nu}{D_{n'\mathbf{k}'}} \quad (\text{B7}) \\ \cdot [M_{n\mathbf{k},n'\mathbf{k}'} e^{\beta\omega_{n'\mathbf{k}'}} (N_{n'\mathbf{k}'}^{\text{eq}})^2 - (n\mathbf{k} \leftrightarrow n'\mathbf{k}')].$$

The longitudinal conductivity is

$$\kappa^{\mu\mu} = \frac{1}{k_B T^2} \frac{1}{V} \sum_{n\mathbf{k}n'\mathbf{k}'} \omega_{n\mathbf{k}} \omega_{n'\mathbf{k}'} v_{n\mathbf{k}}^\mu v_{n'\mathbf{k}'}^\mu \quad (\text{B8}) \\ \cdot \left[ \frac{\delta_{nn'} \delta_{\mathbf{k},\mathbf{k}'}}{D_{n\mathbf{k}}} + \frac{M_{n\mathbf{k},n'\mathbf{k}'}}{D_{n\mathbf{k}} D_{n'\mathbf{k}'}} \right] e^{\beta\omega_{n'\mathbf{k}'}} (N_{n'\mathbf{k}'}^{\text{eq}})^2.$$

Note that we will include all other (diagonal) scattering processes not taken into account here (e.g. boundary scattering, scattering by impurities, phonon-phonon scattering etc.) by adding a phenomenological relaxation rate  $\check{D}_{n\mathbf{k}}$  to the diagonal of the scattering matrix.

## Appendix C: From interaction terms to the collision integral

### 1. General method and definitions

We now aim at deriving an expression for the collision integral of Boltzmann's equation using kinetic theory methods. The probability for the system to be found in a given quantum state  $|\mathbf{i}\rangle = |i_p\rangle|i_s\rangle$  is governed by the master equation

$$\partial_t p_{i_p i_s} = \sum_{f_p f_s} [\Gamma_{f_p f_s \rightarrow i_p i_s} p_{f_p f_s} - \Gamma_{i_p i_s \rightarrow f_p f_s} p_{i_p i_s}], \quad (\text{C1})$$

where we will compute the transition rates  $\Gamma_{i_p i_s \rightarrow f_p f_s}$  using scattering theory. The probability of a phonon state  $|i_p\rangle$  is then obtained by summing over all possible spin configurations of the system,  $p_{i_p} = \sum_{i_s} p_{i_p i_s}$ . Assuming the phonon and spin probabilities are independent, i.e.  $p_{i_p i_s} = p_{i_p} p_{i_s}$ , and defining the transition rates  $\Gamma_{f_p \rightarrow i_p} = \sum_{i_s f_s} \Gamma_{f_p f_s \rightarrow i_p i_s} p_{f_s}$  between phonon states only, we obtain the master equation for the probabilities of phonon states. We may in turn express the collision integral in the RHS of Boltzmann's equation, which is given by the time evolution of the populations in each phonon state  $|i_p\rangle$  through the definition  $\mathcal{C}_{n\mathbf{k}}[\{\bar{N}_{n'\mathbf{k}'}\}] = \sum_{i_p} N_{n\mathbf{k}}(i_p) \partial_t p_{i_p}$ , in terms of transition rates between phonon states:

$$\mathcal{C}_{n\mathbf{k}}[\{\bar{N}_{n'\mathbf{k}'}\}] = \sum_{i_p, f_p} \Gamma_{i_p \rightarrow f_p} (N_{n\mathbf{k}}(f_p) - N_{n\mathbf{k}}(i_p)) p_{i_p}, \quad (\text{C2})$$

where  $N_{n\mathbf{k}}(i_p) = \langle i_p | a_{n\mathbf{k}}^\dagger a_{n\mathbf{k}} | i_p \rangle$  is the number of  $(n, \mathbf{k})$  phonons in the  $|i_p\rangle$  state and  $\bar{N}_{n\mathbf{k}} = \sum_{i_p} N_{n\mathbf{k}}(i_p) p_{i_p}$  is the average population. The only phonon states involved in the sums are those whose populations of  $(n, \mathbf{k})$  phonons are different. Now, in order to obtain the scattering rates between spin-phonon states, we use Fermi's golden rule

$$\Gamma_{i_p i_s \rightarrow f_p f_s} = 2\pi |T_{i_p i_s \rightarrow f_p f_s}|^2 \delta(E_{i_p i_s} - E_{f_p f_s}), \quad (\text{C3})$$

where the factor  $N_{\text{uc}}$  ensures that  $\Gamma_{i_p i_s \rightarrow f_p f_s}$  is a finite quantity in the thermodynamic limit, consistent with the choice of  $H'$  as a hamiltonian *density*. We use Born's expansion of the scattering matrix

$$T_{i_p i_s \rightarrow f_p f_s} = \langle f_p f_s | H' | i_p i_s \rangle + \sum_{n_s n_p} \frac{\langle f_p f_s | H' | n_s n_p \rangle \langle n_s n_p | H' | i_p i_s \rangle}{E_{i_p i_s} - E_{n_s n_p} + i\eta} + \dots, \quad (\text{C4})$$

where  $H'$  is the (perturbative) interaction hamiltonian between the phonons and the  $Q$  fields, and the  $\eta \rightarrow 0^+$

appearing in the denominator of the second-order term ensures causality, which will prove crucial in the following.

To describe the interaction between phonon and spin degrees of freedom, we introduce general coupling terms between phonon creation-annihilation operators  $a_{n\mathbf{k}}^{(\dagger)}$  and general, for now unspecified, fields  $Q_{\{n_j \mathbf{k}_j\}}^{\{q_j\}}$  which depend on the spin structure: denoting  $a_{n\mathbf{k}}^+ \equiv a_{n\mathbf{k}}^\dagger$  and  $a_{n\mathbf{k}}^- \equiv a_{n\mathbf{k}}$ , and similarly for the  $Q$  operators,  $Q_{\{n_i \mathbf{k}_i\}}^+ \equiv Q_{\{n_i \mathbf{k}_i\}}^\dagger$  and  $Q_{\{n_i \mathbf{k}_i\}}^- \equiv Q_{\{n_i \mathbf{k}_i\}}$ , we write the couplings

$$H'_{[1]} = \sum_{n\mathbf{k}} \sum_{q=\pm} a_{n\mathbf{k}}^q Q_{n\mathbf{k}}^q \quad (\text{C5})$$

$$H'_{[2]} = \frac{1}{\sqrt{N_{\text{uc}}}} \sum_{n\mathbf{k}, n'\mathbf{k}'} \sum_{q, q'=\pm} a_{n\mathbf{k}}^q a_{n'\mathbf{k}'}^{q'} Q_{n\mathbf{k}n'\mathbf{k}'}^{qq'}, \quad (\text{C6})$$

where  $Q_{n\mathbf{k}n'\mathbf{k}'}^{qq'} = Q_{n'\mathbf{k}'n\mathbf{k}}^{q'q} = (Q_{n\mathbf{k}n'\mathbf{k}'}^{-q-q'})^\dagger$  ensures the hermiticity of  $H'_{[2]}$ . Here and throughout the manuscript, a square bracket index, e.g.  $[p]$  denotes the number of interacting phonons.

By definition the term  $H'_{[p]}$  involves  $p$  phonon creation-annihilation operators, and as such typically arises from microscopic models as the  $p$ th spatial derivative of orbital overlaps. Consequently, we assume  $H'_{[2]}$  to be of the same order of magnitude as the square of  $H'_{[1]}$ , that is to say,  $Q_{n\mathbf{k}}^q \sim \lambda$ ,  $Q_{n\mathbf{k}n'\mathbf{k}'}^{qq'} \sim \lambda^2$  with  $\lambda$  a small parameter. In this paper, we keep only the first two terms of the expansion (i.e. we take  $H' = H'_{[1]} + H'_{[2]}$ ).

### 2. Computation at first Born order

In this subsection we consider only the first term of Born's expansion. The transition rates associated with  $H' = H'_{[1]} + H'_{[2]}$  at this order derive from the matrix elements:

$$T_{\mathbf{i} \rightarrow \mathbf{f}}^{[1]} = \sum_{n\mathbf{k}q} \sqrt{N_{\mathbf{k},n}^i + \frac{q+1}{2}} \langle f_s | Q_{n\mathbf{k}}^q | i_s \rangle \mathbb{I}(i_p \xrightarrow{q, n\mathbf{k}} f_p), \quad (\text{C7})$$

$$T_{\mathbf{i} \rightarrow \mathbf{f}}^{[2]} = \frac{1}{\sqrt{N_{\text{uc}}}} \sum_{n\mathbf{k}, n'\mathbf{k}'} \sum_{qq'} \sqrt{N_{n\mathbf{k}}^i + \frac{q+1}{2}} \sqrt{N_{n'\mathbf{k}'}^i + \frac{q'+1}{2}} \langle f_s | Q_{n\mathbf{k}n'\mathbf{k}'}^{qq'} | i_s \rangle \mathbb{I}(i_p \xrightarrow{q, n\mathbf{k}; q', n'\mathbf{k}'} f_p), \quad (\text{C8})$$

where  $\mathbb{I}(i_p \xrightarrow{q, n\mathbf{k}} f_p)$  means that the only difference between  $|i_p\rangle$  and  $|f_p\rangle$  is that there is  $q = \pm 1$  more phonon of species  $(n, \mathbf{k})$  in the final state. Note that the cases where  $n\mathbf{k} = n'\mathbf{k}'$  require a formal correction. However, at any given order in the  $\lambda$  expansion, such terms are smaller than all others by a factor  $1/N_{\text{uc}}$ , where  $N_{\text{uc}}$  is the number of unit cells, and therefore vanish in the thermodynamic limit. In this article we thus take  $\sum_{n\mathbf{k}, n'\mathbf{k}'}$  and  $\sum_{n\mathbf{k} \neq n'\mathbf{k}'}$  exchangeably, unless we specify otherwise.

We then compute the squared matrix element. ‘‘Cross terms’’ such as  $\langle \mathbf{i} | H'_{[2]} | \mathbf{f} \rangle \langle \mathbf{f} | H'_{[1]} | \mathbf{i} \rangle$  (which are of order  $\lambda^3$ ) vanish because  $\langle i_p | \hat{A} | i_p \rangle = 0$  for any operator  $\hat{A}$  containing an odd number of phonon creation-annihilation operators. At order  $\lambda^2$ , there thus remains only  $\langle \mathbf{i} | H'_{[1]} | \mathbf{f} \rangle \langle \mathbf{f} | H'_{[1]} | \mathbf{i} \rangle$ , and at order  $\lambda^4$ , only  $\langle \mathbf{i} | H'_{[2]} | \mathbf{f} \rangle \langle \mathbf{f} | H'_{[2]} | \mathbf{i} \rangle$ .

*a. Terms at  $O(\lambda^2)$*

At order  $\lambda^2$ , we have therefore

$$\left| T_{\mathbf{i} \rightarrow \mathbf{f}}^{[1]} \right|^2 = \sum_{n\mathbf{k}q} \left( N_{n\mathbf{k},n}^i + \frac{q+1}{2} \right) \mathbb{I}(i_p \xrightarrow{q,n\mathbf{k}} f_p) \langle i_s | Q_{n\mathbf{k}}^{-q} | f_s \rangle \langle f_s | Q_{n\mathbf{k}}^q | i_s \rangle. \quad (\text{C9})$$

We then enforce the energy conservation  $\delta(E_{\mathbf{f}} - E_{\mathbf{i}}) = \delta(q\omega_{n\mathbf{k}} + E_{f_s} - E_{i_s})$  by writing the latter as a time integral, i.e.  $\int_{-\infty}^{+\infty} dt e^{i\omega t} = 2\pi\delta(\omega)$ , identify  $A(t) = e^{+iHt} A e^{-iHt}$ , use the identity  $1 = \sum_{f_s} |f_s\rangle \langle f_s|$ , and take the spins in the initial state to be in thermal equilibrium  $p_{i_s} = Z^{-1} e^{-\beta E_{i_s}}$ . Finally summing over  $|i_s\rangle$  and identifying  $\langle A \rangle_{\beta} = Z^{-1} \text{Tr}(e^{-\beta H} A)$ , we find

$$W_{n\mathbf{k}q}^{[1];[1]} = 2\pi \sum_{f_s, i_s} \langle i_s | Q_{n\mathbf{k}}^{-q} | f_s \rangle \langle f_s | Q_{n\mathbf{k}}^q | i_s \rangle p_{i_s} \times \delta(q\omega_{n\mathbf{k}} + E_{f_s} - E_{i_s}) = \int_{-\infty}^{\infty} dt e^{-iq\omega_{n\mathbf{k}}t} \langle Q_{n\mathbf{k}}^{-q}(t) Q_{n\mathbf{k}}^q(0) \rangle_{\beta}. \quad (\text{C10})$$

Note that this calculation, in a time-reversal symmetric system, leads to the extra symmetry  $W_{n\mathbf{k}q}^{[1];[1]} = W_{n-\mathbf{k}q}^{[1];[1]}$ .

The scattering rate between phonon states, for the one-phonon interaction term at first Born’s order, then reads

$$\Gamma_{i_p \rightarrow f_p}^{[1];[1]} = \sum_{n\mathbf{k}q} \left( N_{n\mathbf{k}}^i + \frac{q+1}{2} \right) W_{n\mathbf{k}q}^{[1];[1]} \mathbb{I}(i_p \xrightarrow{q,n\mathbf{k}} f_p). \quad (\text{C11})$$

To arrive at the collision integral, the final step involves summing over final phononic states  $f_p$  and taking the average over initial phononic states  $i_p$ . We find, the contributions to  $\mathcal{C}$  at order  $\lambda^2$  to be:

$$O_{n\mathbf{k}}^{[1];[1]} = \sum_{q=\pm} q W_{n,\mathbf{k},q}^{[1];[1]} \left( N_{n,\mathbf{k}}^{\text{eq}} + \frac{q+1}{2} \right), \quad (\text{C12})$$

$$-D_{n\mathbf{k}}^{[1];[1]} = \sum_{q=\pm} q W_{n,\mathbf{k},q}^{[1];[1]}. \quad (\text{C13})$$

We will address the constant term  $O_{n\mathbf{k}}^{[1];[1]}$  (expected to be zero) in more detail in Sec. C 2 c. The collision matrix is clearly diagonal, i.e.  $M_{n\mathbf{k},n'\mathbf{k}'}^{[1];[1]} = 0$ . Therefore this  $\lambda^2$  contribution to  $\mathcal{C}$  may contribute to the longitudinal conductivity, but not to the Hall conductivity.

*b. Terms at  $O(\lambda^4)$*

We address the  $O(\lambda^4)$  term in a similar fashion. There, the energy conservation reads  $\delta(E_{\mathbf{f}} - E_{\mathbf{i}}) = \delta(q\omega_{n\mathbf{k}} + q'\omega_{n'\mathbf{k}'} + E_{f_s} - E_{i_s})$ , and we find

$$\Gamma_{i_p \rightarrow f_p}^{[2];[2]} = \frac{1}{2N_{\text{uc}}} \sum_{n\mathbf{k},n'\mathbf{k}'} \sum_{q,q'=\pm} W_{n\mathbf{k}q,n'\mathbf{k}'q'}^{[2];[2]} \mathbb{I}(i_p \xrightarrow{q,n\mathbf{k},q',n'\mathbf{k}'} f_p) \cdot \left( N_{n\mathbf{k}}^i + \frac{q+1}{2} \right) \left( N_{n'\mathbf{k}'}^i + \frac{q'+1}{2} \right), \quad (\text{C14})$$

where

$$W_{n\mathbf{k}q,n'\mathbf{k}'q'}^{[2];[2]} = 2 \int_{-\infty}^{+\infty} dt e^{-i(q\omega_{n\mathbf{k}} + q'\omega_{n'\mathbf{k}'})t} \langle Q_{n\mathbf{k}n'\mathbf{k}'}^{-q-q'}(t) Q_{n\mathbf{k}n'\mathbf{k}'}^{qq'}(0) \rangle_{\beta}, \quad (\text{C15})$$

and  $W_{n\mathbf{k}q,n'\mathbf{k}'q'}^{[2];[2]} = W_{n'\mathbf{k}'q',n\mathbf{k}q}^{[2];[2]}$ , by definition. The resulting collision integral, up to linear order in the perturbed populations  $\delta\bar{N}$  contains the following contributions:

$$O_{n\mathbf{k}}^{[2];[2]} = \frac{1}{N_{\text{uc}}} \sum_{n'\mathbf{k}'q,q'=\pm} q W_{n\mathbf{k}q,n'\mathbf{k}'q'}^{[2];[2]} \cdot \left( N_{n\mathbf{k}}^{\text{eq}} + \frac{q+1}{2} \right) \left( N_{n'\mathbf{k}'}^{\text{eq}} + \frac{q'+1}{2} \right), \quad (\text{C16})$$

$$-D_{n\mathbf{k}}^{[2];[2]} = \frac{1}{N_{\text{uc}}} \sum_{n'\mathbf{k}'q,q'=\pm} q \left( N_{n'\mathbf{k}'}^{\text{eq}} + \frac{q'+1}{2} \right) W_{n\mathbf{k}q,n'\mathbf{k}'q'}^{[2];[2]}, \quad (\text{C17})$$

$$M_{n\mathbf{k},n'\mathbf{k}'}^{[2];[2]} = \frac{1}{N_{\text{uc}}} \sum_{q,q'=\pm} q \left( N_{n\mathbf{k}}^{\text{eq}} + \frac{q+1}{2} \right) W_{n\mathbf{k}q,n'\mathbf{k}'q'}^{[2];[2]}. \quad (\text{C18})$$

As above, we will address the constant term in Sec. C 2 c. The diagonal contribution is of order  $\lambda^4$ , and we therefore expect it to be subdominant compared with the  $\lambda^2$  contribution from the previous section. Finally, the off-diagonal contribution is nonzero. However, we will show that its contribution to  $C_{n\mathbf{k},n'\mathbf{k}'} e^{\beta\omega_{n'\mathbf{k}'}} (N_{n'\mathbf{k}'}^{\text{eq}})^2$  is purely symmetric under  $n\mathbf{k} \leftrightarrow n'\mathbf{k}'$  and therefore contributes only to the symmetric off-diagonal conductivity but not to the Hall one – see Eq. (B6).

*c. Detailed balance*

First, we notice that a change of variables  $i_s \leftrightarrow f_s$  in Eq. (C10) leads to the detailed-balance relation

$$W_{n\mathbf{k},q}^{[1];[1]} = W_{n\mathbf{k},-q}^{[1];[1]} e^{-q\beta\omega_{n\mathbf{k}}}. \quad (\text{C19})$$

An immediate consequence is that  $O_{n\mathbf{k}}^{[1];[1]} = 0$  if we take the equilibrium phonon population  $N_{n\mathbf{k}}^{\text{eq}}$  to be Bose-Einstein’s distribution, as was physically required. Similarly, for the two-phonon interactions at first order, we find the detailed-balance relation

$$W_{n\mathbf{k}q,n'\mathbf{k}'q'}^{[2];[2]} = e^{-\beta(q\omega_{n\mathbf{k}} + q'\omega_{n'\mathbf{k}'})} W_{n\mathbf{k}-q,n'\mathbf{k}'-q'}^{[2];[2]}. \quad (\text{C20})$$



Again, taking  $N_{n\mathbf{k}}^{\text{eq}}$  to be Bose-Einstein's distribution implies  $O_{n\mathbf{k}}^{[2];[2]} = 0$ . Moreover, the detailed-balance relation also implies

$$M_{n\mathbf{k},n'\mathbf{k}'}^{[2];[2]} e^{\beta\omega_{n'\mathbf{k}'}} (N_{n'\mathbf{k}'}^{\text{eq}})^2 = (n\mathbf{k} \leftrightarrow n'\mathbf{k}'), \quad (\text{C21})$$

i.e. there are no antisymmetric contributions, and hence no thermal Hall effect at first Born's order. While we proved this explicitly for the one-phonon and two-phonon cases, this is true in general (along with  $O_{n\mathbf{k}} = 0$ ) for any number of phonon creation-annihilation operators at first order in Born's expansion (see Sec. D 2 c).

#### d. Extra structure

Independently, by writing

$$Q_{n\mathbf{k}}^{-q}(t)Q_{n\mathbf{k}}^q(0) = \frac{1}{2}[Q_{n\mathbf{k}}^{-q}(t), Q_{n\mathbf{k}}^q(0)] + \frac{1}{2}\{Q_{n\mathbf{k}}^{-q}(t), Q_{n\mathbf{k}}^q(0)\} \quad (\text{C22})$$

it is straightforward to show that only the commutator term contributes to  $W_{n,\mathbf{k},q}^{[1](1)} - W_{n,\mathbf{k},-q}^{[1](1)}$ . The final expression for the diagonal of the collision matrix Eq. (C12) takes the form of the spectral function:

$$D_{n\mathbf{k}}^{[1];[1]} = - \int_{-\infty}^{+\infty} dt e^{-i\omega_{n\mathbf{k}}t} \langle [Q_{n\mathbf{k}}^-(t), Q_{n\mathbf{k}}^+(0)] \rangle_{\beta}. \quad (\text{C23})$$

In the two-phonon case, such a commutator structure does not naturally appear, and

$$D_{n\mathbf{k}}^{[2];[2]} = - \frac{2}{N_{\text{uc}}} \sum_{n'\mathbf{k}',q,q'=\pm} q \left( N_{n'\mathbf{k}'}^{\text{eq}} + \frac{q'+1}{2} \right) \times \int_{\mathbb{R}} dt e^{-i(q\omega_{n\mathbf{k}}+q'\omega_{n'\mathbf{k}'})t} \langle Q_{n\mathbf{k}n'\mathbf{k}'}^{-q-q'}(t) Q_{n\mathbf{k}n'\mathbf{k}'}^{qq'}(0) \rangle_{\beta}, \quad (\text{C24})$$

at order  $\lambda^4$  and first Born's order.

### 3. Energy shift of the phonons

We now address the constant term  $O_{n\mathbf{k}}$  appearing in the collision integral, which must vanish because there is no current in equilibrium. Its cancellation is equivalent to a redefinition of the energies of the phonons, due to their interaction with the  $Q$  degrees of freedom. This energy shift corresponds to the real part of the associated self-energy. Consequently, the equilibrium phonon populations  $N_{n'\mathbf{k}'}^{\text{eq}}$  are a priori not equal to  $N_{n'\mathbf{k}'}^{\text{BE}}$ , the Bose-Einstein populations for the *unperturbed* phonon energies.

In this subsection, we show that the energy shift, although a priori nonzero, does not alter the results which we obtained for the thermal conductivities, up to the order  $\lambda^4$  in our perturbative expansion. To understand this, we decompose

$$O_{n\mathbf{k}}[N_{n'\mathbf{k}'}^{\text{eq}}] = O_{n\mathbf{k}}^{(1)}[N_{n'\mathbf{k}'}^{\text{eq}}] + O_{n\mathbf{k}}^{(2)}[N_{n'\mathbf{k}'}^{\text{eq}}] + \mathcal{O}(\lambda^6) \quad (\text{C25})$$

where, as for  $D_{n\mathbf{k}}$  elsewhere in this paper, the upper index  $O^{(p)}$  indicates a term of order  $\lambda^{2p}$ .

We have shown in Sec. C 2 c that  $O_{n\mathbf{k}}^{(1)}[N_{n'\mathbf{k}'}^{\text{BE}}] = 0$ . However,  $O_{n\mathbf{k}}^{(2)}[N_{n'\mathbf{k}'}^{\text{BE}}] \neq 0$  a priori, so that an energy shift is actually required to cancel the equilibrium current. We thus consider the *physical requirement*,  $O_{n\mathbf{k}}[N_{n'\mathbf{k}'}^{\text{eq}}] = 0$ , to be an equation on the unknown  $N_{n'\mathbf{k}'}^{\text{eq}}$ .

Now expanding  $N_{n'\mathbf{k}'}^{\text{eq}} = N_{n'\mathbf{k}'}^{\text{BE}} + \delta N_{n'\mathbf{k}'}^{\text{eq}}$  (with  $\delta N_{n'\mathbf{k}'}^{\text{eq}}$  at least of order  $\lambda^2$ ), this equation becomes

$$0 = O_{n\mathbf{k}}^{(1)}[N_{n''\mathbf{k}''}^{\text{BE}}] + \sum_{n'\mathbf{k}'} \delta N_{n'\mathbf{k}'}^{\text{eq}} \partial_{N_{n'\mathbf{k}'}^{\text{eq}}} O_{n\mathbf{k}}^{(1)}[N_{n''\mathbf{k}''}^{\text{BE}}] + O_{n\mathbf{k}}^{(2)}[N_{n''\mathbf{k}''}^{\text{BE}}] + \mathcal{O}(\lambda^6) \quad (\text{C26})$$

At order  $\lambda^2$ , one recovers  $O_{n\mathbf{k}}^{(1)}[N_{n'\mathbf{k}'}^{\text{BE}}] = 0$ , as is required by detailed balance (see Sec. D 2 b).

At order  $\lambda^4$ , formally inverting this linear equation, one obtains

$$\delta N_{n\mathbf{k}}^{\text{eq}} = - \sum_{n'\mathbf{k}'} \left( \partial_{N_{n_j\mathbf{k}_j}^{\text{eq}}} O_{n_i\mathbf{k}_i}^{(1)}[N_{n''\mathbf{k}''}^{\text{BE}}] \right)^{-1} \Big|_{n\mathbf{k},n'\mathbf{k}'} \times O_{n'\mathbf{k}'}^{(2)}[N_{n''\mathbf{k}''}^{\text{BE}}] + \mathcal{O}(\lambda^4). \quad (\text{C27})$$

This correction Eq. (17) to the phonon equilibrium populations is of order  $\lambda^2$ .

This ensures that using the approximate populations  $N_{n'\mathbf{k}'}^{\text{eq}} = N_{n'\mathbf{k}'}^{\text{BE}}$  leads to a correct estimation of  $D_{n\mathbf{k}}^{(1)}$  the lowest-order contribution to  $D_{n\mathbf{k}}$ , of order  $\lambda^2$ . However, the next-order contribution  $D_{n\mathbf{k}}^{(2)} \sim \lambda^4$  can only be estimated correctly if one adds to it the correction that  $\delta N_{n\mathbf{k}}^{\text{eq}}$  brings to  $D_{n\mathbf{k}}^{(1)}$ . Similarly, using the approximate populations  $N_{n'\mathbf{k}'}^{\text{eq}} = N_{n'\mathbf{k}'}^{\text{BE}}$  leads to a correct estimation of the lowest-order contribution, of order  $\lambda^4$ , to  $M_{n\mathbf{k}n'\mathbf{k}'}$  as expressed in the main text. Corrections of order  $\lambda^6$ , not considered in the present work, would require that the population corrections  $\delta N_{n\mathbf{k}}^{\text{eq}}$  be taken into account.

### 4. Computation at second Born order

As discussed at length, the first Born approximation alone does not lead to a nonzero thermal Hall effect. Here we compute that which appears when the Born expansion is taken up to the second Born order. More precisely, we consider all possible terms up to second Born order that lead to an off-diagonal scattering rate of order at most  $\lambda^4$ . This includes terms like  $\langle \mathbf{f} | H'_{[1]} | \mathbf{n} \rangle \langle \mathbf{n} | H'_{[1]} | \mathbf{i} \rangle$  as well as  $\langle \mathbf{f} | H'_{[1]} | \mathbf{n} \rangle \langle \mathbf{n} | H'_{[2]} | \mathbf{i} \rangle$ , but not  $\langle \mathbf{i} | H'_{[2]} | \mathbf{n} \rangle \langle \mathbf{n} | H'_{[2]} | \mathbf{i} \rangle$  since this term is already of order  $\lambda^4$  (thus contributes to  $|T_{\mathbf{i} \rightarrow \mathbf{f}}|^2$  at order  $\lambda^5$  at least).

a. *Term with one-phonon interactions only*

The first of these terms reads

$$T_{\mathbf{i} \rightarrow \mathbf{f}}^{[1,1]} = \sum_{n\mathbf{k}, n'\mathbf{k}'} \sum_{q, q' = \pm} \sqrt{N_{n\mathbf{k}}^i + \frac{1+q}{2}} \sqrt{N_{n'\mathbf{k}'}^f + \frac{1-q'}{2}} \cdot \sum_{m_s} \frac{\langle f_s | Q_{n'\mathbf{k}'}^{q'} | m_s \rangle \langle m_s | Q_{n\mathbf{k}}^q | i_s \rangle}{E_{i_s} - E_{m_s} - q\omega_{\mathbf{k},n} + i\eta} \mathbb{I}(i_p \xrightarrow{q \cdot n\mathbf{k}}_{q' \cdot n'\mathbf{k}'} f_p), \quad (\text{C28})$$

where the upper index indicates that within Born's expansion,  $T^{[i,j]} \sim \frac{\langle f | H'_{[j]} | m \rangle \langle m | H'_{[i]} | i \rangle}{E_i - E_m + i\eta}$ .

The squared  $T$ -matrix elements now include cross-terms between the first and second orders of Born's expansion (although we keep only terms of order  $\lambda^4$  at most). Here we give details of the calculation of one term, the square of Eq. (C28),  $\left| T_{\mathbf{i} \rightarrow \mathbf{f}}^{[1,1]} \right|^2$ .

In the numerator, the matrix elements of the

Then, the transition rate coming from this part of the total squared matrix element can be written as a sum of eight terms:

$$\Gamma_{i_p \rightarrow f_p}^{[1,1];[1,1]} = \sum_{n\mathbf{k}, n'\mathbf{k}'} \sum_{q, q'} \left( N_{n\mathbf{k}}^i + \frac{q+1}{2} \right) \left( N_{n'\mathbf{k}'}^f + \frac{q'+1}{2} \right) \cdot \sum_{s, s' = \pm} \sum_{i=a, b} W_{n\mathbf{k}q, n'\mathbf{k}'q'}^{[1,1];[1,1],(i),ss'} \mathbb{I}(i_p \xrightarrow{q \cdot n\mathbf{k}}_{q' \cdot n'\mathbf{k}'} f_p), \quad (\text{C31})$$

where we defined (notice the order of the first two operators in the correlator and the sign  $t_1 \pm t_2$  in the exponential):

$$W_{n\mathbf{k}q, n'\mathbf{k}'q'}^{[1,1];[1,1],(a),ss'} = \int dt dt_1 dt_2 \Theta_{ss'}(t_1, t_2) e^{i(q\omega_{n\mathbf{k}} + q'\omega_{n'\mathbf{k}'})t} e^{i(t_1+t_2)(q\omega_{n\mathbf{k}} - q'\omega_{n'\mathbf{k}'})} \cdot \left\langle Q_{n\mathbf{k}}^{-q}(-t-t_2) Q_{n'\mathbf{k}'}^{-q'}(-t+t_2) Q_{n'\mathbf{k}'}^{q'}(-t_1) Q_{n\mathbf{k}}^q(+t_1) \right\rangle_{\beta} \quad (\text{C32})$$

$$W_{n\mathbf{k}q, n'\mathbf{k}'q'}^{[1,1];[1,1],(b),ss'} = \int dt dt_1 dt_2 \Theta_{ss'}(t_1, t_2) e^{i(q\omega_{n\mathbf{k}} + q'\omega_{n'\mathbf{k}'})t} e^{i(t_1-t_2)(q\omega_{n\mathbf{k}} - q'\omega_{n'\mathbf{k}'})} \cdot \left\langle Q_{n'\mathbf{k}'}^{-q'}(-t-t_2) Q_{n\mathbf{k}}^{-q}(-t+t_2) Q_{n'\mathbf{k}'}^{q'}(-t_1) Q_{n\mathbf{k}}^q(+t_1) \right\rangle_{\beta}. \quad (\text{C33})$$

We will investigate the symmetries of these terms in Sec. C4c, and show that only some combinations contribute to the thermal Hall conductivity. In fact the eight terms from Eq. (C31) can be rewritten as products of (anti-)commutators. Meanwhile, defining the symmetrized in  $(n\mathbf{k}q \leftrightarrow n'\mathbf{k}'q')$  collision rate,

$$\mathcal{W}_{n\mathbf{k}q, n'\mathbf{k}'q'}^{[1,1];[1,1],ss'} = \sum_{i=a, b} W_{n\mathbf{k}q, n'\mathbf{k}'q'}^{[1,1];[1,1],(i),ss'} + (n\mathbf{k}q \leftrightarrow n'\mathbf{k}'q'), \quad (\text{C34})$$

we obtain components of the part of the collision matrix

$Q$  operators can combine themselves in two different ways, which we denote in the following as (a):  $\langle i_s | Q_{n\mathbf{k}}^q | m_s \rangle \langle m_s | Q_{n'\mathbf{k}'}^{q'} | f_s \rangle \langle f_s | Q_{n'\mathbf{k}'}^{-q'} | m'_s \rangle \langle m'_s | Q_{n\mathbf{k}}^{-q} | i_s \rangle$ , and (b):  $\langle i_s | Q_{n\mathbf{k}}^q | m_s \rangle \langle m_s | Q_{n'\mathbf{k}'}^{q'} | f_s \rangle \langle f_s | Q_{n\mathbf{k}}^{-q} | m'_s \rangle \langle m'_s | Q_{n'\mathbf{k}'}^{-q'} | i_s \rangle$ .

We use the following time integral representation of each of the denominators (using a regularized definition of the sign function),

$$\frac{1}{x \pm i\eta} = \text{PP} \frac{1}{x} \mp i\pi\delta(x) \quad (\text{C29})$$

$$= \frac{1}{2i} \int_{-\infty}^{+\infty} dt_1 e^{it_1 x} \text{sign}(t_1) \pm \frac{1}{2i} \int_{-\infty}^{+\infty} dt_1 e^{it_1 x}.$$

and a introduce a third time integral to enforce the energy conservation  $E_{\mathbf{f}} - E_{\mathbf{i}} = q'\omega_{n'\mathbf{k}'} + q\omega_{n\mathbf{k}} + E_{f_s} - E_{i_s}$ . The product of the denominators (cf. Eq. (C29)) leads to four terms, which can be labeled by two signs  $s, s' = \pm$ , and we define, for convenience,

$$\Theta_{ss'}(t_1, t_2) := [-\text{sign}(t_1)]^{\frac{1-s}{2}} [\text{sign}(t_2)]^{\frac{1-s'}{2}}. \quad (\text{C30})$$

due to  $\left| T_{\mathbf{i} \rightarrow \mathbf{f}}^{[1,1]} \right|^2$ :

$$O_{n, \mathbf{k}}^{[1,1];[1,1]} = \sum_{n'\mathbf{k}'} \sum_{q, q'} q \sum_{s, s'} \mathcal{W}_{n\mathbf{k}q, n'\mathbf{k}'q'}^{[1,1];[1,1],ss'} \quad (\text{C35})$$

$$- D_{n, \mathbf{k}}^{[1,1];[1,1]} = \sum_{n'\mathbf{k}'} \sum_{q, q'} q \left( N_{n, \mathbf{k}}^{\text{eq}} + \frac{q+1}{2} \right) \left( N_{n'\mathbf{k}'}^{\text{eq}} + \frac{q'+1}{2} \right) \sum_{s, s'} \mathcal{W}_{n\mathbf{k}q, n'\mathbf{k}'q'}^{[1](2),ss'}, \quad (\text{C36})$$

$$M_{n\mathbf{k}, n'\mathbf{k}'}^{[1,1];[1,1]} = \sum_{q, q'} q \left( N_{n, \mathbf{k}}^{\text{eq}} + \frac{q+1}{2} \right) \sum_{s, s'} \mathcal{W}_{n\mathbf{k}q, n'\mathbf{k}'q'}^{[1](2),ss'}. \quad (\text{C37})$$

b. *Commutators and anticommutators*

In what follows, we write  $\llbracket A, B \rrbracket_{\pm} = AB \pm BA$ .

Upon replacing  $Q_{n\mathbf{k}}^{-q}(-t-t_2)Q_{n'\mathbf{k}'}^{-q'}(-t+t_2)$  by  $Q_{n\mathbf{k}}^{-q}(-t-t_2)Q_{n'\mathbf{k}'}^{-q'}(-t+t_2) - \llbracket Q_{n\mathbf{k}}^{-q}(-t-t_2), Q_{n'\mathbf{k}'}^{-q'}(-t+t_2) \rrbracket_{s'}$  in the definition of  $W_{n\mathbf{k}q, n'\mathbf{k}'q'}^{[1,1];[1,1],(a),ss'}$  hereabove, (after changing  $t_2 \leftrightarrow -t_2$  if  $s' = -$ ) one obtains  $-W_{n\mathbf{k}q, n'\mathbf{k}'q'}^{[1,1];[1,1],(b),ss'}$ . Therefore,

$$W_{n\mathbf{k}q, n'\mathbf{k}'q'}^{[1,1];[1,1],(a),ss'} + W_{n\mathbf{k}q, n'\mathbf{k}'q'}^{[1,1];[1,1],(b),ss'} = \int dt dt_1 dt_2 \Theta_{ss'}(t_1, t_2) e^{i(q\omega_{n\mathbf{k}} + q'\omega_{n'\mathbf{k}'})t} e^{i(t_1+t_2)(q\omega_{n\mathbf{k}} - q'\omega_{n'\mathbf{k}'})} \cdot \langle \llbracket Q_{n\mathbf{k}}^{-q}(-t-t_2), Q_{n'\mathbf{k}'}^{-q'}(-t+t_2) \rrbracket_{s'} Q_{n'\mathbf{k}'}^{q'}(-t_1) Q_{n\mathbf{k}}^q(+t_1) \rangle_{\beta}. \quad (\text{C38})$$

Similarly, upon replacing  $Q_{n'\mathbf{k}'}^{q'}(-t_1)Q_{n\mathbf{k}}^q(t_1)$  by  $Q_{n'\mathbf{k}'}^{q'}(-t_1), Q_{n\mathbf{k}}^q(t_1) - \llbracket Q_{n'\mathbf{k}'}^{q'}(-t_1), Q_{n\mathbf{k}}^q(t_1) \rrbracket_s$  into  $W_{n\mathbf{k}q, n'\mathbf{k}'q'}^{[1,1];[1,1],(a),ss'} + W_{n\mathbf{k}q, n'\mathbf{k}'q'}^{[1,1];[1,1],(b),ss'}$  i.e. Eq.(C38), (after changing  $t_1 \leftrightarrow -t_1$  if  $s = -$ ) one obtains  $-W_{n'\mathbf{k}'q', n\mathbf{k}q}^{[1,1];[1,1],(b),ss'} - W_{n'\mathbf{k}'q', n\mathbf{k}q}^{[1,1];[1,1],(a),ss'}$ .

Therefore, the only nonzero contribution to  $W_{n\mathbf{k}q, n'\mathbf{k}'q'}^{[1,1];[1,1],(a),ss'} + W_{n'\mathbf{k}'q', n\mathbf{k}q}^{[1,1];[1,1],(b),ss'} + (n\mathbf{k}q \leftrightarrow n'\mathbf{k}'q')$ , i.e. Eq. (C34), takes the form

$$\mathcal{W}_{n\mathbf{k}q, n'\mathbf{k}'q'}^{[1,1];[1,1],ss'} = \int dt dt_1 dt_2 \Theta_{ss'}(t_1, t_2) e^{i(q\omega_{n\mathbf{k}} + q'\omega_{n'\mathbf{k}'})t} e^{i(t_1+t_2)(q\omega_{n\mathbf{k}} - q'\omega_{n'\mathbf{k}'})} \quad (\text{C39})$$

$$\cdot \langle \llbracket Q_{n\mathbf{k}}^{-q}(-t-t_2), Q_{n'\mathbf{k}'}^{-q'}(-t+t_2) \rrbracket_{s'} \llbracket Q_{n'\mathbf{k}'}^{q'}(-t_1), Q_{n\mathbf{k}}^q(+t_1) \rrbracket_s \rangle_{\beta}, \quad (\text{C40})$$

where  $s, s' = +$  corresponds to an energy conservation constraint, i.e. to on-shell scattering event, while  $s, s' = -$  corresponds to a  $\text{PP}(E_i - E_n)^{-1}$  term, i.e. off-shell scattering (with  $i, n, f$  the initial, intermediate, and final states in the second-order process).

Note that, in a time-reversal symmetric system, these satisfy the symmetry

$$\mathcal{W}_{n\mathbf{k}q, n'\mathbf{k}'q'}^{[1,1];[1,1],ss'} = ss' \mathcal{W}_{n-\mathbf{k}q, n'-\mathbf{k}'q'}^{[1,1];[1,1],s's}, \quad (\text{C41})$$

reflecting the role of  $\pm i\eta$  in the denominators in terms of causality.

### c. Detailed balance

Using the method of the previous subsection Sec. C 2 c, we show the following (“anti-”)detailed-balance relations

$$W_{n\mathbf{k}q, n'\mathbf{k}'q'}^{[1,1];[1,1],(a),ss'} = ss' W_{n'\mathbf{k}'-q', n\mathbf{k}-q}^{[1,1];[1,1],(a),s's} e^{-\beta(q\omega_{\mathbf{k}} + q'\omega_{\mathbf{k}'})}, \quad (\text{C42})$$

$$W_{n\mathbf{k}q, n'\mathbf{k}'q'}^{[1,1];[1,1],(b),ss'} = ss' W_{n\mathbf{k}-q, n'\mathbf{k}'-q'}^{[1,1];[1,1],(b),s's} e^{-\beta(q\omega_{\mathbf{k}} + q'\omega_{\mathbf{k}'})}. \quad (\text{C43})$$

From this, the same holds for the symmetrized in  $n\mathbf{k}q \leftrightarrow n'\mathbf{k}'q'$  scattering rate:

$$\mathcal{W}_{n\mathbf{k}q, n'\mathbf{k}'q'}^{[1,1];[1,1],ss'} = ss' e^{-\beta(q\omega_{\mathbf{k}} + q'\omega_{\mathbf{k}'})} \mathcal{W}_{n\mathbf{k}-q, n'\mathbf{k}'-q'}^{[1,1];[1,1],ss'}. \quad (\text{C44})$$

One contribution comes from the “cross-term”  $2\Re\{ (T_{i \rightarrow f}^{[2]})^* T_{i \rightarrow f}^{[1,1]} \}$ , which contributes to the scattering rates in the form of

$$\mathfrak{W}_{n\mathbf{k}n'\mathbf{k}'}^{\ominus, [1,1];[2], qq'} = \frac{2N_{\text{uc}}^{1/2}}{\hbar^4} \Im \int_{t, t_1} \langle Q_{n\mathbf{k}n'\mathbf{k}'}^{-q, -q'}(-t) \{ Q_{n'\mathbf{k}'}^{q'}(-t_1), Q_{n\mathbf{k}}^q(t_1) \} \rangle \quad (\text{C48})$$

$$\mathfrak{W}_{n\mathbf{k}n'\mathbf{k}'}^{\oplus, [1,1];[2], qq'} = -\frac{2N_{\text{uc}}^{1/2}}{\hbar^4} \Im \int_{t, t_1} \langle Q_{n\mathbf{k}n'\mathbf{k}'}^{-q, -q'}(-t) \llbracket Q_{n'\mathbf{k}'}^{q'}(-t_1), Q_{n\mathbf{k}}^q(t_1) \rrbracket \rangle, \quad (\text{C49})$$

We now identify

$$\mathfrak{W}_{n\mathbf{k}, n'\mathbf{k}'}^{\ominus, [1,1];[1,1], qq'} = N_{\text{uc}} \sum_{s=\pm} \mathcal{W}_{n\mathbf{k}q, n'\mathbf{k}'q'}^{[1,1];[1,1], s, -s}, \quad (\text{C45})$$

$$\mathfrak{W}_{n\mathbf{k}, n'\mathbf{k}'}^{\oplus, [1,1];[1,1], qq'} = N_{\text{uc}} \sum_{s=\pm} \mathcal{W}_{n\mathbf{k}q, n'\mathbf{k}'q'}^{[1,1];[1,1], ss}, \quad (\text{C46})$$

complete expressions of which are given in the main text.

By construction, these enforce

$$\mathfrak{W}_{n\mathbf{k}, n'\mathbf{k}'}^{\sigma, [1,1];[1,1], qq'} = \sigma e^{-\beta(q\omega_{\mathbf{k}} + q'\omega_{\mathbf{k}'})} \mathfrak{W}_{n\mathbf{k}, n'\mathbf{k}'}^{\sigma, [1,1];[1,1], -q-q'}, \quad (\text{C47})$$

where  $\sigma = \oplus$  (resp.  $\sigma = \ominus$ ) indicates that  $\mathfrak{W}$  enforces detailed balance (resp. “anti-detailed balance”).

### d. All contributions

As mentioned at the beginning of this subsection, other terms of order  $\lambda^4$  contribute to the thermal conductivity at second Born’s order. In the following, we use the shorthand  $\llbracket A(-t), B(t') \rrbracket = \text{sign}(t+t') [A(-t), B(t')]$  and  $f_{t, \{t_j\}}$  (resp.  $f'_{t, \{t_j\}}$ ),  $j = 1, \dots, l$ , denotes the set of  $1+l$  inverse Fourier transforms evaluated once at  $\Sigma_{n\mathbf{k}q}^{n'\mathbf{k}'q'} = q\omega_{n\mathbf{k}} + q'\omega_{n'\mathbf{k}'}$  and  $l$  times at  $\Delta_{n\mathbf{k}q}^{n'\mathbf{k}'q'} = q\omega_{n\mathbf{k}} - q'\omega_{n'\mathbf{k}'}$ , i.e.  $f_{t, \{t_j\}} = \int dt dt_1 \dots dt_l e^{i\Sigma_{n\mathbf{k}q}^{n'\mathbf{k}'q'} t} e^{i\Delta_{n\mathbf{k}q}^{n'\mathbf{k}'q'} (t_1 + \dots + t_l)}$ , (resp. once at  $q\omega_{n\mathbf{k}}$  and  $l$  times at  $q'\omega_{n'\mathbf{k}'}$ , i.e.  $f'_{t, \{t_j\}} = \int dt dt_1 \dots dt_l e^{iq\omega_{n\mathbf{k}} t} e^{iq'\omega_{n'\mathbf{k}'} (t_1 + \dots + t_l)}$ ).

The last contribution comes from considering the second Born's order matrix element

$$T_{\mathbf{i} \rightarrow \mathbf{f}}^{[2,1]} = \frac{1}{\sqrt{N_{\text{uc}}}} \sum_{n\mathbf{k}, n'\mathbf{k}'} \sum_{q, q' = \pm} \left( N_{n'\mathbf{k}'}^i + \frac{1+q'}{2} \right) \sqrt{N_{n\mathbf{k}}^i + \frac{1+q}{2}} \mathbb{I}(i_p \xrightarrow{q, n\mathbf{k}} \mathbf{f}_p) \quad (\text{C50})$$

$$\sum_{\mathbf{m}_s} \left\{ \frac{\langle \mathbf{f}_s | Q_{n'\mathbf{k}'}^{-q'} | \mathbf{m}_s \rangle \langle \mathbf{m}_s | Q_{n\mathbf{k}, n'\mathbf{k}'}^{qq'} | \mathbf{i}_s \rangle}{E_{\mathbf{f}_s} - E_{\mathbf{m}_s} - q'\omega_{n'\mathbf{k}'} + i\eta} + \frac{\langle \mathbf{f}_s | Q_{n\mathbf{k}, n'\mathbf{k}'}^{qq'} | \mathbf{m}_s \rangle \langle \mathbf{m}_s | Q_{n'\mathbf{k}'}^{-q'} | \mathbf{i}_s \rangle}{E_{\mathbf{i}_s} - E_{\mathbf{m}_s} + q'\omega_{n'\mathbf{k}'} + i\eta} \right\},$$

which contains two-phonon operators, of order  $\lambda^2$ . At order  $\lambda^4$ , it is thus involved in the ‘‘cross-term’’  $2 \Re\{ (T_{\mathbf{i} \rightarrow \mathbf{f}}^{[1]})^* T_{\mathbf{i} \rightarrow \mathbf{f}}^{[2,1]} \}$ , which contributes to scattering rates in the form of  $\mathfrak{W}_{n\mathbf{k}n'\mathbf{k}'}^{[2,1];[1],qq'} = \sum_{s=\pm} \mathfrak{W}_{n\mathbf{k}n'\mathbf{k}'|s}^{[2,1];[1],qq'}$ , where

$$\mathfrak{W}_{n\mathbf{k}n'\mathbf{k}'|s}^{[2,1];[1],qq'} = \frac{N_{\text{uc}}^{1/2}}{\hbar^4} \Im \int_{t, t_1}^{t'} \langle Q_{n\mathbf{k}}^{-q}(-t) [\text{sign}(t_1)]^{\frac{1-s}{2}} \llbracket Q_{n'\mathbf{k}'}^{-q'}(-t_1), Q_{n\mathbf{k}n'\mathbf{k}'}^{qq'}(0) \rrbracket_s \rangle, \quad (\text{C51})$$

and we recall the shorthand  $\llbracket A, B \rrbracket_{\pm} = AB \pm BA$ .

The first two terms enforce the usual, ‘‘two-phonon’’, (anti-)detailed balance relations

$$\mathfrak{W}_{n\mathbf{k}q, n'\mathbf{k}'q'}^{\sigma, [2];[1,1], qq'} = \sigma e^{-\beta(q\omega_{\mathbf{k}} + q'\omega_{\mathbf{k}'})} \mathfrak{W}_{n\mathbf{k}q, n'\mathbf{k}'q'}^{\sigma, [2];[1,1], qq'}, \quad (\text{C52})$$

with  $\sigma = \oplus, \ominus$ . Meanwhile, the last term satisfies ‘‘one-phonon’’ (anti-)detailed balance,

$$\mathfrak{W}_{n\mathbf{k}, n'\mathbf{k}'|s}^{[2,1];[1], qq'} = s e^{-q\beta\omega_{n\mathbf{k}}} \mathfrak{W}_{n\mathbf{k}, n'\mathbf{k}'|s}^{[2,1];[1], -q-q'}, \quad (\text{C53})$$

where we used a different notation ( $s = \pm$  as a lower index) to emphasize the difference with the other terms derived hereabove.

## 5. Computation at third Born's order

The only third-order element of  $T_{\mathbf{i} \rightarrow \mathbf{f}}$  which can appear in a term of order  $\lambda^4$  in  $|T_{\mathbf{i} \rightarrow \mathbf{f}}|^2$  is

$$T_{\mathbf{i} \rightarrow \mathbf{f}}^{[1,1,1]} = \sum_{n\mathbf{k}q, n'\mathbf{k}'q'} \sqrt{N_{n\mathbf{k}}^i + \frac{1+q}{2}} \left( N_{n'\mathbf{k}'}^i + \frac{1+q'}{2} \right) \mathbb{I}(i_p \xrightarrow{q, n\mathbf{k}} \mathbf{f}_p) \times \sum_{m_s, m'_s} \left\{ \frac{\langle f_s | Q_{n'\mathbf{k}'}^{-q'} | m'_s \rangle \langle m'_s | Q_{n'\mathbf{k}'}^{q'} | m_s \rangle \langle m_s | Q_{n\mathbf{k}}^q | i_s \rangle}{(E_{i_s} - E_{m_s} - q\omega_{n\mathbf{k}} + i\eta)(E_{f_s} - E_{m'_s} - q'\omega_{n'\mathbf{k}'} + i\eta)} \right.$$

$$\left. + \frac{\langle f_s | Q_{n'\mathbf{k}'}^{-q'} | m'_s \rangle \langle m'_s | Q_{n\mathbf{k}}^q | m_s \rangle \langle m_s | Q_{n'\mathbf{k}'}^{q'} | i_s \rangle}{(E_{i_s} - E_{m_s} - q'\omega_{n'\mathbf{k}'} + i\eta)(E_{f_s} - E_{m'_s} - q\omega_{n\mathbf{k}} + i\eta)} + \frac{\langle f_s | Q_{n\mathbf{k}}^q | m'_s \rangle \langle m'_s | Q_{n'\mathbf{k}'}^{-q'} | m_s \rangle \langle m_s | Q_{n'\mathbf{k}'}^{q'} | i_s \rangle}{(E_{i_s} - E_{m_s} - q'\omega_{n'\mathbf{k}'} + i\eta)(E_{f_s} - E_{m'_s} + q\omega_{n\mathbf{k}} + i\eta)} \right\}, \quad (\text{C54})$$

which is involved in the scattering rate

$$\mathfrak{W}_{n\mathbf{k}n'\mathbf{k}'}^{[1,1,1];[1], qq'} = 2\Re \left[ (T_{\mathbf{i} \rightarrow \mathbf{f}}^{[1,1,1]})^* T_{\mathbf{i} \rightarrow \mathbf{f}}^{[1]} \right] = \sum_{s, s' = \pm} \mathfrak{W}_{n\mathbf{k}n'\mathbf{k}'|ss'}^{[1,1,1];[1], qq'}, \quad (\text{C55})$$

where we denote

$$\mathfrak{W}_{n\mathbf{k}n'\mathbf{k}'|ss'}^{[1,1,1];[1], qq'} = \frac{-1}{2\hbar^4} \Re \int_{t, t_1, t_2}^{t'} \left\langle Q_{n\mathbf{k}}^{-q}(-t) \left( Q_{n'\mathbf{k}'}^{-q'}(-t_1), Q_{n\mathbf{k}}^q(0), Q_{n'\mathbf{k}'}^{q'}(t_2) \right)_{s, s'} \right\rangle, \quad (\text{C56})$$

$$\left( A(t), B(t'), C(t'') \right)_{s, s'} = [\text{sign}(t - t')]^{\frac{1-s}{2}} [\text{sign}(t' - t'')]^{\frac{1-s'}{2}} \left( A(t)B(t')C(t'') + sB(t')A(t)C(t'') + s'A(t)C(t'')B(t'') \right).$$

This term enforces an unusual version of (anti-)detailed balance, namely

$$\mathfrak{W}_{n\mathbf{k}n'\mathbf{k}'|ss'}^{[1,1,1];[1], qq'} = s s' e^{-q\beta\omega_{n\mathbf{k}}} \mathfrak{W}_{n\mathbf{k}n'\mathbf{k}'|ss'}^{[1,1,1];[1], -q, q'}, \quad (\text{C57})$$

where the index  $q'$  remains unchanged.

## Appendix D: Generalizations

### 1. Generalized model and higher perturbative orders

To describe the interaction between phonon and another degree of freedom, we introduce general coupling terms between phonon annihilation (creation) operators  $a_{n\mathbf{k}}^{(\dagger)}$  and general, for now unspecified, fields  $Q_{\{n_j, \mathbf{k}_j\}}^{\{q_j\}}$

which are operators acting in their own Hilbert space, i.e. we write  $H' = \sum_l H'_{[l]}$ , with

$$H'_{[l]} = \frac{1}{\sqrt{N_{\text{uc}}^l}} \sum_{\{n_i \mathbf{k}_i\}} \sum_{\{q_i = \pm\}} \left( \prod_{j=1}^m a_{n_j \mathbf{k}_j}^{q_j} \right) Q_{\{n_j \mathbf{k}_j\}}^{\{q_j\}}. \quad (\text{D1})$$

In this expression,  $m$  is the number of phonon creation-annihilation operators coupled to  $Q_{\{n_j \mathbf{k}_j\}}^{\{q_j\}}_{i=1..l}$ . In terms of the perturbative expansion introduced in the main text and the other appendices, this means  $Q_{\{n_j \mathbf{k}_j\}}^{\{q_j\}}_{i=1..l} \sim \lambda^l$ ; note that since the perturbative expansion is considered (formally) up to *infinite* order in this appendix, we make this specification only for the sake of clarity. To avoid ambiguities, we assume that all the  $n_j \mathbf{k}_j$  indices involved in a given term of  $H'_{[l]}$  are distinct; this is correct in the thermodynamic limit. Note also that, for the sake of clarity in the following developments, the normalization factors of  $N_{\text{uc}}$  are not defined following the same convention as in the rest of the paper.

In what follows, we take special notations for the first two indices:  $n_1 \mathbf{k}_1 \equiv n \mathbf{k}$ ,  $n_2 \mathbf{k}_2 \equiv n' \mathbf{k}'$ . Using the model Eq. (68) and following the general procedure described in Sec. C and in the main text, one can then (at least formally) derive the collision integral which always takes the form

$$\mathcal{C}_{n \mathbf{k}} = \sum_{p=1}^{\infty} \frac{1}{N_{\text{uc}}^p} \sum_{\{n_i \mathbf{k}_i\}_{i=2, \dots, p}} \sum_{\{q_i\}_{i=1, \dots, p}} q_1 \quad (\text{D2}) \\ \times \left[ \prod_{i=1}^p \left( \bar{N}_{n_i \mathbf{k}_i} + \frac{q_i + 1}{2} \right) \right] W_{\{n_i \mathbf{k}_i\}}^{(p), \{q_i\}},$$

where the index  $(p)$  denotes a term of order  $\lambda^{2p}$ . The scattering rate  $W_{\{n_i \mathbf{k}_i\}}^{(p), \{q_i\}} = W_{\{n_i \mathbf{k}_i\}}^{(p), \{q_i\}}_{i=1, \dots, p}$  is the sum of all the scattering rates of the  $[l_1, \dots, l_m]; [l'_1, \dots, l'_{m'}]$  kind (according to the nomenclature introduced in the main text) such that  $\sum_{i=1}^m l_i + \sum_{j=1}^{m'} l'_j = 2p$ . In terms of physical process, each of these terms corresponds to the interference between two scattering channels,  $[l_1, \dots, l_m]$  and  $[l'_1, \dots, l'_{m'}]$ , such that in all,  $2p$  phonon creations or annihilations occur between the initial  $\mathbf{i}$  and final  $\mathbf{f}$  states. Note that in the present paper, we compute explicitly this expansion up to  $p = 2$ .

We then expand the phonon average populations as  $\bar{N}_{n_i \mathbf{k}_i} = N_{n_i \mathbf{k}_i}^{\text{eq}} + \delta \bar{N}_{n_i \mathbf{k}_i}$ . Following Eq.(11), the diagonal scattering rate is obtained as  $D_{n \mathbf{k}} = -\partial_{\bar{N}_{n \mathbf{k}}} \mathcal{C}_{n \mathbf{k}} \Big|_{\bar{N} = N^{\text{eq}}}$ .

It can be decomposed as  $D_{n \mathbf{k}} = \sum_{p=1}^{\infty} D_{n \mathbf{k}}^{(p)}$ , where

$$D_{n \mathbf{k}}^{(p)} = \frac{-1}{N_{\text{uc}}^p} \sum_{\{n_i \mathbf{k}_i\}_{i=2, \dots, p}} \sum_{\{q_i\}_{i=1, \dots, p}} q_1 \quad (\text{D3}) \\ \times \left[ \prod_{i=2}^p \left( N_{n_i \mathbf{k}_i}^{\text{eq}} + \frac{q_i + 1}{2} \right) \right] W_{\{n_i \mathbf{k}_i\}}^{(p), \{q_i\}}.$$

Similarly, the off-diagonal scattering rate is obtained as  $M_{n \mathbf{k}, n' \mathbf{k}'} = \partial_{\bar{N}_{n' \mathbf{k}'}} \mathcal{C}_{n \mathbf{k}} \Big|_{\bar{N} = N^{\text{eq}}}$ . It can be decomposed as  $M_{n \mathbf{k}, n' \mathbf{k}'} = \sum_{p=2}^{\infty} M_{n \mathbf{k}, n' \mathbf{k}'}^{(p)}$ , where

$$M_{n \mathbf{k}, n' \mathbf{k}'}^{(p)} = \frac{1}{N_{\text{uc}}^p} \sum_{\{n_i \mathbf{k}_i\}_{i=3, \dots, p}} \sum_{\{q_i\}_{i=1, \dots, p}} q_1 \quad (\text{D4}) \\ \times \left( N_{n \mathbf{k}}^{\text{eq}} + \frac{q_1 + 1}{2} \right) \left[ \prod_{i=3}^p \left( N_{n_i \mathbf{k}_i}^{\text{eq}} + \frac{q_i + 1}{2} \right) \right] W_{\{n_i \mathbf{k}_i\}}^{(p), \{q_i\}}.$$

Like in the equations for  $p = 1, 2$  derived explicitly in Appendix C,  $q_1$  always factorizes in the collision integral, as the change in number of  $n \mathbf{k}$  phonons due to the scattering event.

## 2. Special properties of first Born's order

### a. Definitions and basic results

At first order of the Born expansion, all contributions to the collision integral are ‘‘semiclassical’’, in the sense defined in Sec. III D 3; i.e. an operator  $Q_{n_1 \mathbf{k}_1, \dots, n_l \mathbf{k}_l}^{q_1, \dots, q_l}$  does only appear in the collision integral as  $|Q_{n_1 \mathbf{k}_1, \dots, n_l \mathbf{k}_l}^{q_1, \dots, q_l}|^2$ .

To make this statement more precise, we rewrite

$$H'_{[l]} = \frac{1}{\sqrt{N_{\text{uc}}^l}} \sum_{r=0}^l \sum_{\{n_i \mathbf{k}_i\}_{i=1..l}} \left( \prod_{j=1}^r a_{n_j \mathbf{k}_j}^+ \right) \left( \prod_{j=r+1}^l a_{n_j \mathbf{k}_j}^- \right) \\ \times \frac{1}{\sqrt{r!(l-r)!}} Q_{n_1 \mathbf{k}_1 \dots n_r \mathbf{k}_r | n_{r+1} \mathbf{k}_{r+1} \dots n_l \mathbf{k}_l}^{+, \dots, + | -, \dots, -}, \quad (\text{D5})$$

where the upper indices of  $Q$  are  $r$  times ‘+’ and  $l - r$  times ‘-’, and  $Q$  is by definition symmetric under permutation of its lower indices in the two blocks  $\{n_i \mathbf{k}_i\}_{i=1, \dots, r}$  and  $\{n_i \mathbf{k}_i\}_{i=r+1, \dots, l}$  separately. Hermiticity is guaranteed by  $Q_{n_1 \mathbf{k}_1 \dots n_r \mathbf{k}_r | n_{r+1} \mathbf{k}_{r+1} \dots n_l \mathbf{k}_l}^{+, \dots, + | -, \dots, -} = (Q_{n_{r+1} \mathbf{k}_{r+1} \dots n_l \mathbf{k}_l | n_1 \mathbf{k}_1 \dots n_r \mathbf{k}_r}^{+, \dots, + | -, \dots, -})^\dagger$ . Note that at first Born's order, distinct scattering channels  $[l]$  and  $[l']$  do not interfere for  $l \neq l'$ ; one can thus study independently the contribution of each  $H'_{[l]}$  to the collision integral.

The contribution to the squared T-matrix obtained from  $H'_{[l]}$  at first Born's order is

$$\begin{aligned} |T_{i \rightarrow f}^{[l]}|^2 &= \frac{1}{N_{\text{uc}}^l} \sum_{r=0}^l \frac{1}{r!(l-r)!} \sum_{\{n_i \mathbf{k}_i\}_{i=1..l}} \left[ \prod_{j=1}^r (N_{n_j \mathbf{k}_j}^i + 1) \right] \left[ \prod_{j=r+1}^l (N_{n_j \mathbf{k}_j}^i) \right] \\ &\times \mathbb{I}(i_p \xrightarrow{+\{n_j \mathbf{k}_j\}_1^r} f_p) \langle i_s | Q_{\{n_j \mathbf{k}_j\}_{r+1}^l}^{+, \dots, +, |-, \dots, -} | f_s \rangle \langle f_s | Q_{\{n_j \mathbf{k}_j\}_1^r | \{n_j \mathbf{k}_j\}_{r+1}^l}^{+, \dots, +, |-, \dots, -} | i_s \rangle, \end{aligned} \quad (\text{D6})$$

Summing over all scattering channels, the first Born's order contribution to the collision integral is

$$\mathcal{C}_{n\mathbf{k}}^{1\text{B}} = \sum_{l=1}^{\infty} \frac{1}{N_{\text{uc}}^l} \sum_{r=0}^l \sum_{\{n_i \mathbf{k}_i\}_{i=1..l}} \prod_{j=1}^r (\bar{N}_{n_j \mathbf{k}_j} + 1) \prod_{j=r+1}^l (\bar{N}_{n_j \mathbf{k}_j}) \left( \frac{r \delta_{n, n_1} \delta_{\mathbf{k}, \mathbf{k}_1}}{r!(l-r)!} - \frac{(l-r) \delta_{n, n_{r+1}} \delta_{\mathbf{k}, \mathbf{k}_{r+1}}}{r!(l-r)!} \right) W_{\{n_j \mathbf{k}_j\}_1^r | \{n_j \mathbf{k}_j\}_{r+1}^l}^{[l]; [l]}, \quad (\text{D7})$$

where

$$W_{\{n_j \mathbf{k}_j\}_1^r | \{n_j \mathbf{k}_j\}_{r+1}^l}^{[l]; [l]} = \int dt e^{-i(\sum_{j=1}^r \omega_{n_j \mathbf{k}_j} - \sum_{j=r+1}^l \omega_{n_j \mathbf{k}_j})t} \left\langle Q_{\{n_j \mathbf{k}_j\}_{r+1}^l | \{n_j \mathbf{k}_j\}_1^r}^{+, \dots, +, |-, \dots, -}(t) Q_{\{n_j \mathbf{k}_j\}_1^r | \{n_j \mathbf{k}_j\}_{r+1}^l}^{+, \dots, +, |-, \dots, -} \right\rangle. \quad (\text{D8})$$

Following the same steps as in Sec. C2c, it is easy to see that  $W_{\{n_j \mathbf{k}_j\}_1^r | \{n_j \mathbf{k}_j\}_{r+1}^l}^{[l]; [l]}$  *always* enforces detailed-balance, namely

$$\begin{aligned} W_{\{n_j \mathbf{k}_j\}_1^r | \{n_j \mathbf{k}_j\}_{r+1}^l}^{[l]; [l]} &= e^{-\beta(\sum_{j=1}^r \omega_{n_j \mathbf{k}_j} - \sum_{j=r+1}^l \omega_{n_j \mathbf{k}_j})} \\ &\times W_{\{n_j \mathbf{k}_j\}_{r+1}^l | \{n_j \mathbf{k}_j\}_1^r}^{[l]; [l]}. \end{aligned} \quad (\text{D9})$$

We now prove two important properties of the collision integral, as obtained from first Born's order, which derive therefrom.

#### b. No equilibrium current

The equilibrium current is due to  $O_{n\mathbf{k}} = C_{n\mathbf{k}}[\bar{N}_{n'\mathbf{k}'} \mapsto N_{n'\mathbf{k}'}^{\text{eq}}]$ , the constant term in the collision integral.

In the present case, by performing a change of index  $r \mapsto l-r$  in the second term of  $(\dots - \dots)$  in Eq. (D7), and resorting to the detailed balance relation Eq. (D9) and taking  $N_{n'\mathbf{k}'}^{\text{eq}} = \frac{1}{e^{\beta\omega_{n'\mathbf{k}'}} - 1}$ , one can easily show that

$$O_{n\mathbf{k}}^{1\text{B}} = C_{n\mathbf{k}}^{1\text{B}}[\bar{N}_{n_j \mathbf{k}_j} \mapsto N_{n_j \mathbf{k}_j}^{\text{eq}}] = 0. \quad (\text{D10})$$

This means that no shift of the phonons' energies is needed at first Born's order to guarantee cancellation of the equilibrium current.

#### c. No phonon Hall effect

The off-diagonal contribution to the collision matrix at first Born's order,  $M_{n\mathbf{k}, n'\mathbf{k}'}^{1\text{B}} = \partial_{\bar{N}_{n'\mathbf{k}'}} C_{n\mathbf{k}}^{1\text{B}}$ , reads

$$\begin{aligned} M_{n\mathbf{k}, n'\mathbf{k}'}^{1\text{B}} &= \sum_{l=1}^{\infty} \frac{1}{N_{\text{uc}}^l} \sum_{r=0}^l \sum_{\{n_i \mathbf{k}_i\}_{i=1..l}} \prod_{j=1}^r (N_{n_j \mathbf{k}_j}^{\text{eq}} + 1) \prod_{j=r+1}^l (N_{n_j \mathbf{k}_j}^{\text{eq}}) W_{\{n_j \mathbf{k}_j\}_1^r | \{n_j \mathbf{k}_j\}_{r+1}^l}^{[l]; [l]} \\ &\times \frac{1}{r!(l-r)!} \left( r \delta_{n, n_1} \delta_{\mathbf{k}, \mathbf{k}_1} \left( (r-1) \delta_{n', n_2} \delta_{\mathbf{k}', \mathbf{k}_2} + (l-r) \delta_{n', n_{r+1}} \delta_{\mathbf{k}', \mathbf{k}_{r+1}} \right) \right. \\ &\quad \left. - (l-r) \delta_{n, n_{r+1}} \delta_{\mathbf{k}, \mathbf{k}_{r+1}} \left( r \delta_{n', n_1} \delta_{\mathbf{k}', \mathbf{k}_1} + (l-r-1) \delta_{n', n_{r+2}} \delta_{\mathbf{k}', \mathbf{k}_{r+2}} \right) \right) \end{aligned} \quad (\text{D11})$$

After some algebra, following essentially the same steps as outlined hereabove, it is possible to show that

$$M_{n\mathbf{k}, n'\mathbf{k}'}^{1\text{B}} e^{\beta\omega_{n'\mathbf{k}'}} (N_{n'\mathbf{k}'}^{\text{eq}})^2 = M_{n'\mathbf{k}', n\mathbf{k}}^{1\text{B}} e^{\beta\omega_{n\mathbf{k}}} (N_{n\mathbf{k}}^{\text{eq}})^2. \quad (\text{D12})$$

This, as was illustrated several times in the main text and the appendices, entails that  $M^{1\text{B}}$  does not contribute

to  $\kappa_H$  – see Eq. B6. We have thus shown that no contribution to the thermal Hall conductivity can possibly come from first Born's order, regardless of the number of phonon operators in the Hamiltonian and of the nature of the operators  $Q$  to which they are coupled.

## Appendix E: Application—further technical details

### 1. Solving the delta functions

In order to solve the two simultaneous delta functions, we use the following rewriting of  $\mathfrak{W}^\ominus$ ,

$$\begin{aligned} \mathfrak{W}_{n\mathbf{k},n'\mathbf{k}'}^{\ominus,qq'} &= \frac{64\pi^2}{\hbar^4 N_{\text{uc}}^{2d}} \sum_{\mathbf{p}} \sum_{\{\ell_i, q_i\}} \mathcal{F}^{\ell_3, \ell_1, \ell_2 | q_4, q_1, q_2} \mathfrak{Jm} \left\{ \mathcal{B}_{\mathbf{k}, \mathbf{p} + \frac{1}{2} q \mathbf{k} + q' \mathbf{k}'}^{n\ell_2 \ell_3 | q_2 q_3 q} \mathcal{B}_{\mathbf{k}', \mathbf{p} + \frac{1}{2} q' \mathbf{k}'}^{n' \ell_3 \ell_1 | -q_3 q_1 q'} \right. \\ &\quad \left. \text{PP} \left[ \frac{\mathcal{B}_{\mathbf{k}, \mathbf{p} + \frac{1}{2} q \mathbf{k}}^{n\ell_1 \ell_4 | -q_1 q_4 - q} \mathcal{B}_{\mathbf{k}', \mathbf{p} + q \mathbf{k} + \frac{1}{2} q' \mathbf{k}'}^{n' \ell_4 \ell_2 | -q_4 - q_2 - q'}}{2v_m q_1 \left( \frac{q_1 q \omega_{n\mathbf{k}}}{v_m} + \hat{\Omega}_{\ell_1, \mathbf{p}} - q_1 q_4 \hat{\Omega}_{\ell_4, \mathbf{p} + q \mathbf{k}} \right)} + (n, q, \mathbf{k}, q_4) \leftrightarrow (n', q', \mathbf{k}', -q_4) \right] \right\} \\ &\quad \delta \left( v_m q_1 \left[ \frac{q_1 \sum_{n\mathbf{k}n'\mathbf{k}'}^{qq'}}{v_m} + \hat{\Omega}_{\ell_1, \mathbf{p}} + q_1 q_2 \hat{\Omega}_{\ell_2, \mathbf{p} + q \mathbf{k} + q' \mathbf{k}'} \right] \right) \delta \left( -2v_m q_1 \left[ \frac{q_1 q' \omega_{n'\mathbf{k}'}}{v_m} + \hat{\Omega}_{\ell_1, \mathbf{p}} - q_1 q_3 \hat{\Omega}_{\ell_3, \mathbf{p} + q' \mathbf{k}'} \right] \right), \end{aligned} \quad (\text{E1})$$

where  $\hat{\Omega}_{\ell, \mathbf{p}} = \Omega_{\ell, \mathbf{p}}/v_m$  and

$$\mathcal{F}_{\mathbf{p}, q \mathbf{k}, q' \mathbf{k}'}^{\ell_3, \ell_1, \ell_2 | q_4, q_1, q_2} = q_4 (2n_B(\Omega_{\ell_3, \mathbf{p} + q' \mathbf{k}'} + 1) (2n_B(\Omega_{\ell_1, \mathbf{p}}) + q_1 + 1) (2n_B(\Omega_{\ell_2, \mathbf{p} + q \mathbf{k} + q' \mathbf{k}'} + q_2 + 1) \quad (\text{E2})$$

is a product of thermal factors (note  $\hat{\mathcal{F}} = q_1 \mathcal{F}$ , cf. Eq. (94)). Now collapsing the delta functions, we can write:

$$\begin{aligned} \mathfrak{W}_{n\mathbf{k},n'\mathbf{k}'}^{\ominus,qq'} &= \frac{8a^2}{\hbar^4 v_m^2} \sum_j \sum_{\ell, \{q_i\}} \mathfrak{Jm} \left\{ \mathcal{B}_{\mathbf{k}, \mathbf{p}_j + \frac{1}{2} q \mathbf{k} + q' \mathbf{k}'}^{n\ell \ell | q_2 q_3 q} \mathcal{B}_{\mathbf{k}', \mathbf{p}_j + \frac{1}{2} q' \mathbf{k}'}^{n' \ell \ell | -q_3 q_1 q'} \text{PP} \left[ \frac{\mathcal{B}_{\mathbf{k}, \mathbf{p}_j + \frac{1}{2} q \mathbf{k}}^{n\ell \ell | -q_1 q_4 - q} \mathcal{B}_{\mathbf{k}', \mathbf{p}_j + q \mathbf{k} + \frac{1}{2} q' \mathbf{k}'}^{n' \ell \ell | -q_4 - q_2 - q'}}{2v_m q_1 \left( \frac{q_1 q \omega_{n\mathbf{k}}}{v_m} + \hat{\Omega}_{\ell, \mathbf{p}_j} - q_1 q_4 \hat{\Omega}_{\ell, \mathbf{p}_j + q \mathbf{k}} \right)} \right. \right. \\ &\quad \left. \left. + (n, q, \mathbf{k}, q_4) \leftrightarrow (n', q', \mathbf{k}', -q_4) \right] \right\} J_{\mathfrak{W}}(\mathbf{p}_j) \mathcal{F}_{\mathbf{p}_j, q \mathbf{k}, q' \mathbf{k}'}^{\ell, \ell | q_4, q_1, q_2}, \end{aligned} \quad (\text{E3})$$

where, when they exist, the solutions,  $j = 0, \dots, 3$  take the form (recall  $\mathbf{v}_i = \underline{\mathbf{v}}_i$ ,  $\mathbf{w}_i = \underline{\mathbf{w}}_i$ ,  $\mathbf{p}_j = \underline{\mathbf{p}}_j$ )

$$\mathbf{p}_j = t_{\lfloor j/2 \rfloor} \mathbf{v}_{\lfloor j/2 \rfloor} + u_{\lfloor j/2 \rfloor}^{(j \text{ [2]})} \mathbf{w}_{\lfloor j/2 \rfloor}, \quad (\text{E4})$$

where, for  $i = 0, 1$

$$\mathbf{v}_i = a_2 \mathbf{k}_1 + (-1)^i a_1 \mathbf{k}_2, \quad \mathbf{w}_i = \hat{\mathbf{z}} \times \mathbf{v}_i, \quad (\text{E5})$$

$$t_i = \frac{a_2 \mathbf{k}_1^2 + (-1)^i a_1 \mathbf{k}_2^2 - a_1 a_2 (a_1 + (-1)^i a_2)}{2\mathbf{v}_i^2}, \quad u_i^{(\pm)} = \frac{-B_i \pm \sqrt{B_i^2 - 4A_i C_i}}{2A_i}, \quad (\text{E6})$$

$$A_i = 4a_{i+1}^2 (\mathbf{v}_i^2 - (\mathbf{k}_1 \wedge \mathbf{k}_2)^2), \quad (\text{E7})$$

$$B_i = (-1)^i 4a_{i+1} (\mathbf{k}_1 \wedge \mathbf{k}_2) (a_{i+1}^2 - \mathbf{k}_{i+1}^2 + 2(\mathbf{v}_i \cdot \mathbf{k}_{i+1}) t_i),$$

$$C_i = - (a_{i+1} (a_{i+1} - 2\delta_\ell) - \mathbf{k}_{i+1}^2) (a_{i+1} (a_{i+1} + 2\delta_\ell) - \mathbf{k}_{i+1}^2) - 4(a_{i+1}^2 - \mathbf{k}_{i+1}^2) (\mathbf{v}_i \cdot \mathbf{k}_{i+1}) t_i + 4(a_{i+1}^2 \mathbf{v}_i^2 - (\mathbf{v}_i \cdot \mathbf{k}_{i+1})^2) t_i^2,$$

and  $J_{\mathfrak{W}}(\mathbf{p}_j)$  is given in the main text, Eq. (96).

### 2. Choice of polarization vectors

Below, we enumerate possible explicit choices for a basis of polarization vectors ( $\boldsymbol{\varepsilon}_{0, \mathbf{k}}$ ,  $\boldsymbol{\varepsilon}_{1, \mathbf{k}}$ ,  $\boldsymbol{\varepsilon}_{2, \mathbf{k}}$ ). In the numer-

ical calculations, we use choice 2.

a. *Choice 1*

A simple choice is that of momentum-independent polarization vectors, which can be, for example:  $\boldsymbol{\varepsilon}_0(\mathbf{k}) = \hat{\mathbf{x}}$ ,  $\boldsymbol{\varepsilon}_1(\mathbf{k}) = \hat{\mathbf{y}}$ ,  $\boldsymbol{\varepsilon}_2(\mathbf{k}) = \hat{\mathbf{z}}$ .

b. *Choice 2*

Below, we describe the choice of polarization vectors used in the numerical implementation. Its polarization vectors  $\boldsymbol{\varepsilon}_{n,\mathbf{k}}$  form an orthonormal basis in which  $\mathbf{k}$  points along the  $[1, 1, 1]$  axis, so that  $\mathbf{k} \cdot \boldsymbol{\varepsilon}_{n,\mathbf{k}} = \frac{|\mathbf{k}|}{\sqrt{3}} \forall n$ . This, as explained in the main text, ensures that the structure factor  $\mathcal{S}^{\alpha,\beta}$  does not vanish for  $\alpha = \beta$ , corresponding to the largest coupling constants  $\Lambda_{1..5}$  (as opposed to anisotropic  $\Lambda_{6,7}$  for which  $\alpha \neq \beta$ ).

The starting point is the orthonormal basis made of three vectors  $\mathbf{e}_n, n = 0, 1, 2$ , defined as

$$\begin{cases} \mathbf{e}_0 = \frac{1}{\sqrt{3}} (\sqrt{2}\hat{\mathbf{x}} + \hat{\mathbf{z}}) \\ \mathbf{e}_1 = \frac{1}{\sqrt{6}} (-\hat{\mathbf{x}} + \sqrt{3}\hat{\mathbf{y}} + \sqrt{2}\hat{\mathbf{z}}) \\ \mathbf{e}_2 = \frac{1}{\sqrt{6}} (-\hat{\mathbf{x}} - \sqrt{3}\hat{\mathbf{y}} + \sqrt{2}\hat{\mathbf{z}}) \end{cases} ; \quad (\text{E8})$$

in this basis,  $\hat{\mathbf{z}} = [1, 1, 1]$ . To rotate the  $\hat{\mathbf{z}}$  axis into  $\hat{\mathbf{k}}$ 's direction, we define the polar angles of  $\hat{\mathbf{k}}$ ,

$$\theta = \arccos(k_z/|\mathbf{k}|), \quad (\text{E9})$$

$$\phi = \text{Arg}(k_x + ik_y), \quad (\text{E10})$$

so that a good choice for the three polarization vectors is

$$\boldsymbol{\varepsilon}_{n,\mathbf{k}} = i R_{\hat{\mathbf{z}}}(\phi) \cdot R_{\hat{\mathbf{y}}}(\theta) \cdot \text{diag}[s(\mathbf{k}), 1, 1] \cdot \mathbf{e}_n \quad (\text{E11})$$

for  $n = 0, 1, 2$ . In the above, we defined  $R_{\hat{\boldsymbol{\mu}}}(\gamma)$  to be the direct rotation matrix around the  $\boldsymbol{\mu}$  axis by an angle  $\gamma$ , and we used the ‘‘sign’’ function

$$s(\mathbf{k}) = \begin{cases} +1 & \text{if } \mathbf{k} \in \mathcal{D}_+ \\ -1 & \text{if } \mathbf{k} \in \mathcal{D}_- \end{cases} \quad (\text{E12})$$

with respect to two domains  $\mathcal{D}_{\pm}$ , corresponding (up to unimportant details in a set of null measure contained in the  $k_z = 0$  plane) to the ‘‘upper’’ ( $k_z > 0$ ) and ‘‘lower’’ ( $k_z < 0$ ) halves of  $\mathbb{R}^3$ , and more precisely defined by

$$\mathcal{D}_+ = \left\{ \mathbf{k} \mid k_z > 0 \text{ or } (k_z = 0 \text{ and } (k_y > 0 \text{ or } (k_y = 0 \text{ and } k_x > 0))) \right\}, \quad (\text{E13})$$

$$\mathcal{D}_- = \left\{ \mathbf{k} \mid k_z < 0 \text{ or } (k_z = 0 \text{ and } (k_y < 0 \text{ or } (k_y = 0 \text{ and } k_x < 0))) \right\} \quad (\text{E14})$$

such that  $\mathbb{R}^3 = \mathcal{D}_+ \cup \mathcal{D}_- \cup \{\mathbf{0}\}$ . The role of this  $s(\mathbf{k})$  function is to help ensure that this choice of polarizations enforces  $\boldsymbol{\varepsilon}_n(-\mathbf{k}) = \boldsymbol{\varepsilon}_n(\mathbf{k})^*$ , as well as all the tetragonal symmetry group of the crystal. This last statement

means that under a symmetry operation  $g$  belonging to  $D_{4h}$  the symmetry group of the crystal, they transform as

$$\boldsymbol{\varepsilon}_n(g \cdot \mathbf{k}) = \sum_{n'} c_{nn'}^g(\mathbf{k}) g \cdot \boldsymbol{\varepsilon}_{n'}(\mathbf{k}), \quad (\text{E15})$$

where  $g \cdot$  denotes the action of  $g$  on a vector, and most importantly the  $c_{nn'}^g$  coefficient either is  $\delta_{nn'}$  or exchanges the  $n = 1$  and  $n = 2$  polarizations, depending on whether  $\mathbf{k}$  is in a high-symmetry position. Indeed  $n = 1, 2$  are constructed degenerate (as eigenvectors of the dynamical matrix) at the high-symmetry planes and axes of the Brillouin zone. See Ref. [27] for details and further discussion on the behavior of polarization vectors under symmetry operations.

c. *Choice 3*

One may also use the Hall-plane-dependent basis for the polarization vectors and label  $\boldsymbol{\varepsilon}_{n\mathbf{k}}$ , assuming  $\mu\nu$  is the Hall plane,  $\rho$  is the direction transverse to the plane, and  $\mu\nu\rho$  forms a direct orthonormal basis:

$$\boldsymbol{\varepsilon}_{0,\mathbf{k}} = i\mathbf{k}/|\mathbf{k}| \quad (\text{longitudinal}),$$

$$\boldsymbol{\varepsilon}_{1,\mathbf{k}} = i \frac{\hat{\mathbf{u}}_{\rho} \times \mathbf{k}}{|\hat{\mathbf{u}}_{\rho} \times \mathbf{k}|} \quad (\text{transverse, in Hall plane}),$$

$$\boldsymbol{\varepsilon}_{2,\mathbf{k}} = \boldsymbol{\varepsilon}_{0,\mathbf{k}} \times \boldsymbol{\varepsilon}_{1,\mathbf{k}} = \frac{k^{\rho}\mathbf{k} - \mathbf{k}^2\hat{\mathbf{u}}_{\rho}}{|\mathbf{k}||\hat{\mathbf{u}}_{\rho} \times \mathbf{k}|} \quad (\text{transverse}). \quad (\text{E16})$$

Then, if  $\alpha, \beta, \mu, \nu, \rho \in \{x, y, z\}$ , we can write:

$$\mathcal{S}_{0\mathbf{k}}^{q;\alpha\beta} = \frac{1}{\sqrt{\omega_{0\mathbf{k}}}} \frac{2qi}{|\mathbf{k}|} k^{\alpha} k^{\beta}, \quad (\text{E17})$$

$$\mathcal{S}_{1\mathbf{k}}^{q;\alpha\beta} = \frac{1}{\sqrt{\omega_{1\mathbf{k}}}} \frac{qi}{|\hat{\mathbf{u}}_{\rho} \times \mathbf{k}|} (k^{\mu} (k^{\alpha} \delta_{\beta,\nu} + k^{\beta} \delta_{\alpha,\nu}) - k^{\nu} (k^{\alpha} \delta_{\beta,\mu} + k^{\beta} \delta_{\alpha,\mu})),$$

$$\mathcal{S}_{2\mathbf{k}}^{q;\alpha\beta} = \frac{1}{\sqrt{\omega_{2\mathbf{k}}}} \frac{-1}{|\mathbf{k}||\hat{\mathbf{u}}_{\rho} \times \mathbf{k}|} (\mathbf{k}^2 (k^{\alpha} \delta_{\beta,\rho} + k^{\beta} \delta_{\alpha,\rho}) - 2k^{\alpha} k^{\beta} k^{\rho}),$$

so that  $\mathcal{L}_0 \propto \mathbf{k} \cdot \boldsymbol{\lambda} \cdot \mathbf{k}$ ,  $\mathcal{L}_1 \propto [\mathbf{k} \times (\boldsymbol{\lambda} \cdot \mathbf{k})]^{\rho}$ ,  $\mathcal{L}_2 \propto [\mathbf{k}^2 (\boldsymbol{\lambda} \cdot \mathbf{k}) - (\mathbf{k} \cdot \boldsymbol{\lambda} \cdot \mathbf{k}) \mathbf{k}]^{\rho}$ .

For this choice of polarization vectors, the phonon-magnon coupling constants can be decomposed in such a way that their behavior under operations of the  $D_{4h}$  point-group defined in the  $(\mu, \nu, \rho)$  basis becomes transparent, in other words in terms of the basis harmonics of the ‘‘Hall geometry’’ point-group. Note that, because the magnetic space group of the system is a priori independent of the symmetries associated with the choice of ‘‘Hall geometry,’’ the coefficients of the harmonics need not be independent. (In the the square lattice case discussed here, some of the symmetries of the system coincide with those of the Hall geometry, so that these coefficients are not entirely independent. Note that this causes



additional constraints for the existence of a nonzero Hall effect.)

### 3. Numerical implementation

We define  $\hat{\lambda}_{\xi, \xi'}^{\ell_1, \ell_2; \alpha \beta} = \lambda_{\xi \ell_1 + \bar{\xi} + 1, \tilde{\xi}' \ell_2 + \bar{\xi}' + 1; \xi \xi'}$ , so that, in particular,

$$\begin{aligned} \hat{\lambda}_{1,1}^{\ell_1, \ell_2; \alpha \beta} &= \lambda_{\ell_1 + 1, \ell_2 + 1; 11}, \\ \hat{\lambda}_{0,0}^{\ell_1, \ell_2; \alpha \beta} &= \lambda_{\ell_1 + 1, \bar{\ell}_2 + 1; 00}, \\ \hat{\lambda}_{1,0}^{\ell_1, \ell_2; \alpha \beta} &= \lambda_{\ell_1 + 1, \bar{\ell}_2 + 1; 10}, \end{aligned} \quad (\text{E18})$$

(note the bars) and

$$\mathcal{L}_{\mathbf{nk}; \xi, \xi'}^{q, \ell_1, \ell_2} = \text{Tr} \left[ (\hat{\lambda}_{\xi \xi'}^{\ell_1, \ell_2})^T \cdot \mathcal{S}_{\mathbf{nk}}^q \right] = \sum_{\alpha, \beta = x, y, z} \hat{\lambda}_{\xi, \xi'}^{\ell_1, \ell_2; \alpha \beta} \mathcal{S}_{\mathbf{nk}}^{q; \alpha \beta}. \quad (\text{E19})$$

Moreover, given (i) our choice of isotropic elasticity, (ii) a given Hall plane  $\mu\nu$  and perpendicular Hall axis,  $\rho$ , (iii)  $\ell_1 = \ell_2 = \ell$ ,  $\hat{\lambda}$  is a function of  $\Lambda_{1, \dots, 7}^{\xi(\ell)}$  contains 72 values, which can be parametrized by a single index  $i = 0, \dots, 71$  through, e.g.  $i = 36\xi + 18\xi' + 9\ell + 3\alpha + \beta$  if we identify  $(x, y, z)$  with  $(0, 1, 2)$  for  $\alpha$  and  $\beta$ ,  $\mathcal{S}$  is a complex function of  $n, \rho, \mathbf{k}, q, \ell, \alpha, \beta$ .

### 4. Details of the derivation of the general forms of the scaling relations

Here we give details about the results and calculations in Sec. V E 5.

#### a. Dimensionless functions

The functional forms of the scaling functions introduced in Eq. (110) are

$$\tilde{c}_\eta(\tilde{y}) = \frac{1}{2} (|\sin \theta| + \eta v^{-1} X(\tilde{y})), \quad (\text{E20})$$

$$\tilde{\Omega}_\ell^{\pm \eta}(\tilde{y}) = \frac{1}{2} \sqrt{\sin^2 \theta X^2(\tilde{y}) + v^{-2} \pm 2\eta |\sin \theta| v^{-1} X(\tilde{y})},$$

with

$$X(\tilde{y}) = \sqrt{1 + 4 \frac{\tilde{y}^2}{\sin^2 \theta - v^{-2}}}, \quad (\text{E21})$$

and

$$\begin{aligned} \tilde{\mathbf{f}}_\eta^{s=1}(\tilde{y}) &= \Theta(v^{-2} - \sin^2 \theta - 4|\tilde{y}|^2), \\ \tilde{\mathbf{f}}_\eta^{s=-1}(\tilde{y}) &= \delta_{\eta, 1} \Theta(\sin^2 \theta - v^{-2}), \\ \tilde{J}_D^s(\tilde{y}) &= \left| \sum_{r=\pm 1} \frac{s^{(r-1)/2} r \tilde{c}_r(\tilde{y})}{\sqrt{\tilde{c}_r(\tilde{y})^2 + \tilde{y}^2}} \right|^{-1}. \end{aligned} \quad (\text{E22})$$

Inserting the expressions for  $\mathcal{L}$  and  $\mathbf{F}$  into that of  $\mathcal{B}$ , we find

$$\begin{aligned} &\mathcal{B}_{\mathbf{k}; -\mathbf{p}_{\ell, \mathbf{k}}^{(\eta)}(y) + \frac{\mathbf{k}}{2}}^{n, \ell \ell | + s -} \quad (\text{E23}) \\ &= \frac{-i}{2\sqrt{2}M_{\text{uc}}} \sum_{\xi \xi'} n_0^{-\xi - \xi'} \sum_{\alpha, \beta = x, y, z} \hat{\lambda}_{\xi \xi'}^{\ell \ell; \alpha \beta} i^{\bar{\xi}}(si)^{\bar{\xi}'} (-1)^{(\bar{\xi} + \bar{\xi}') \ell} \\ &\quad \frac{k^\alpha \varepsilon_{\mathbf{nk}}^\beta + k^\beta \varepsilon_{\mathbf{nk}}^\alpha}{\sqrt{\omega_{\mathbf{nk}}}} (\chi \Omega_{\ell \mathbf{p}_{\ell \mathbf{k}}^{(\eta)}(y)})^{\xi - \frac{1}{2}} (\chi \Omega_{\ell \mathbf{p}_{\ell \mathbf{k}}^{(-\eta)}(y)})^{\xi' - \frac{1}{2}} \end{aligned}$$

because  $F_{\xi q \ell}(-\mathbf{p}) = F_{\xi q \ell}(\mathbf{p})$ . Then, for  $\delta_\ell = 0$ , and defining  $\hat{k}^\alpha = (\hat{\mathbf{k}})^\alpha$ , the  $\tilde{\mathcal{B}}_{\xi \xi'}$  introduced in Eq. (110) are:

$$\tilde{\mathcal{B}}_{nn} = \frac{is \chi^{-1} v_m^{-1}}{2\sqrt{2}M_{\text{uc}} v_{\text{ph}}} \sum_{\alpha, \beta = x, y, z} \hat{\lambda}_{00}^{\ell \ell; \alpha \beta} (\hat{k}^\alpha \varepsilon_{\mathbf{nk}}^\beta + \hat{k}^\beta \varepsilon_{\mathbf{nk}}^\alpha) (\tilde{\Omega}^\eta(\tilde{y}) \tilde{\Omega}^{-\eta}(\tilde{y}))^{-\frac{1}{2}}, \quad (\text{E24})$$

$$\tilde{\mathcal{B}}_{mm} = \frac{-in_0^{-2} \chi v_m}{2\sqrt{2}M_{\text{uc}} v_{\text{ph}}} \sum_{\alpha, \beta = x, y, z} \hat{\lambda}_{11}^{\ell \ell; \alpha \beta} (\hat{k}^\alpha \varepsilon_{\mathbf{nk}}^\beta + \hat{k}^\beta \varepsilon_{\mathbf{nk}}^\alpha) (\tilde{\Omega}^\eta(\tilde{y}) \tilde{\Omega}^{-\eta}(\tilde{y}))^{\frac{1}{2}}, \quad (\text{E25})$$

and

$$\begin{aligned} \tilde{\mathcal{B}}_{mn} &= \frac{(-1)^\ell n_0^{-1}}{2\sqrt{2}M_{\text{uc}} v_{\text{ph}}} \sum_{\alpha, \beta = x, y, z} (\hat{k}^\alpha \varepsilon_{\mathbf{nk}}^\beta + \hat{k}^\beta \varepsilon_{\mathbf{nk}}^\alpha) \\ &\quad \left[ \hat{\lambda}_{01}^{\ell \ell; \alpha \beta} (\tilde{\Omega}^\eta(\tilde{y}))^{-\frac{1}{2}} (\tilde{\Omega}^{-\eta}(\tilde{y}))^{\frac{1}{2}} \right. \\ &\quad \left. + s \hat{\lambda}_{10}^{\ell \ell; \alpha \beta} (\tilde{\Omega}^\eta(\tilde{y}))^{\frac{1}{2}} (\tilde{\Omega}^{-\eta}(\tilde{y}))^{-\frac{1}{2}} \right]. \end{aligned} \quad (\text{E26})$$

#### b. Details of the behavior of the scaling function $\mathbf{F}$

Here we derive the behavior of the scaling functions  $F_x(\varkappa, v, \theta)$  defined in Eq. (112) at small and large  $\varkappa$ .

Let us first consider the large- $\varkappa$  limit. The hyperbolic sines in the denominator of the integrand grow exponentially in this limit (because the two  $\tilde{\Omega}_\ell^{\pm \eta}(\tilde{y})$  functions cannot be simultaneously be made to vanish), so that they can be approximated by their leading exponential forms. An application of the saddle point method then shows that the integral is dominated by region around  $\tilde{y} = 0$ , and is exponentially suppressed for large  $\varkappa$ . For  $v|\sin \theta| > 1$ , i.e. when the azimuthal angle of  $\mathbf{k}$  is smaller than  $v^{-1}$ , this suppression exceeds the exponential growth of the  $\sinh \varkappa/2$  prefactor, and the scaling function decays exponentially:

$$F_x(\varkappa, v > |\sin \theta|^{-1}) \underset{\varkappa \gg 1}{\sim} \exp \left[ \frac{\varkappa}{2} (1 - v|\sin \theta|) \right]. \quad (\text{E27})$$

For smaller angles where  $v|\sin \theta| < 1$ ,  $\mathbf{F}$  does not decay exponentially in the large  $\varkappa$  limit. Here Eq. (E27) is correct to exponential accuracy, i.e. it is asymptotically correct for  $\ln(\mathbf{F})$  at large  $\varkappa$ . To this accuracy, the asymptotics are independent of  $x$ .

Now consider the small  $\varkappa$  limit. The naïve result for the scaling function is obtained by expanding both the

hyperbolic sine in the numerator and the two in the denominator of the integrand around zero leads to

$$F_x^{(s)}(\varkappa \ll 1, v, \theta) \underset{?}{\sim} \frac{1}{\varkappa} \frac{(3-s)\mathbf{a}^2}{2\pi v_m h^2 v^2} \quad (\text{E28})$$

$$\int_{-\infty}^{+\infty} d\tilde{y} \sum_{\eta} \tilde{f}_{\eta}^s(\tilde{y}) \tilde{J}_D^s(\tilde{y}) \sum_{\ell} \frac{\tilde{C}_x(\tilde{y})}{\tilde{\Omega}_{\ell}^{+\eta}(\tilde{y}) \tilde{\Omega}_{\ell}^{-\eta}(\tilde{y})}.$$

This expression is correct provided the integral in the second line converges. The convergence is problematic only at large  $\tilde{y}$  for the case  $s = -1$  (in the case  $s = 1$ , the integral is confined by the  $\tilde{f}^{s=1}$  factor to a finite domain). In this limit the Jacobean  $\tilde{J}^{s=-1}$  grows linearly in  $\tilde{y}$  as does  $\tilde{\Omega}$ , while the factor  $\tilde{C}_x(\tilde{y})$  behaves as  $\tilde{y}^{2x}$ . As a result, the integral converges for the case  $x = -1$  and the  $1/\varkappa$  scaling is correct in this case. In the cases  $x = 0, 1$ , the integral is logarithmically and quadratically divergent at large  $\tilde{y}$ , respectively.

In the latter two cases, we must reconsider the naïve result in Eq. (E28). The divergence in this equation is an artificial result because the hyperbolic sines in the original expression in Eq. (112) grow rapidly once  $\tilde{\Omega} > \varkappa^{-1}$  and ensure convergence of the integral (i.e. the large  $\tilde{y} > |v\varkappa|^{-1}$  contribution is negligible). Proper behavior is restored for small  $\varkappa$  by simply using the expanded form of Eq. (E28) but only integrating up to an upper cutoff  $|\tilde{y}| < |\varkappa v|^{-1}$ . This regulates the divergences and one obtains additional  $\ln(1/\varkappa)$  and  $\varkappa^{-2}$  factors multiplying the  $1/\varkappa$

form for the cases  $x = 0, 1$ , respectively. Collecting the above results we see that

$$F_x^{(-1)}(\varkappa) \underset{\varkappa \ll 1}{\sim} \begin{cases} \frac{1}{\varkappa^3} & x = 1 \\ \frac{\ln(1/\varkappa)}{\varkappa} & x = 0 \\ \frac{1}{\varkappa} & x = -1 \end{cases}. \quad (\text{E29})$$

This function is non-zero for  $|v \sin \theta| > 1$ , while  $F^{(+1)}$  is non-zero when  $|v \sin \theta| < 1$ .

In the latter case, as mentioned above, the integral over  $\tilde{y}$  always converges because the set of integration is an ellipse instead of a half-hyperbola. Therefore the naïve scaling is the correct one and the  $F_x^{(+1)}(\varkappa) \underset{\varkappa \ll 1}{\sim} 1/\varkappa$  behavior holds for all  $x$ .

## Appendix F: Application—further physical details

### 1. Microscopic derivation of the coupling constants

We consider the most general coupling between the strain tensor and bilinears of the  $\mathbf{m}, \mathbf{n}$  fields, exhibiting all the symmetries allowed by the crystal symmetry group in the paramagnetic phase: the  $D_{4h}$  tetragonal point-group; translations of one unit cell—which forbids interactions of the  $m_a n_b$  type; and time-reversal. The corresponding hamiltonian density (where for the sake of readability we have replaced  $n_0 \rightarrow 1$ ) reads:

$$\mathcal{H}'_{\text{tetra}} = \Lambda_1^{(m)} \left( m_x m_x \mathcal{E}^{xx} + m_y m_y \mathcal{E}^{yy} \right) + \Lambda_1^{(n)} \left( n_x n_x \mathcal{E}^{xx} + n_y n_y \mathcal{E}^{yy} \right) + \Lambda_5^{(m)} m_z m_z \mathcal{E}^{zz} + \Lambda_5^{(n)} n_z n_z \mathcal{E}^{zz} \quad (\text{F1})$$

$$+ \Lambda_2^{(m)} \left( m_x m_x \mathcal{E}^{yy} + m_y m_y \mathcal{E}^{xx} \right) + \Lambda_2^{(n)} \left( n_x n_x \mathcal{E}^{yy} + n_y n_y \mathcal{E}^{xx} \right) \quad (\text{F2})$$

$$+ \left( \Lambda_3^{(m)} m_z m_z + \Lambda_3^{(n)} n_z n_z \right) \left( \mathcal{E}^{xx} + \mathcal{E}^{yy} \right) + \Lambda_4^{(m)} \left( m_x m_x + m_y m_y \right) \mathcal{E}^{zz} + \Lambda_4^{(n)} \left( n_x n_x + n_y n_y \right) \mathcal{E}^{zz} \quad (\text{F3})$$

$$+ 4\Lambda_6^{(m)} m_x m_y \mathcal{E}^{xy} + 4\Lambda_6^{(n)} n_x n_y \mathcal{E}^{xy} + 4\Lambda_7^{(m)} \left( m_x m_z \mathcal{E}^{xz} + m_y m_z \mathcal{E}^{yz} \right) + 4\Lambda_7^{(n)} \left( n_x n_z \mathcal{E}^{xz} + n_y n_z \mathcal{E}^{yz} \right). \quad (\text{F4})$$

We now propose a microscopic origin to the  $\Lambda_I^{(\xi)}$  coefficients appearing in it.

We start from a generic spin exchange hamiltonian of the form

$$H_{\text{ex}} = \sum_{\mathbf{R}, \mathbf{R}'} \sum_{a, b} S_{\mathbf{R}}^a J_{\mathbf{R}-\mathbf{R}'}^{ab} S_{\mathbf{R}'}^b, \quad (\text{F5})$$

where  $\mathbf{R}, \mathbf{R}'$  indicate the actual locations of the sites in the *distorted* lattice, and each sum spans the whole distorted lattice.

We then express  $\mathbf{R} = \mathbf{r} + \mathbf{u}_{\mathbf{r}}$ , where  $\mathbf{r}$  belongs to the undistorted lattice and  $\mathbf{u}_{\mathbf{r}}$  is the displacement field at site  $\mathbf{r}$ . Taylor-expanding the coefficients  $J_{\mathbf{R}-\mathbf{R}'}^{ab}$  with respect to the displacement field (and identifying  $S_{\mathbf{R}}^a = S_{\mathbf{r}}^a$ ), we thus obtain  $H_{\text{ex}} = H_{\text{ex}}^0 + H'_{\text{ex}} + O(u^2)$ , where  $H_{\text{ex}}^0 =$

$H_{\text{ex}}|_{\mathbf{R}, \mathbf{R}' \rightarrow \mathbf{r}, \mathbf{r}'}$  and

$$H'_{\text{ex}} = \sum_{\mathbf{r}, \mathbf{r}'} \sum_{ab, \nu} S_{\mathbf{r}}^a (u_{\mathbf{r}}^{\nu} - u_{\mathbf{r}'}^{\nu}) \partial_{\eta^{\nu}} J_{\eta}^{ab} \Big|_{\eta=\mathbf{r}-\mathbf{r}'} S_{\mathbf{r}'}^b. \quad (\text{F6})$$

Then, identifying  $\mathcal{E}_{\alpha\beta} = \frac{1}{2}(\partial_{\alpha} u_{\beta} + \partial_{\beta} u_{\alpha})$  the symmetric rank-2 elasticity tensor (i.e. strain tensor), we identify  $H'_{\text{ex}} = H'_{ss\varepsilon} + \dots$ , where

$$H'_{ss\varepsilon} = \frac{1}{2} \sum_{\mathbf{r}, \boldsymbol{\eta}} S_{\mathbf{r}+\boldsymbol{\eta}}^a S_{\mathbf{r}}^b [\eta_{\alpha} \partial_{\eta^{\beta}} + \eta_{\beta} \partial_{\eta^{\alpha}}] J_{\boldsymbol{\eta}}^{ab} \Big|_{\boldsymbol{\eta}} \mathcal{E}_{\alpha\beta}(\mathbf{r}) + \dots, \quad (\text{F7})$$

where  $a, b = x, y, z$  is a spin axis index,  $\alpha, \beta = x, y, z$  is a spatial index, and “ $+\dots$ ” encompasses terms featuring  $\omega_{\alpha\beta}$  the anti-symmetric rank-2 elasticity tensor, as well as higher-order derivatives of the displacement field.

Note that in this microscopic derivation, we identify  $S_{\mathbf{R}}^a \mapsto S_{\mathbf{r}}^a$ . In fact, also expanding the *magnetization fields* (and not only the magnetic exchange) with respect to displacement yields an interaction term which is *formally* of the same order as that derived here. However, magnetization in an ordered magnet is a slow variable, while  $J$  varies over distances of the order of the lattice parameter  $\mathbf{a}$ , therefore such terms are *quantitatively* much smaller by a factor  $O(k_B T \mathbf{a} / v_m)$ , both within and beyond the Born-Oppenheimer approximation.

Finally, we take the particular case of a square lattice with tetragonal symmetry, and describe the spins in terms of  $\mathbf{m}, \mathbf{n}$  fields as in the main text, namely  $\mathbf{S}_{\mathbf{r}} = (-1)^{\mathbf{r}} \mu_0 \mathbf{n}(\mathbf{r}) + \mathbf{a}^2 \mathbf{m}(\mathbf{r})$ . We identify  $H'_{ss\epsilon} = \sum_{\mathbf{r}} \mathcal{H}'_{\text{tetra}}(\mathbf{r}) + \dots$  where “+...” is made of rapidly oscillating (time-reversal breaking) terms, and  $\mathcal{H}'_{\text{tetra}}$  is as displayed in Eq. (F1), with identification

$$\Lambda_{ab}^{(m),\alpha\beta} = \frac{1}{2} \sum_{\boldsymbol{\eta}} (\eta_{\alpha} \partial_{\beta} + \eta_{\beta} \partial_{\alpha}) J^{ab} \Big|_{\boldsymbol{\eta}}, \quad (\text{F8})$$

$$\Lambda_{ab}^{(n),\alpha\beta} = \frac{1}{2} \sum_{\boldsymbol{\eta}} e^{i\boldsymbol{\pi}\boldsymbol{\eta}} (\eta_{\alpha} \partial_{\beta} + \eta_{\beta} \partial_{\alpha}) J^{ab} \Big|_{\boldsymbol{\eta}}, \quad (\text{F9})$$

where the sum over  $\boldsymbol{\eta}$  spans the whole direct (two-dimensional square) lattice, and  $\boldsymbol{\pi} = (\frac{\pi}{\mathbf{a}}, \frac{\pi}{\mathbf{a}})$  with  $\mathbf{a}$  the square lattice parameter.

## 2. Contributions to intervalley couplings

In the main text, the  $n_a, m_a$  fields live in the valleys identified by:

$$\begin{aligned} \ell = 0 : & \quad n_y, m_z \\ \ell = 1 : & \quad n_z, m_y. \end{aligned} \quad (\text{F10})$$

Therefore, intervalley couplings are of the form  $\lambda_{ab;\xi\xi'}$  with  $\delta_{\xi\xi'} + \delta_{ab} = 1$ . More explicitly, using Eq. (73), they

are:

$$\begin{aligned} \lambda_{yz;00}^{\alpha\beta} &= \Lambda_{yz}^{(n),\alpha\beta}, \\ \lambda_{yz;11}^{\alpha\beta} &= \Lambda_{yz}^{(m),\alpha\beta}, \\ \lambda_{yy;01}^{\alpha\beta} &= \frac{-1}{n_0} \left[ m_0^y \Lambda_{yx}^{(m),\alpha\beta} + m_0^z \Lambda_{zx}^{(m),\alpha\beta} + m_0^y \Lambda_{yx}^{(n),\alpha\beta} \right], \\ \lambda_{zz;01}^{\alpha\beta} &= \frac{-1}{n_0} \left[ m_0^z \Lambda_{zx}^{(m),\alpha\beta} + m_0^y \Lambda_{yx}^{(m),\alpha\beta} + m_0^z \Lambda_{zx}^{(n),\alpha\beta} \right]. \end{aligned} \quad (\text{F11})$$

Also recall from Eq. (70) that

$$\begin{aligned} \Lambda_{yx}^{(\xi),xy} &= \Lambda_{yx}^{(\xi),yx} = \Lambda_{xy}^{(\xi),xy} = \Lambda_{xy}^{(\xi),yx} = \Lambda_6^{(\xi)}, \\ \Lambda_{zx}^{(\xi),xz} &= \Lambda_{zx}^{(\xi),zx} = \Lambda_{yz}^{(\xi),yz} = \Lambda_{yz}^{(\xi),zy} = \Lambda_7^{(\xi)}, \end{aligned} \quad (\text{F12})$$

and all other values of  $\alpha, \beta$  yield 0 for this set of lower indices. From this, it is clear that the  $\Lambda_7^{(\xi)}$  couplings always mix valleys, regardless of  $\mathbf{m}_0$ , and contribute a  $\lambda_{yz;\xi\xi}$  term. This intervalley coupling is a small contribution which does not contribute to  $\mathcal{T}$  breaking. Meanwhile, the  $\mathcal{T}$ -odd  $\lambda_{yy;01}$  and  $\lambda_{zz;01}$  intervalley couplings both contain contributions from both  $\Lambda_7^{(\xi)} m_0^z$  and  $\Lambda_6^{(\xi)} m_0^y$ .

### 3. Derivation of the gaps from a sigma model

Here we provide a heuristic microscopic argument for expressing the gaps in terms of spin-spin couplings. We ignore spin-lattice coupling, and just consider corrections to the isotropic Heisenberg model. We assume the addition of a term of the XXZ anisotropy form:

$$H_{\text{XXZ}} = gJ \sum_{\langle ij \rangle} (2S_i^z S_j^z - S_i^x S_j^x - S_i^y S_j^y). \quad (\text{F13})$$

This is to be added to the isotropic Heisenberg model, along with a Zeeman coupling to the transverse field.

Carrying out the long-wavelength expansion in terms of  $\mathbf{m}$  and  $\mathbf{n}$  fields, we obtain the corrected potential part (i.e. without gradient terms) of the nonlinear sigma-model Eq. (50):

$$\begin{aligned} \mathcal{H}_{\text{NLS}}^{g,h} &= \frac{1}{2\chi} |\mathbf{m}|^2 + 2gJ \mathbf{a}^2 (2m_z^2 - m_x^2 - m_y^2) \\ &\quad - 2gJ \frac{\mu_0^2}{\mathbf{a}^2} (2n_z^2 - n_x^2 - n_y^2) - h_y m_y - h_z m_z. \end{aligned} \quad (\text{F14})$$

Note that the first term includes an  $m_x^2$  term, which is absent in the quadratic expansion describing linear spin waves in the main text. Indeed this term is higher order in the small fluctuations around an  $x$ -ordered state when carrying out a zero field spin wave expansion, which was the case in the main text where the external field had already been integrated out to yield the  $n_a n_b$  mass term. We also included an external uniform field which lies in the  $y - z$  plane.

---

Expanding around the  $x$ -ordered state, using that  $m_x = -m_y n_y - m_z n_z$  and  $n_x = 1 - \frac{1}{2}(n_y^2 + n_z^2 + \frac{1}{n_0^2}(m_y^2 + m_z^2))$ ,

yields

$$\begin{aligned} \mathcal{H}_{\text{NLS}}^{g,h} = & \frac{1}{2\chi} (m_y^2 + m_z^2) + 2gJ\mathbf{a}^2 (2m_z^2 - m_y^2) - 2gJ\frac{\mu_0^2}{\mathbf{a}^2} (2n_z^2 - n_y^2) - h_y m_y - h_z m_z \\ & + \left( \frac{1}{2\chi} - 2gJ\mathbf{a}^2 \right) (m_y^2 n_y^2 + m_z^2 n_z^2 + 2m_y m_z n_y n_z) + 2gJ\frac{\mu_0^2}{\mathbf{a}^2} \left[ 1 - \frac{1}{2}(n_y^2 + n_z^2 + \frac{1}{n_0^2}(m_y^2 + m_z^2)) \right]^2. \end{aligned} \quad (\text{F15})$$

Note that the first term on the second line is of the form  $(\mathbf{m}_\perp \cdot \mathbf{n}_\perp)^2$ , where the  $\perp$  indicates the components of the vectors normal to the ordering direction. Since we in the next step shift the magnetization by its value induced by the field, this is proportional to  $(\mathbf{h} \cdot \mathbf{n})^2$ , as is postulated

in the main text on symmetry grounds.

We now show this explicitly. We shift the definition  $m_a = m_a + \chi_a h_a$  for  $a = y, z$ , and expand the result to quadratic order in  $m, n$ . Here  $\chi_z = (1/\chi + 4gJ\mathbf{a}^2)^{-1}$  and  $\chi_y = (1/\chi - 2gJ\mathbf{a}^2)^{-1}$ .

This gives

$$\begin{aligned} \mathcal{H}_{\text{NLS}}^{g,h} = & \frac{1}{2\chi} (m_y^2 + m_z^2) + 2gJ\mathbf{a}^2 (2m_z^2 - m_y^2) - 2gJ\frac{\mu_0^2}{\mathbf{a}^2} (2n_z^2 - n_y^2) \\ & + \left( \frac{1}{2\chi} - 2gJ\mathbf{a}^2 \right) (\chi_y^2 h_y^2 n_y^2 + \chi_z^2 h_z^2 n_z^2 + 2\chi_y \chi_z h_y h_z n_y n_z) - 2gJ\frac{\mu_0^2}{\mathbf{a}^2} [n_y^2 + n_z^2 + \dots], \end{aligned} \quad (\text{F16})$$

where the ‘ $\dots$ ’ in the last brackets account for terms higher order in field, magnetization fluctuations, etc.

The anisotropy coefficients, denoted by  $\Gamma_{ab}$  in the text, can now be extracted. The terms in  $\mathcal{H}_{\text{NLS}}^{g,h}$  which are quadratic in the  $n_y, n_z$  fields read

$$\mathcal{H}_{nn} = \chi_y^2 h_y^2 \left( \frac{1}{2\chi} - 2gJ\mathbf{a}^2 \right) n_y^2 + \left[ \chi_z^2 h_z^2 \left( \frac{1}{2\chi} - 2gJ\mathbf{a}^2 \right) - 6gJ\frac{\mu_0^2}{\mathbf{a}^2} \right] n_z^2 + 2\chi_y \chi_z h_y h_z \left( \frac{1}{2\chi} - 2gJ\mathbf{a}^2 \right) n_y n_z. \quad (\text{F17})$$

Note that the two terms proportional to  $n_y^2$  from the right-most contributions on each line of Eq. (F16) above canceled. That means the the coefficient of  $n_y^2$  in Eq. (F17) vanishes if  $h_y = 0$ . This occurs because of Goldstone’s theorem and the assumed XXZ form of the anisotropy: if the field is purely along the  $z$  direction, XY symmetry of the Hamiltonian under rotations about the  $z$  axis is preserved, and this makes one of the spin wave modes remain gapless. Conversely, for a field along the  $y$  direction, and in the presence of anisotropy, both modes are generally gapped.

We can simplify the above expression if we assume  $|g| \ll 1$ , which means  $\chi_y^{-1} \approx \chi_z^{-1} \approx \chi^{-1} = 4\mathbf{a}^2 J$  and therefore  $1/\chi \gg gJ\mathbf{a}^2$ ; hence

$$\mathcal{H}_{nn} \approx \frac{\chi h_y^2}{2} n_y^2 + \left[ \frac{\chi h_z^2}{2} - 6gJ\frac{\mu_0^2}{\mathbf{a}^2} \right] n_z^2 + \chi h_y h_z n_y n_z. \quad (\text{F18})$$

The above shows that if  $h_z$  is small or zero, stability requires  $g < 0$ . This can be understood from the fact that, if the field is along  $y$ , then  $H_{\text{XXZ}}$  is the only term, in the pure spin hamiltonian, breaking explicitly the  $O(2)$  symmetry in the  $x - z$  plane. It should therefore favor antiferromagnetic alignment along the  $x$  axis, which is the initial assumption of this derivation. It also proves the  $\frac{\chi}{2}$  prefactor used in the main text.

The coefficients in Eq. (F18) give contributions to  $\Gamma_{yy}$ ,  $\Gamma_{zz}$  and  $\Gamma_{yz}$ , respectively. In this Appendix, as opposed to the more general expressions given in the main text, we assume they are the only contribution.

Since taking the magnetic field purely along one of the two axes  $y, z$  guarantees that  $\Gamma_{yz} = 0$ , so that (as explained in the main text) the two magnon valleys are independent, let us assume that the field is along the  $y$  axis. Then one gap is  $\Delta_1 = |h_y|$ , the Zeeman energy associated with the field along  $y$ . The other gap gets contributions both from the anisotropy and the Zeeman energy associated with the field along  $z$ .

Note that the anisotropy-induced gap involves the square root of the anisotropy, i.e.  $\Delta_0|_{h_z=0} = 4\sqrt{3|g|}J\mu_0$ , which is not necessarily *very* small for reasonably small values of  $g$ .

### Appendix G: Application—Supplementary figures

Here we present further calculations of scattering rates and (diagonal) thermal conductivity for the model of Sec. V, as supplemental figures.

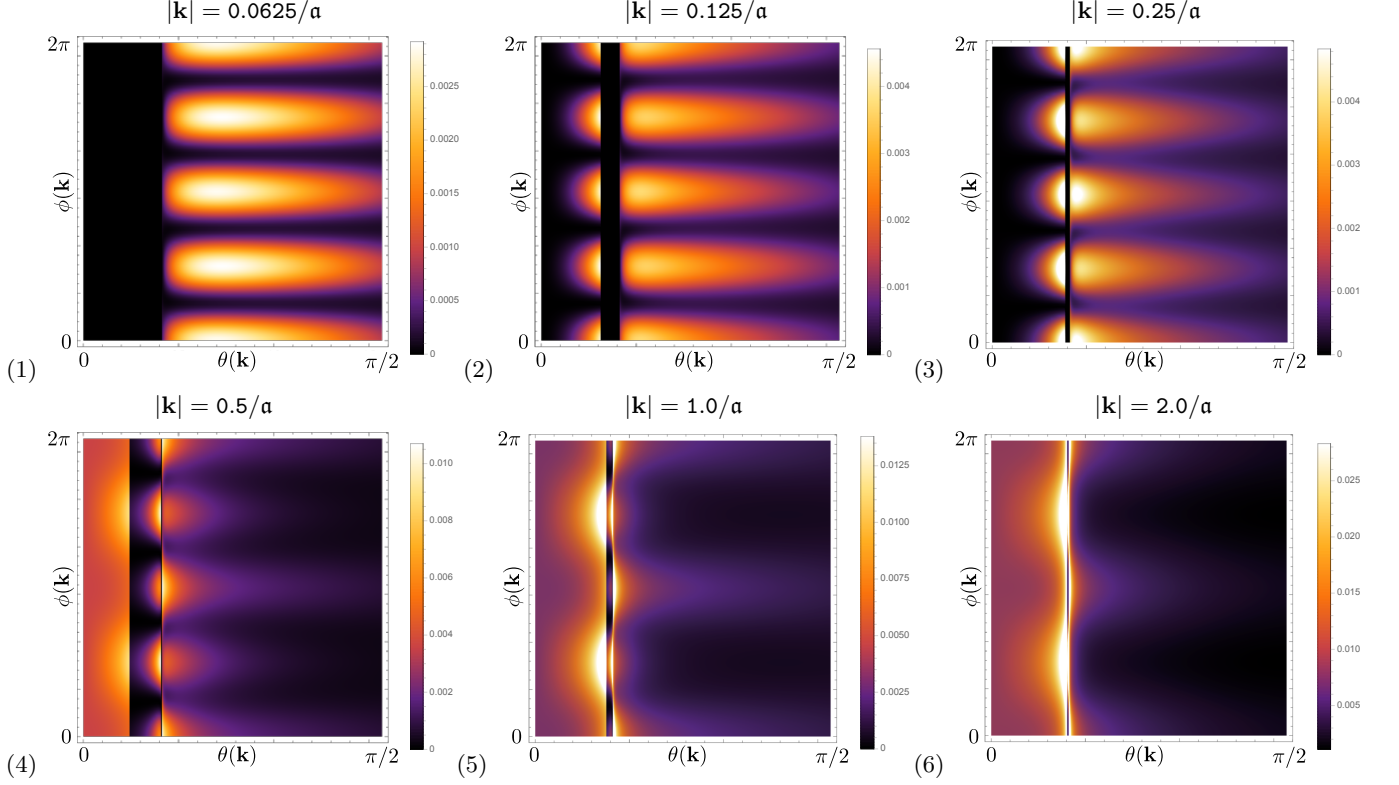


FIG. 6: Diagonal scattering rate  $D_{n\mathbf{k}}$  with respect to  $\theta(\mathbf{k}) \in [0, \pi/2]$  (horizontal axis) and  $\phi(\mathbf{k}) \in [0, 2\pi]$  (vertical axis) for fixed temperature  $T = 0.5T_0$ , polarization  $n = 0$ , and momentum (1)  $|\mathbf{k}| = 0.0625/a$ , (2)  $|\mathbf{k}| = 0.125/a$ , (3)  $|\mathbf{k}| = 0.25/a$ , (4)  $|\mathbf{k}| = 0.5/a$ , (5)  $|\mathbf{k}| = 1.0/a$ , (6)  $|\mathbf{k}| = 2.0/a$ . Color scales vary from figure to figure. Note that the  $C_4$  symmetry is approximately preserved for small  $|\mathbf{k}|$  but broken at large  $|\mathbf{k}|$ , as stated in the main text. Also note how scattering processes at  $\theta(\mathbf{k}) < \theta_-$  become allowed for  $\omega_{n\mathbf{k}} \geq 2\Delta, 2\Delta'$ , then dominant at large  $|\mathbf{k}|$ .

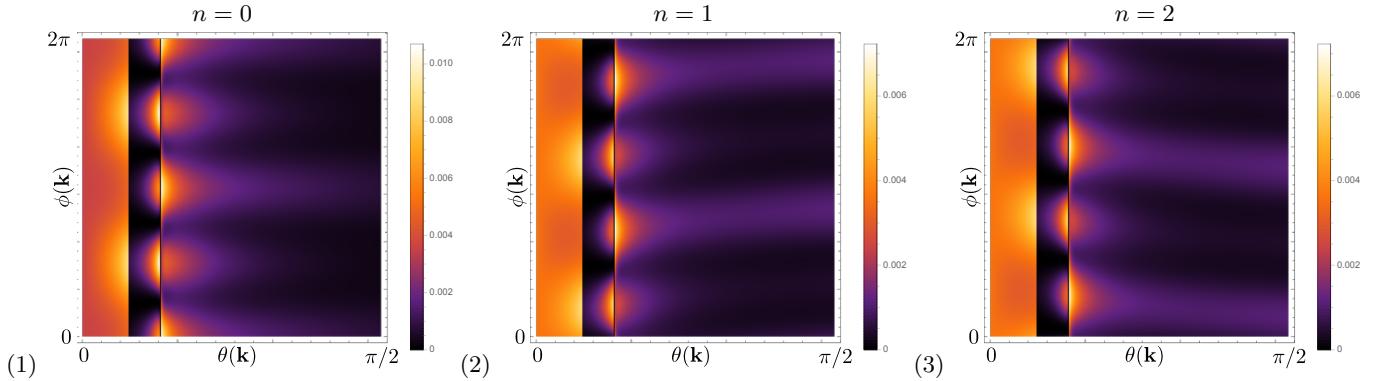


FIG. 7: Diagonal scattering rate  $D_{n\mathbf{k}}$  with respect to  $\theta(\mathbf{k}) \in [0, \pi/2]$  (horizontal axis) and  $\phi(\mathbf{k}) \in [0, 2\pi]$  (vertical axis) for fixed temperature  $T = 0.5T_0$ , momentum  $|\mathbf{k}| = 0.5/a$ , and polarizations (1)  $n = 0$ , (2)  $n = 1$ , (3)  $n = 2$ . Color scales are different in (1) and (2,3). Subfigure (1) is reproduced from the main text. Note that with our choice of polarization vectors  $\mathbf{\varepsilon}_{n,\mathbf{k}}$ , results for  $n = 1$  and  $n = 2$  are simply related by the mirror symmetry  $\phi \mapsto \pi - \phi$ .

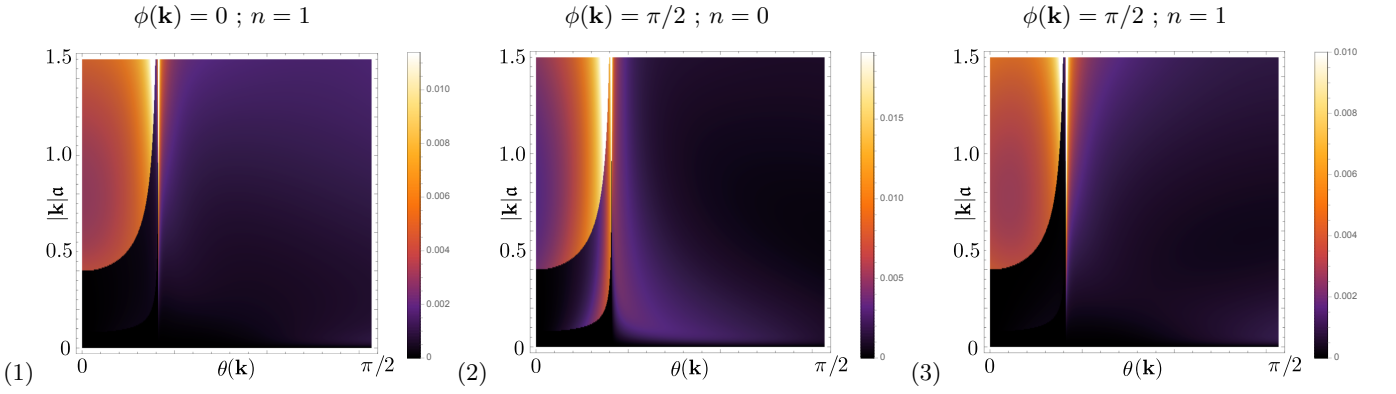


FIG. 8: Diagonal scattering rate  $D_{n\mathbf{k}}$  with respect to  $\theta(\mathbf{k}) \in [0, \pi/2]$  (horizontal axis) and  $|\mathbf{k}|a$  (vertical axis) for fixed temperature  $T = 0.5T_0$  and (1)  $\phi(\mathbf{k}) = 0$  and  $n = 1$ , (2)  $\phi(\mathbf{k}) = \pi/2$  and  $n = 0$ , (3)  $\phi(\mathbf{k}) = \pi/2$  and  $n = 1$ . Color scales are different for the three subfigures. The  $\phi(\mathbf{k}) = 0$  and  $n = 0$  case is displayed in the main text. Note that polarizations  $n = 1$  and  $n = 2$  yield the same results here. Note also that the general features are the same for polarizations  $n = 1, 2$  as for  $n = 0$ : although the scattering rates of  $n = 1, 2$  polarizations for energies  $\omega_{n\mathbf{k}} \gtrsim 2\Delta$  are not as clearly visible as they are for  $n = 0$ , they are finite (of order  $10^{-4}$  in our units) and are only *parametrically* smaller than those for the  $n = 0$  polarization, due to purely geometrical factors ( $S_{n\mathbf{k}}^{q;\alpha\beta}$  in the main text).

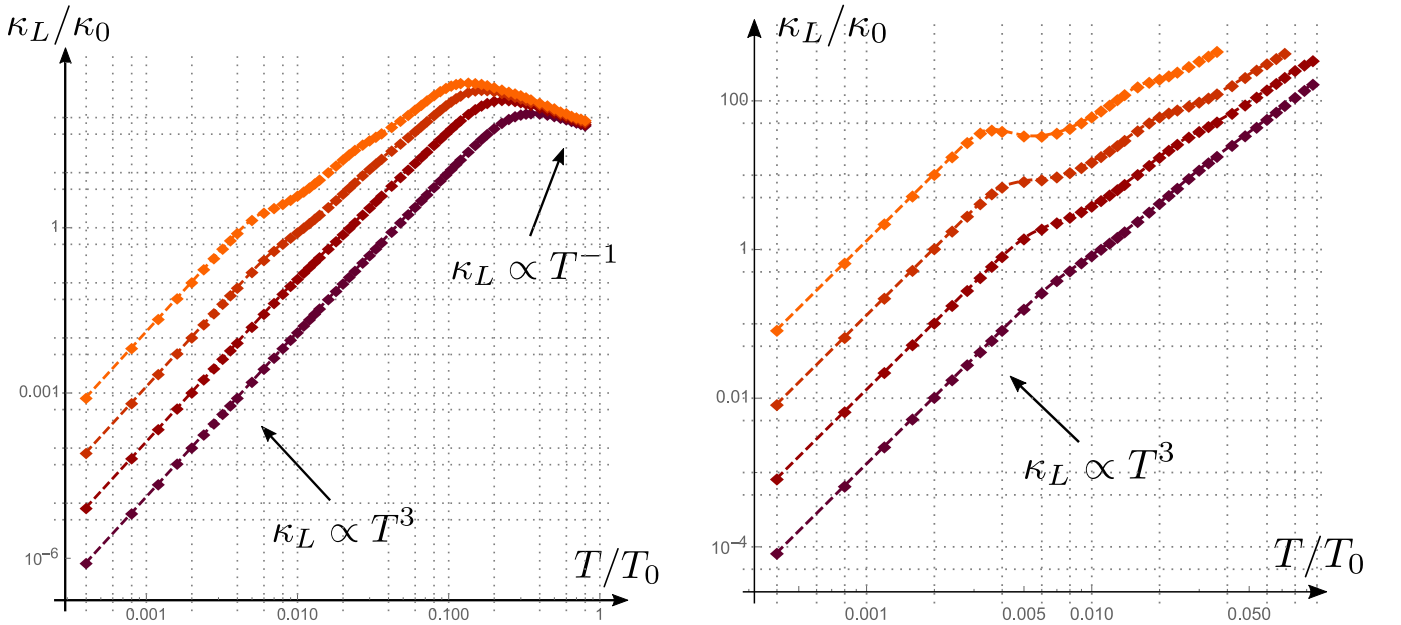


FIG. 9: Longitudinal thermal conductivity  $\kappa_L$  with respect to temperature  $T$ , in log-log scale, (*left*) for four different values of  $\gamma_{\text{ext}} = 1 \cdot 10^{-z}(v_{\text{ph}}/a)$ ,  $z \in \llbracket 4, 7 \rrbracket$ , from darker ( $z = 4$ ) to lighter ( $z = 7$ ) shade, (*right*) for four different values  $\gamma_{\text{ext}} = 1 \cdot 10^{-z}(v_{\text{ph}}/a)$ ,  $z \in \llbracket 6, 9 \rrbracket$ , from darker ( $z = 6$ ) to lighter ( $z = 9$ ) shade. Note that the two “bumps” come from the competition between  $\gamma_{\text{ext}}$  and  $D_{nn,\ell}$  for valley index  $\ell = 0, 1$ , as explained in the main text.

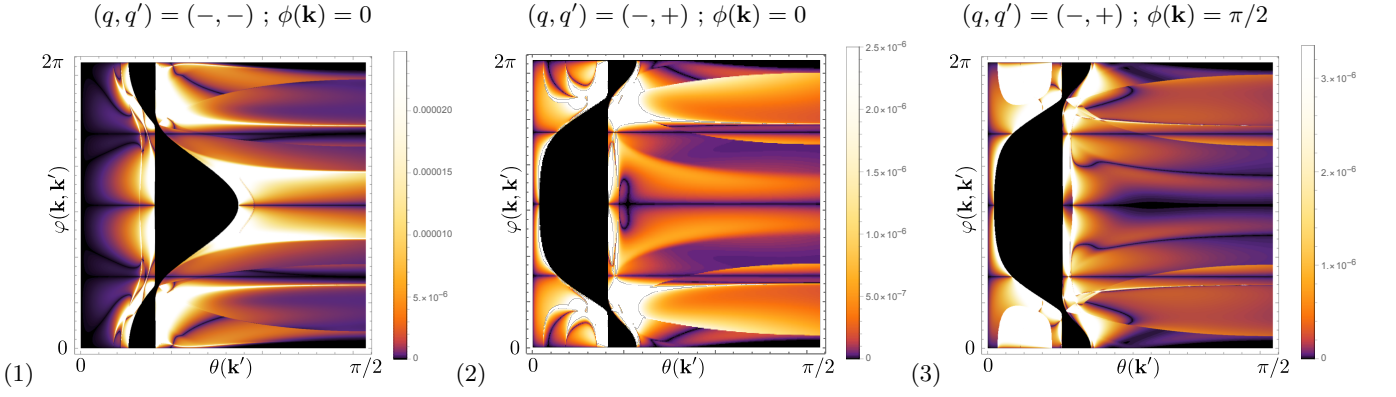


FIG. 10: Skew-scattering rates (1)  $\mathfrak{W}_{n\mathbf{k}n'\mathbf{k}'}^{\ominus,--}$  and (2,3)  $\mathfrak{W}_{n\mathbf{k}n'\mathbf{k}'}^{\ominus,+}$ , with respect to  $\theta(\mathbf{k}') \in [0, \pi/2]$  (horizontal axis) and  $\varphi(\mathbf{k}, \mathbf{k}') = \phi(\mathbf{k}') - \phi(\mathbf{k})$  (vertical axis), for fixed magnetization  $\mathbf{m}_0 = 0.05\hat{z}$ , temperature  $T = 0.5T_0$ , momentum  $|\mathbf{k}'| = 0.8/a$ ,  $k_z = 0.1/a$ , and (1,2)  $k_x = 0.2/a$ ,  $k_y = 0$ , (3)  $k_x = 0$ ,  $k_y = 0.2/a$ . The case  $\mathfrak{W}_{n\mathbf{k}n'\mathbf{k}'}^{\ominus,--}$ ,  $k_x = 0$ ,  $k_y = 0.2/a$  is in the main text. The colorbars are different for each figure and not linearly scaled. Note that thanks to anti-detailed-balance, angular dependences of  $\mathfrak{W}_{n\mathbf{k}n'\mathbf{k}'}^{\ominus,++}$ ,  $\mathfrak{W}_{n\mathbf{k}n'\mathbf{k}'}^{\ominus,+}$  are identical to those of  $\mathfrak{W}_{n\mathbf{k}n'\mathbf{k}'}^{\ominus,--}$ ,  $\mathfrak{W}_{n\mathbf{k}n'\mathbf{k}'}^{\ominus,-}$ , respectively, for an isotropic phonon dispersion.